UNIVERSITA' di PISA

Dipartimento di Chimica e Chimica Industriale

"Scuola di Dottorato Galileo Galilei"

PhD course in Chemical Science (CHIM/06)

XXVI cycle

(2011-2013)

Conjugated Organic Polymers: Effects of Chirality on Aggregation and Optical Properties

Claudio Resta

Supervisors:

Prof. Lorenzo Di Bari

Dr. Gennaro Pescitelli

Table of Contents

1 Introduction

1.1 Conjugated Organic Polymers

It was 1977 when Alan Heeger, Alan MacDiarmid and Hideki Shirakawa observed and explained the particularly high electrical conductivity of iodine-treated *trans*-polyacetylene.[1] This pathbreaking discovery was rewarded in 2000 with the Nobel Prize and, together with the studies on the light emitting properties of phenyl-based organic semiconductors in the early '90s, constitutes the capstone of one of the most important research fields in material science. The vast portfolio of new polymeric structures with unique and tailored properties makes this kind of molecules suitable for lots of applications ranging from optical switching to solar cells, light emitting devices, sensors, organic transistors, etc... Researches carried out over the last decade have demonstrated the commercial opportunities associated with the implementation of devices using this kind of technology. As a result, lines of research aiming at the study and the development of new conjugated polymers are worldwide active and ongoing.[2] The reason of this lies on the fact that these materials combine the optoelectronic properties of classic semiconductors with the processability of plastics, paving the way to devices with new intriguing features (e.g. flexibility and lightness). Moreover, one of the greatest advantages of conjugated polymers is that, to some extent, it is possible to control and vary their properties through appropriate modifications on their structure; for example, by altering the local arrangement of carbon atoms on the backbone, for instance by incorporating heteroatoms, or replacing the hydrogen atoms with side chains of various nature.

The typical monomer repeat units are based on five- or six-membered rings directly bonded one to each other, such as polyphenylenes, polypyrroles, polythiophenes and polyanilines, or more frequently linked by a double or a triple bond, or a condensed system. Some of the most common architectures are shown in Figure 1.
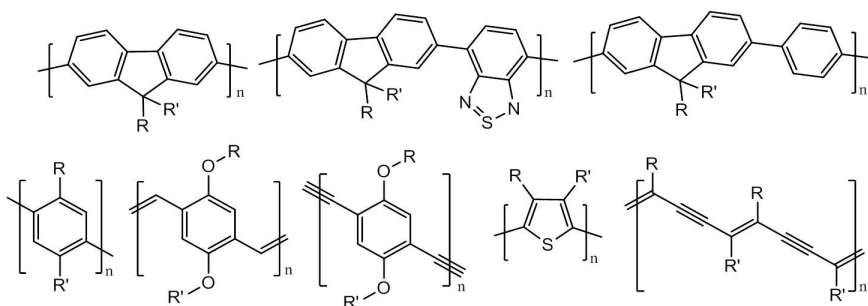
FIGURE 1: SOME EXAMPLE OF THE MOST COMMONLY USED CONJUGATED POLYMERS

The progress in understanding the fundamental physics of conjugated polymers, which provides a crucial underpinning to the technological applications, has also been large and it has been driven by experimental, theoretical and computational developments.

1.1.1 Basic Electronic Structure and Dynamics of π-Conjugated Materials

1.1.1.1 Bands Structure

As expectable from Figure 1 most of electro- and photo-active organic polymers are characterized by an extensive π-conjugation along the backbone, which results in a significant increase in the degree of electron delocalization. We can model our infinite π-system as a polymer with butadiene as the "monomer". (Figure 2) We are considering only π-orbitals. For butadiene number of units (*n.u.*) = 1, we have the usual four π-orbitals. For *n.u.*= 2 (octatetraene) the eight molecular orbitals (MOs) can be considered to be the in-phase and the out-of-phase combinations of the four butadiene MOs; each butadiene MO gives rise to two octatetraene MOs. There is a

slight split in energy, with the in-phase lying below the out-of-phase. The 12 MOs for *n.u.*= 3 can similarly be thought of as four sets of three, each set containing the three linear combinations of one of the four original butadiene orbitals. The pattern continues, and as we add more and more diene monomers, the set of MOs related to an individual butadiene MO contains more and more orbitals and spans a wider range of energies.
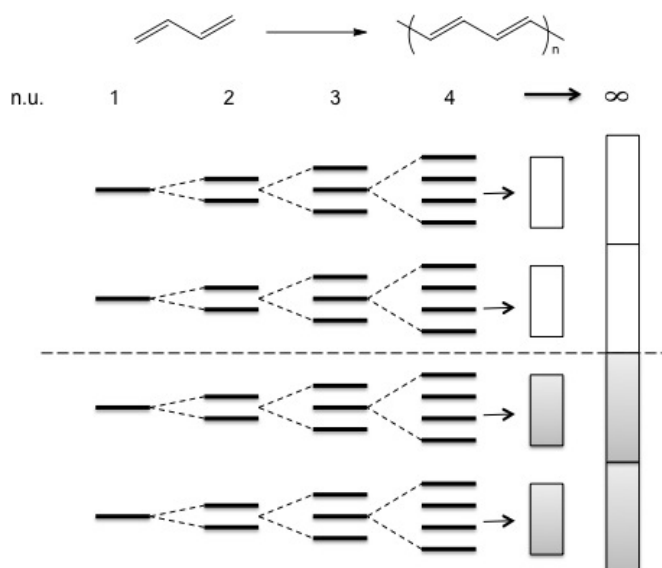
FIGURE 2: EVOLUTION FROM π-MOs IN FINITE POLYENES TO BANDS IN AN INFINITE SYSTEM

At the infinite polyene, each of the four sets of MOs contains an infinite number of MOs, each of which is a particular linear combination of one of the MOs of the monomer. All MOs in a given set trace their origin to the same monomer MO. Such a collection of orbitals is called a band. An individual MO within a band is called a band orbital. Just like MOs, band orbitals can hold two electrons, the spins of which must be paired . The eigenenergies for these systems are derivable from Eq. 1.

$$E_n = \frac{\hbar^2 \pi^2}{2mL^2} n^2$$

EQ. 1: EIGENENERGIES FOR PARTICLE IN A BOX

1.1.1 - Basic Electronic Structure and Dynamics of π-Conjugated Materials

Suppose that such as a polymer is composed by a linear chain of N atoms, each separated by a distance d; the total length of the chain is $(N-1)d$, which for a large number of atoms approximates to Nd. Eigenenergies are then (Eq. 2):

$$E_n = \frac{\hbar^2 \pi^2}{2m(Nd)^2} n^2$$

EQ. 2

Assuming that the π-electrons from the N π-orbitals are available, with two electrons per molecular orbital, the HOMO will be given by $n = N/2$, and the LUMO by $n = (N/2)+1$. (Eq. 3)

$$E_{HOMO} = \left(\frac{N}{2}\right)^2 \frac{\hbar^2 \pi^2}{2m(Nd)^2} \; ; E_{LUMO} = \left(\frac{N}{2}+1\right)^2 \frac{\hbar^2 \pi^2}{2m(Nd)^2}$$

EQ. 3

The energy required to excite an electron from the HOMO to the LUMO level is the band gap of the polymer, E_g, and becomes (Eq. 4):

$$E_g = E_{HOMO} - E_{LUMO} = (N+1)\frac{\hbar^2 \pi^2}{2m(Nd)^2} \approx \frac{\hbar^2 \pi^2}{2md^2} \cdot \frac{1}{N}$$

EQ. 4

The band gap is therefore predicted to decrease with increasing length of the polymer chain, and will practically vanish for macroscopic dimensions. From the above, it might be expected that a linear polymer backbone consisting of many strongly interacting coplanar p_z orbitals, each contributing with one electron to the resultant π-system, would behave as a one-dimensional system with conductive metallic properties. In 1955 Peierls[3] showed that quasi-one-dimensional metals spontaneously tend to distort their geometry by introducing an alternation of *short*

and *long* bonds between successive atoms along the chain. When each atom contributes with one electron, the tendency toward spontaneous symmetry breaking is particularly strong because of pairing the electrons of adjacent atoms. This opens an energy gap at the Fermi surface, thereby lowering the energy of the occupied states and stabilizing the distortion. Moving to conjugated polymers the described phenomenon leads to a formal alternation between *double* (*short*) and *single* (*long*) bonds, with a π-cloud denser in the first case then in the second one. This effect results in a semiconductive rather than a metallic conductive structure, and the difference between the distances, or, equivalently, between the densities of the π-electrons is a measure of the "alternation parameter," and it may strongly impact the electronic structure of the polymer.[4]

In summary, a completely delocalized electron system in one dimension is expected to lead to the metallic state, but due to the Peierls distortion we observe a bond alternation, a doubling of the unit cell and a semiconductive state. Moreover the energies of the individual orbitals within a band are not equally spaced, although the picture of a band might give this impression. Instead, the band orbitals may cluster around certain energies within a band, generating different densities of states. The *density of states* refers to the number of orbitals around a given energy.

1.1.1.2 Exciton Model: Electron-Hole and Charge Carriers Generation

The explanation of certain phenomena typical of conjugated polymers is provided by the *exciton model*. This model was originally developed for inorganic semiconductors and dielectrics,[5] and descends from the observation that the light-induced transition of an electron from the ground to the excited state causes a pronounced polarization of the chromophoric group. Because of the relatively high stability of this state, this is considered to be an entity of special nature. This entity, called *exciton*, is an excited state of quasi-particle character. It resembles a hydrogen-like system with a certain binding energy, which can, besides other non-radiative or radiative deactivation routes, also give rise to the formation of a geminate

electron/hole pair. The electron and hole are bound together, i.e. they cannot move independently of one another in the medium. Significantly, however, excitons obtained after photoexcitation exist within the effective conjugation length of the chromophore, and are considered to be able to diffuse along the whole chain of the polymer. The exciton can be destroyed when it encounters a perturbation and the electron returns to the ground state via a radiative or non-radiative process to recombine with the hole. (Figure 3)
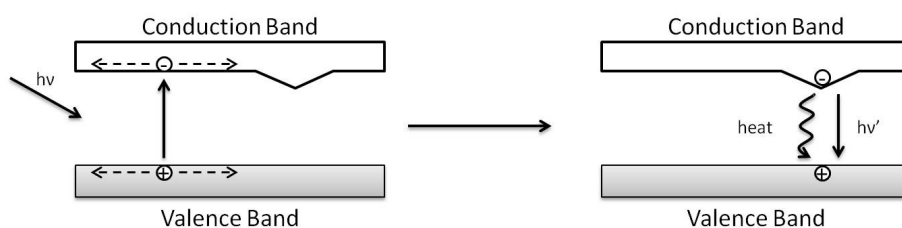
FIGURE 3: SIMPLIFIED MODEL SHOWING THE EXCITON FORMATION, ITS DIFFUSION AND THE DECAY OF THE ELECTRON TO GROUND STATE

Exciton travel in these polymers is portrayed as the exciton hopping along chromophore segments of 5–10 monomer units, generally moving down a "funnel" of segments of decreasing energy, eventually arriving at a low-energy segment which acts as an exciton trap and leads to emission.[6] As the polymer chain coils or bends back on itself, the conjugated segments may align, allowing transfer between noncontiguous chain segments; this has been referred to as interchain transfer, despite the segments being part of same chain. Polymer chains can also aggregate in solution and are adjacent in solid materials, again affecting the exciton migration and lifetime by allowing transfer between two chains. Interchain transfer has been shown to be faster than exciton travel down adjacent chain segments.[7]

Under certain circumstances, it is possible for an exciton to dissociate into free charge carriers. It is generally accepted that the dissociation of electron/hole pairs is induced, or at least strongly assisted, by an external electric field. It is demonstrated that electron/hole pair dissociation can also occur intrinsically. In these cases,

electron/hole pair dissociation is likely to be due to the presence of impurities such as oxidized sites and/or structural defects in the macromolecular system such as conformational kinks or chain twists. The existence of these sites and the capability of excitons to approach them are presumably prerequisites for dissociation. In this connection, it is notable that excitons are conjectured to diffuse over certain distances. It has been suggested that charge generation occurs preferentially at specially structured sites on the surface of the sample. This capability, used with appropriate arrangements, makes these materials suitable for photovoltaic applications.

In the earlier literature, charge carriers generated in polymers are frequently denoted as *polarons*. The definition of the term polaron, which can sometimes be elusive in older works, has been subject to alterations and many authors now denote the products of the dissociation of electron/hole pairs as negative and positive polarons. However, by doing so, the difficulty of precisely describing the chemical nature of the charge carriers is merely circumvented. As a matter of fact, the release of an electron should lead to a radical cation and the capture of an electron to a radical anion. The charge carrier generation is reversible, and the hole-electron (polarons) recombination, due to the same defects that origin the generation, can lead to both radiative and non-radiative decay. The first case is the source of electroluminescence generated with OLED and PLED (Organic/Polymeric Light Emitting Devices).[8] A perhaps counterintuitive result of charge separation is the development of a so-called mid-gap states. One way to think of the band gap is as an energy region where no orbitals are found. Structural and electronic defects, however, introduce orbitals into this region. For instance, examining the formation of a positive polaron, when we remove an electron from the pristine polymer, we simply have a hole in the top of the valence band. This leads to a geometrical change in the system. The radical ion delocalizes to make the polaron, and this relaxation of the structure stabilizes the system. What may not be immediately obvious is that this

relaxation leads to a singly occupied orbital lying in the band gap, isolated from the rest of the valence band.

The formation and fate of excitons are affected by the extent of polarization and conjugation of the polymer. Greater polarizability of the polymer increases the likelihood of free-carrier generation, which also reduces emission.[9] In summary a simplified sketch of the possible fates of an exciton are shown in Figure 4 .
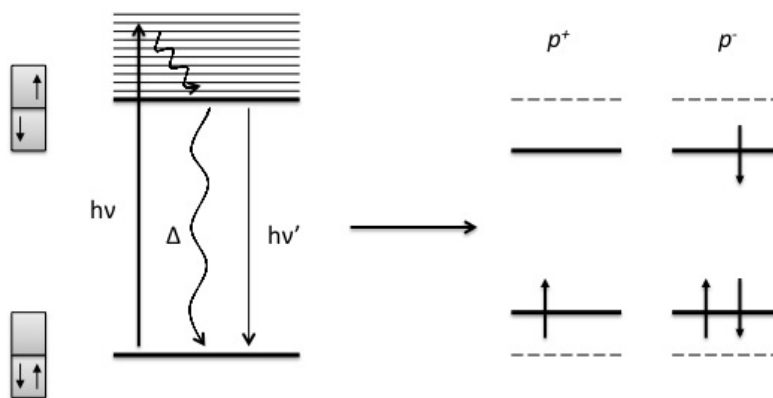
FIGURE 4: SIMPLIFIED DIAGRAM FOR THE POSSIBLE DECAYS OF THE EXCITON

1.1.1.3 Conformational and Optical Properties

Optical properties and dynamics of conjugated polymers are strongly influenced by chain conformation.[10] In fact these systems are characterized by an awkward interplay of π-system conjugation length and conformational disorder owing to the relatively low energy barrier for disruptive small angle rotations around σ-bonds along the backbone.[11] The breaks in conjugation can arise from chemical defects, configurational imperfections, and torsional disorder (which is dynamic).[12] Conformational disorder in the polymer backbone is of utmost importance as it directly dictates the electronic properties of the polymer by disrupting intrinsic π-system conjugation.[13] The distribution function of the different conjugation lengths approximately appears as a Gaussian curve.[14] In real cases, the length of a conjugated segment typically ranges from five to fifteen repeat units, and so the HOMO-LUMO

gap decreases with increasing conjugation length to an asymptotic value reached at ten subunits.

A further investigation of conjugated polymers starts from the idea that these materials should be considered as a distribution of strongly interacting chromophores, whose length is determined by breaks of conjugation. These interactions give rise to coupled collective states, whose comprehension is crucial to elucidate nature, properties, structure and dynamics of these systems. It is important to note that the disorder in conjugated polymers is dynamic: conjugation breaks depend on many factors and give raise to many possible structures. Each of these different structures constitutes a different chromophore, so for these systems chromophores are not a static entities and the size and nature of an *individual* chromophore are strongly influenced by many factors (*e.g.* solvent, temperature, concentration etc…).[15]

The typical absorption spectrum of conjugated polymers (Figure 5) presents a maximum in the visible region and appears as an inhomogeneous broad band originated from a series of vibronic sublevels and contributions from coupled quasi-localized chromophores arising from breaks in conjugation.[16]

As shown in Figure 5, most of conjugated polymers show (at least in solution) intense fluorescence or more generally photoluminescence. The analysis of these properties furnishes lots of information about excited states of these systems and it becomes very useful in comparison to absorption properties.

The asymmetry between absorption and fluorescence spectra arises from torsional disorder along the polymer backbone.[17] This is supported by the asymmetry observed in oligomers of similar structure.[18] As said, disorder in conjugated polymers is dynamic, at room temperature torsional motions weakening conjugation and changing the length of chromophores.
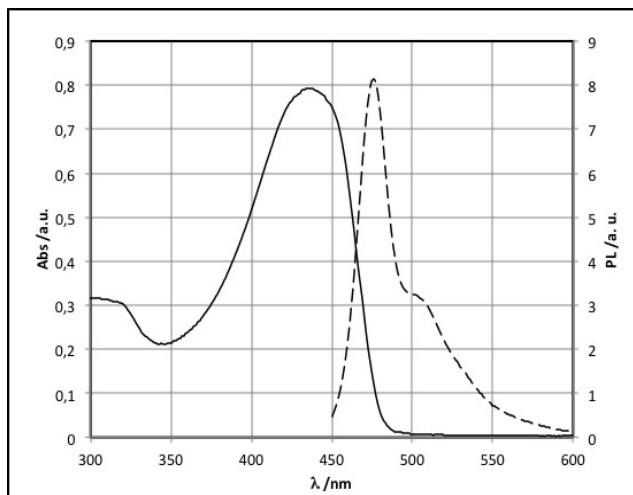
FIGURE 5: EXAMPLE OF ABSORPTION AND FLUORESCENCE SPECTRA (IN DILUTE SOLUTION) FOR A CONJUGATED ORGANIC POLYMER.

At low temperatures, when these torsional motions are frozen out, MEH-PPV, one of the most studied among these materials, indeed exhibits mirror-image symmetry between absorption and fluorescence. [19]

The Stokes' shift arises from the energy for the intramolecular geometry reorganization in going from the ground to the excited state. The planarization upon excitation has been shown theoretically by Tretiak *et al.*[19] The more planar structure of the excited state is also consistent with the sharper fluorescence spectra (as compared to absorption) because of a decrease in torsional disorder. [20]The *true* Stokes' shift is much smaller than the *apparent* Stokes' shift. The observed shift is larger because it reflects energy migration to the longest, red-most chromophores in the ensemble.

1.1.2   Supramolecular Organization of π-Conjugated Materials

π-Conjugated systems, especially when functionalized with various side chains, in order to enhance solubility, are compatible with solution-processing techniques. This peculiarity eliminates the need for expensive lithography and vacuum deposition

steps, which are mandatory for inorganic-based devices. Moreover, the possibility of room temperature solution processing expands the repertoire of tolerant substrates, and allows flexible plastics or fabrics to be used in conjunction with methods such as spin-coating, stamping, or inkjet printing. [21] The optoelectronic properties of conjugated materials in the solid state are quite different from those in solution and they are intimately related to the supramolecular organization of the molecules/polymer chains. The transport processes of electronic excitations and charge carriers are very strongly affected by the degree of order in thin films. On the other hand the efficiency of radiative decay (for LEDs) is governed by the spatial arrangement of the chromophores, which is, in turn, dependent on the nature of the intermolecular interactions. So, when producing thin polymer deposits from solution, it is therefore essential to control the degree of ordering, from the supramolecular scale to the mesoscale (few hundred nanometers to few micrometers).

For this reason, the control of supramolecular order and microscopic morphology is very intensively investigated; several reviews describe the aggregation processes of conjugated compounds from solution to solid state. [22]

Programmed self-assembly of π-conjugated oligomers and low molecular weight polymers has been achieved using supramolecular design rules. Supramolecular chemistry is the chemistry of molecular assemblies using non-covalent bonds.[23] While a covalent bond normally has a homolytic bond dissociation energy that ranges between 100 and 400 $kJ \cdot mol^{-1}$, non-covalent interactions are generally weaker and vary from less than 5 $kJ \cdot mol^{-1}$ for van der Waals forces, up to approximately 50 $kJ \cdot mol^{-1}$ for strong hydrogen bonds. (Table 1)[24]

Two important secondary interactions in the design of supramolecular materials are π − π stacking and hydrogen bond interactions. Logically, π − π stacking interactions often occurs in π-materials.

TABLE 1: STRENGTH OF SEVERAL NON COVALENT FORCES

Type of Interaction	Diss. En. / kJ·mol^{-1}
Covalent Bond	100 – 400
Coulombic Forces	250
Hydrogen Bond	10-70
Ion-Dipole	50 -200
Dipole-Dipole	5 – 50
Cation-π	5 - 80
π – π stacking	5 – 50
Van der Waals Forces	< 5

A simple model, which is entirely electrostatic, to predict the effects of π-stacking interactions was developed by Hunter and Sanders.[25] They assigned three point charges to the atoms in an aromatic molecule, one at the site of the atom (often a positively charged carbon atom) and one above and one below the plane of the π system (π point charges of -1/2 each) and maximize the interaction in function of the geometry.
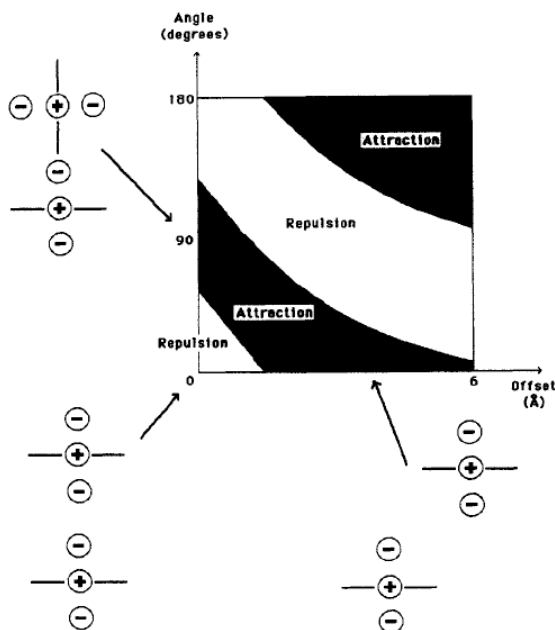
FIGURE 6[25] : INTERACTION BETWEEN TWO IDEALIZED π-ATOMS AS FUNTION OF ORIENTATION

Figure 6 illustrates, according to Hunter and Sanders model, the interaction between two idealized π-atoms as function of orientation highlighting two attractive geometries and the repulsive face to face geometry. The previous model is accompanied in some particular cases by the *Electron Donor-Acceptor Model.* It has been suggested that the strong attraction is due to an electronic interaction between an electron donor and an electron acceptor.[26] Charge-transfer complexes and $\pi - \pi^*$ complexes formed between good electron donors and good electron acceptors are well known and typically they are characterized either by charge-transfer transitions in the UV-visible absorption spectrum or by a broadened UV-visible spectrum.[27] Tipically donor/acceptor interactions and charge transfer phenomena require partners with different electronic properties; but with highly polarizable systems this interactions become achievable also homoaggregates.

Hydrogen bonds provides another ideal secondary interactions to build supramolecular architectures since they are highly selective and directional, and their strength in a macromolecular architecture depends largely on the solvent, number and relative position and geometry.[28] This high tunability makes hydrogen bonding very attractive in order to modulate and control the aggregation properties. Therefore hydrogen bonds have largely been used to position conjugated molecules in self-assembled architectures. Moreover by using hydrogen bonds is also possible to modify the entity, the efficiency and the geometry obtained with $\pi - \pi$ interactions only. [22a]

1.1.2.1 *Solvent and Temperature Dependence*

Solvent and temperature are factors well know to play an important rule on aggregation properties and behavior of conjugated systems. In a poor solvent or at low temperature chain planarization and concomitant interchain $\pi - \pi$ stacking interactions take place, generating an increase of the conjugation length.[29] As a result, a bathochromic shift in the UV-Vis absorption spectra and the appearance of vibronic fine structures are generally observed. Solution self-assembled aggregates, in function

of different solvent conditions, often constitute a reasonable and more easily accessible model to explore solid-state interactions occurring in these systems. The original studies on organization processes of polythiophenes in solution attributed the spectral changes either to the existence of two distinct phases, disordered polymers and ordered polymers in the form of microcrystalline aggregate[30] or to intramolecular conformational transitions. [31] McCullough, Yamamoto, and Leclerc [32] extensively studied the self-organization of poly(3-alkylthiophene)s in solution and in the solid state, exploring the effect of temperature, regioregularity, and solvent by means of spectroscopy and light-scattering techniques. Similar studies on polymer chain aggregation of 2-(2-etylhexyloxy)-5-methoxy-*p*-polyphenylene-vinylene (MEH-PPV) and poly(*p*-phenyleneethynylene)s (PPEs) have been reviewed by Schwartz and Bunz [33] respectively. A high number of substituents is found to prevent π-stacking between polymeric chains. When the concentration of the side chains is reduced, an increase of the planarity of the polymeric chain will result in stronger π-stacking, leading to lamellar arrangements. These solution properties were compared to the optical properties of the same polymers in thin films. The aggregates formed in a non-solvent are often comparable to those found in the solid state, although the ordering in the solid state can be smaller.

1.1.2.2   Effects of Aggregation on Photophysical Properties

Numerous theoretical[34] and experimental[35] research papers have revealed how intermolecular interactions have a large impact on the optoelectronic properties of conjugated polymers. More specifically in the case of photoluminescence, a number of experimental studies have highlighted the influence of interchain interactions when going from dilute solutions to the solid state.[36] Interactions may occur both in ground and excited state. By definition, a dimer obtained from the interaction between a molecule in excited state and another one in its ground state is called an excimer. Because of its nature, an excimer is not directly excitable. On the other hand, a ground-state aggregate can be supposed as a dimer of aggregated molecules in

their ground state. This aggregation give rise to a new chromophore that is directly excitable. The understanding of the ground-state aggregation, in the case of small molecules, has been well established. The interactions between two generic chromophores can be explained by considering energetically delocalized states. Let's define E_{exc} and E_{gr} as the unperturbed energy levels of an isolated molecule in dilute solution and ΔE_m its relative energy gap. When two or more of these molecules are brought close together, the transition dipoles interact and multiple excitation energy levels are observed. The splitting of energy levels is named as *Davydov splitting*. For a simple dimer, the energy gap ΔE_d between the ground state and the two excited states is given by Eq. 5:

$$\Delta E_d = \Delta E_m + D \pm \varepsilon$$

EQ. 5

where, ε is the exciton interaction energy (half of the Davydov splitting) and D is a dispersion energy term, given by the difference between w' and w in Figure 7; this depends on many factors: intermolecular interactions, solvent etc..., and it is generally referred to it as gas-to-crystal shift. Eq. 5 shows that for a dimer the excited energy state has two possible levels. These descend from the phase relationship between the relative transition dipole moments.
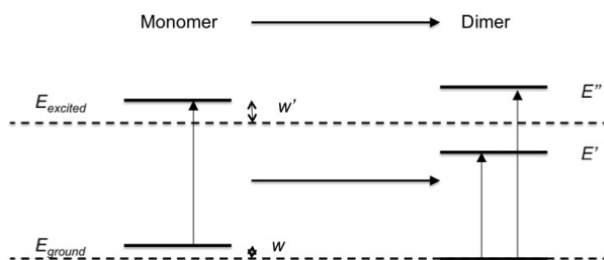
FIGURE 7 : DIAGRAM OF DAVYDOV SPLITTING FOR THE FORMATION OF A DIMER

If the dipole moments of the two molecules are parallel (H-aggregates), as shown in Figure 8 (left), the lower energy state E' for the dimer resulting from

excitonic splitting has a zero net transition moment, making this transition forbidden. Only transitions to the higher energy state E'' are allowed, leading to a hypsochromic or blue shift. If the transition dipoles are in-line rather than parallel, the transition to the higher energy state is forbidden and a bathochromic or red shift is observed. Higher aggregates of this type exhibit a large bathochromic shift, with an intense, narrow absorption; these are termed J-aggregates (Figure 8, right).[35]
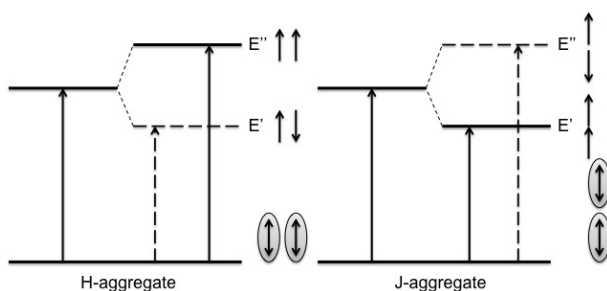
FIGURE 8 : CONSEQUENCES OF MUTUAL ORIENTATION OF TRANSITION: H AND J AGGREGATES.

However, in the case of conjugated polymers, the ambiguity in defining chromophores, the amorphous character, and the large molecular weight have made it very difficult for a systematic investigation. Moreover perfect *parallel* and *in-line* architectures are the two extreme forms of molecular aggregation and the transition dipoles can be mutually oriented at some angle to each other (usually small), resulting in more complex spectral changes.

Even though the detailed identity of interchain aggregate species is controversial, a generally accepted understanding is that interchain aggregation produces lower-energy sites where singlet excitons efficiently migrate to emit red-shifted light. This phenomenon has been mostly attributed to the formation a ground-state aggregate based on strong intermolecular interactions. The evident effect due to formation of a ground-state aggregate is the presence of a directly excitable red-shifted absorption band. This fact has been used to discriminate the presence of a ground-state aggregation in conjugated polymer films. However, in 2000 Bunz and

coworkers suggested that the additional absorption band observed in the PPE films that is absent in solution is not due to the ground-state aggregation but to the planarization of PPE backbones induced by aggregations.[37] Their claim is based on the fact that planarization is a necessary condition for the formation of a ground-state aggregate. As discussed in a previous section, planarization of a conjugated polymer backbone maximizes the effective conjugation length by enhancing π-orbital overlap. Experimentally and computationally, it was clearly shown that planarization of PPEs indeed produced a red-shifted absorption band. However, it was also demonstrated that co-present ground-state aggregation could induce the red-shift even further. Moreover, the presence of the red-shifted absorption band can be manipulated by changing the side-chain of PPEs that determines the interpolymer spacing in the ordered structures.[35] In addition, detailed photophysical studies of the solid solutions of PPE/PMMA showed the appearance and increase of a red-shifted absorption band as the average interpolymer distance is reduced. These results strongly indicated that intermolecular aggregation is responsible for the red-shifted additional absorption band.[35] Moreover, the role of aggregation in producing a red-shifted absorption band was evidently supported by photophysical studies of 1,4-diethynyl-2-fluorobenzene. This small molecule analogous of PPE is the simplest aryl-ethynyl compound free from the planarization effect.[38] In any case, too strong intermolecular interactions affect the emission properties of conjugated polymers. To prevent the self-quenching due to the strong intermolecular interactions, several effective methods have been devised. Bulky side-groups were introduced[39] and a dendrimer approach is also promising because the highly branched structure likely prevents close cofacial intermolecular aggregation.[40] Interesting results in preventing cofacial aggregation and preserving the photoluminescence properties of PPE were achieved by introducing a twist in the supramolecular scaffold driven by the presence of a chiral pendant on the side chains. This particular case constitutes the *leitmotif* at the basis of the work presented in this thesis and can represent a really tunable and easily achievable way to control the supramolecular textures of these systems in aggregation conditions.

1.1.3 Synthetic Approaches

The need to obtain materials with well defined structural properties together with the desired absorption and emission wavelength, high efficiency and good stability, presented, and still presents, a really fascinating challenge to synthetic chemists. In particular the control of the emission color, of the charge-accepting and transporting properties, which are important for optimizing device efficiency, and of electrical and optical stability must be addressed.

In this section is presented a brief overview of the main synthetic methods by which the two classes of conjugated polymers we treated in this thesis, poly-(phenylene-vinylene)s (PPVs) and poly-(phenylene-ethynylene)s (PPEs), can be prepared. A bit of emphasis will be placed on how synthetic design can contribute to the meeting of the above-mentioned device performance. A short view will be given also on the effects the substituents on the aromatic ring have on the macrosopical properties of synthesized materials.

1.1.3.1 Poly-p(phenylene-vinylene)s

Poly-(phenylene-vinylene)s (PPVs) represent the most widely studied group of electroluminescent polymers. The parent compound poly(p-phenylene-vinylene) is insoluble and so must be processed as a precursor polymer, but derivatives with solubilizing alkyl, aryl, silyl, or alkoxy chains show good solubility in organic solvents and so can be readily processed by techniques such as spin casting. There are four main routes to the synthesis of PPVs:

- polymerizations via quinodimethane intermediates,
- polycondensations,
- transition-metal-mediated couplings,
- metathesis polymerizations.

Other methods such as chemical vapor deposition and electropolymerization have also been used on occasion but generally give poorer quality polymers.

Quinodimethane polymerization is the most widely used way to obtain PPVs. The first to be developed was the Wessling–Zimmerman route. (Scheme 1)
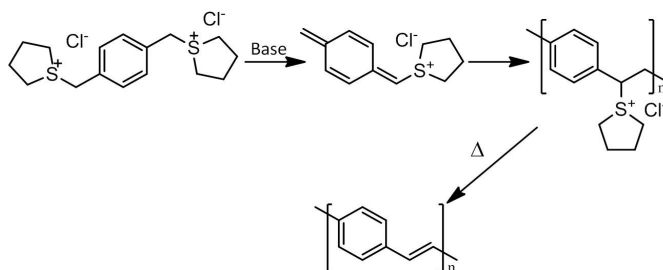
SCHEME 1 : WESSLING-ZIMMERMAN ROUTE FOR THE SYNTHESIS OF PPV

The starting material is a p-xylenyl(bis(sulfonium salt)), which on treatment with 1 equivalent of base generates a quinodimethane that evolves to produce the sulfonium precursor polymer. This is soluble and can be used to make thin films that are thermally converted to the final films of PPV by heating at 220–250 °C under vacuum. By far the most popular method for making PPVs is the Gilch synthesis [41], illustrated in Scheme 2 for the synthesis of MEH-PPV .
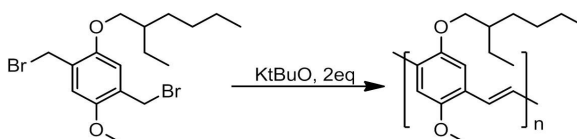
SCHEME 2 : GILCH ROUTE FOR THE SYNTHESIS OF PPVs

Here a dihalomethyl monomer is converted directly to the PPV by means of an excess of base. If only 1 equivalent of base is used a halo-precursor polymer can be obtained that is then convertible to the conjugated material by treatment with base or by thermal elimination in vacuum. Since the molecular weight of materials in Gilch syntheses can be controlled by addition of benzyl bromide as a chain stopper, [42] or of

4-methoxyphenol,[43] a known anionic initiator, an anionic mechanism has been proposed, but most recent studies [44] suggest that, as for the Wessling synthesis, the primary mechanism is a radical pathway, with only low molecular weight materials arising from anionic routes.

There are two major limitations to the quinodimethane-based polymerization methods for making PPVs. First, they do not work for all aromatic systems.[45] A second problem is that the formation of defects that lower the emission efficiency is intrinsic in the polymerization process due to non-regular coupling of the quinodimethane intermediates.[46]

PPVs via Polycondesation were prepared both via Wittig and Horner reaction of arylbisaldehydes with, respectively, aryl bisphosphonium salts and bisphosphonates. One advantage of these methods is the possibility to obtain alternating copolymers. The polymers so obtained are generally of much lower molecular weight than the materials obtained from the Gilch route, but lack the ethane and ethyne defects discussed above and so may show better optical properties. Comparative studies have shown the Horner condensation to be the superior method as it produces relatively higher molecular weight materials with virtually all the double bonds being *trans*, whereas the Wittig condensation results in a high proportion of *cis*-vinylene units, so that the latter material has poorer optical properties.[47] Hörhold and coworker [48] have used a Horner polycondensation route to prepare MEH-PPV (Scheme 3) that is much more soluble than the material obtained by the Gilch route, due to its lower molar mass, but whose electroluminescence and photoluminescence properties match those of the higher mass polymer.
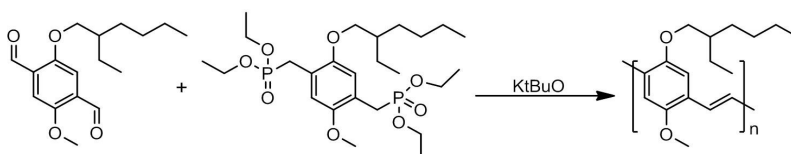
SCHEME 3 : MEH-PPV THROUGH HORNER POLYCONDENSATION REACTION

Transition Metal Mediated Metods are mostly based on Heck and Stille coupling reactions. Heck coupling of a dihaloarene with a divinylarene offers a direct route to PPVs, either homopolymers or alternating copolymers. As with the condensation method discussed above, the molecular weights are generally lower than those obtained by the Gilch route, but the materials are relatively defect-free. Stille coupling of haloarenes with bisstannyl ethene has also been used to make PPVs. Swager and coworkers [49] used it to prepare PPyV in both regiorandom and regioregular forms as depicted in Scheme 4. Stille coupling was also used to obtain a huge series of PPVs derivatives showing a really high versatility of this method. [50] The polymers obtained this way generally have low molecular weight and can be considered completely defect-free.
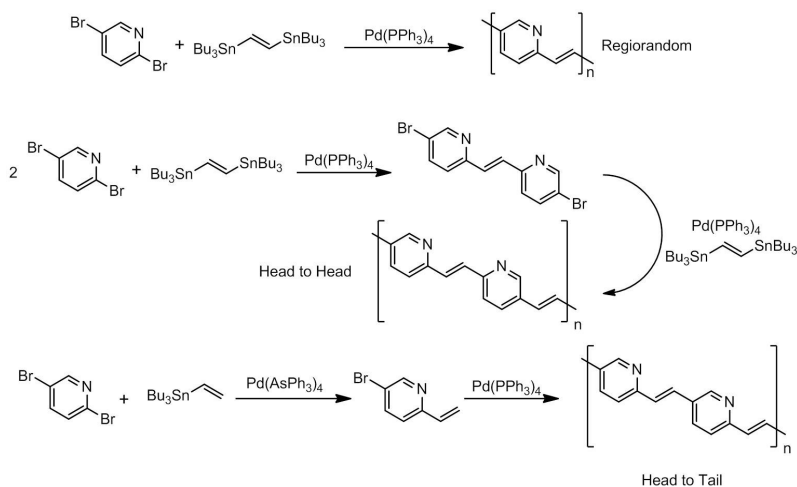
SCHEME 4 : SYNTHESIS OF REGIORANDOM AND REGIOREGULAR PPyV EMPLOYNG STILLE AND HECK COUPLING REACTIONS

The Suzuki reaction provides another useful tool for the synthesis of PPVs. Several PPVs were prepared by Koch and Heitz from *trans*-1,2-dibromoethylene and different *p*-aryldiboronic acids (Scheme 5 - I).[51] Moreover, Suzuki coupling has been employed more extensively for the preparation of modified PPV derivatives such as poly(terphenylenevinylene)s and poly(fluorenevinylene-co-phenylenevinylene)s (Scheme 5 – II, III).[52]
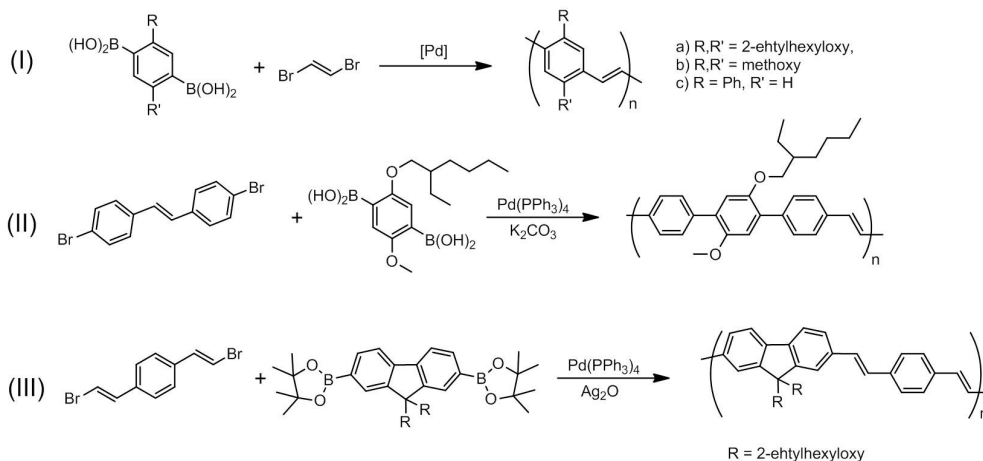
**SCHEME 5: EXAMPLES OF SUZUKI COUPLING REACTION FOR THE PREPARATION OF PPVs,
POLY(TERPHENYLENEVINYLENE)S - POLY(FLUORENEVINYLENE-CO-PHENYLENEVINYLENE)S**

Two types of **Methathesis Polymerization** have been used to make PPVs:

- transition-metal-mediated metathesis of divinylbenzenes to make alkyl- and alkoxy-substituted PPVs, but the products are primarily oligomers.[53]

- Ring-opening metathesis polymerization (ROMP) has been used to make precursor polymers to PPVs for the synthesis of poly (naphthalene vinylene)s.[54]

The advantage of ROMP is that it is a living polymerization method, which permits very precise control of the molecular weight of the polymer and is also applicable to the synthesis of block copolymers. The disadvantages are that the monomers required may be difficult to prepare, and it cannot be used for a direct synthesis of PPVs.

1.1.3.2 Poly-p(phenylene-ethynylene)s

Poly(phenylene-ethynylene)s (PPEs) are more rigid than PPVs and show a greater tendency towards aggregation, which produces marked red-shifts in their solid-state luminescence. They have been less utilized in LEDs than PPVs, largely due

to the lack of good-quality polymers. Two routes have been used to prepare them: Cassar-Heck-Sonogashira coupling and alkyne metathesis (Scheme 6).
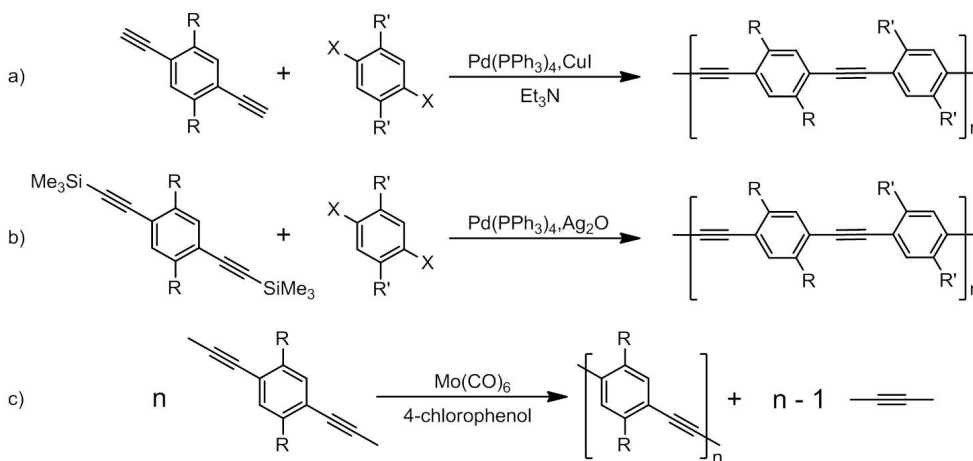
SCHEME 6: ROUTES FOR THE PREPARATION OF PPEs

The former involves the polycoupling of an aryldiyne with either bromo or iodoarenes, the latter being much more reactive. The advantages of this method are the wide range of substrates it is applicable to, and the ability to make alternating copolymers. Disadvantages are the need for exact stoichiometry, the presence of potentially fluorescence-quenching halogens as endgroups, and the formation of diyne defects due to alkyne homocoupling.

This latter problem can be solved by preventing the oxidation of Pd(0) active species or by using the trimethylsilylated diyne with iodoarenes in presence of silver oxide (Scheme 6-b). This cross-coupling process has been reported to afford polymers with a lower amount of defects, deriving from oxidative homocoupling reactions, compared to the classic Cassar-Heck-Sonogashira methodology, and it has already been successfully used for the synthesis of various PPEs.[55]

The metathesis procedure (Scheme 6 - c) has been developed by Bunz[56] and has the advantage of producing materials with well-defined endgroups. The

disadvantages of this method include the greater experimental difficulty, to the more limited scope (it is not applicable to all alkynes), and that it is useful only for homopolymers or statistical copolymers.

1.2 Chiroptical Techniques

Circular dichroism (CD) is defined as the differential absorption of left- and right-circularly polarized electromagnetic radiation by a sample. In particular, electronic CD (ECD, often shortened itself as CD) occurs in correspondence with electronic transitions and represents the chiroptical counterpart of the more common UV-vis absorption spectroscopy. Similarly, vibrational CD (VCD) has its counterpart in infrared spectroscopy and moving to emission techniques Raman optical activity (ROA) and circularly polarized luminescence (CPL), can be considered the chiroptical relatives of Raman and fluorescence spectroscopies.

1.2.1 Circular Dichroism: General Overview

1.2.1.1 Phenomenological and Theoretical Aspects

As said Circular Dichroism descends from the difference in the interaction between left and right circularly polarized light with a sample. The nature of this phenomenon can be described as a *diasteromeric* interaction between circularly polarized light and a chiral non-racemic sample. If we define A^l and A^r as the absorptions of left and right circularly polarized light, CD can be expressed as:

$$CD = A^l - A^r$$

EQ. 6

This quantity is usually measured in *mdeg* units. To define a molar quantity $\Delta\varepsilon$, expressed in the same units [$M^{-1}cm^{-1}$] of molar extinction coefficient ε, we use an analogous of Lambert and Beer's expression. (Eq. 7)

$$\Delta\varepsilon = \varepsilon^l - \varepsilon^r = \frac{CD}{33000 \cdot c \cdot b}$$

EQ. 7

This quantity is independent of concentration c (*mol/l*) or path length b (*cm*). Non-negligible CD signals (also called Cotton effects) can be measured only in correspondence to absorption bands, i.e., when resonance occurs in light/matter interaction and this usually involves either electronic or vibrational transitions. The ratio between CD and absorption intensity is called *dissymmetry factor g*: (Eq. 8)

$$g = \frac{\Delta\varepsilon}{\varepsilon} = \frac{CD}{A}$$

EQ. 8

This is a pure number and it's specific for the system (in given solvent/solid state and temperature conditions). It can be positive or negative depending on whether ε^l is greater or smaller than ε^r, and in fact the CD spectra of two enantiomers are the mirror image (with respect to the *x*-axis) of each other. When this interaction involves electronic transitions we talk about Electronic Circular Dichroism (ECD). On the most common applications, ECD is connected with relatively low-lying excited states, as found in unsaturated (or even conjugated) organic chromophores (Figure 9) or in the mixed orbitals of transition metal ions.
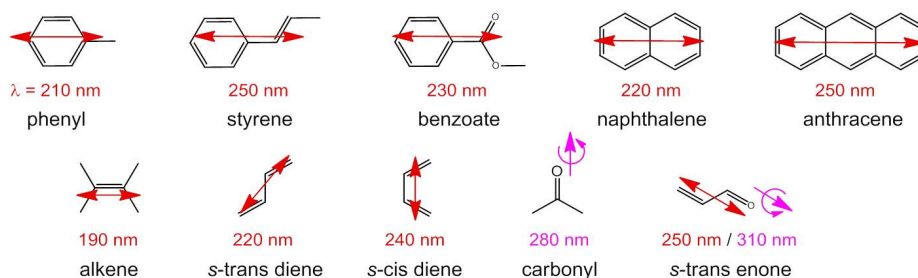
FIGURE 9: A FEW SIMPLE COMMON ORGANIC CHROMOFORES WITH THEIR MAIN UV TRANSITIONS SHOWING ELECTRIC TRANSITION MOMENTS IN RED AND MAGNETIC IN PURPLE.

For electronic transitions it's possible to observe absorption only when the corresponding electronic transition is characterized by a non-vanishing electric transition dipole. This transition is associated to a non-negligible CD only if it is allied to an overall roto-translation of the electronic charge, along a helical path. This brings about a magnetic transition dipole. non-orthogonal to the electric dipole. In fact, CD is related to the quantum-mechanical quantity called *rotational strength*, defined as the product between the electric and magnetic transition moments allied to an electronic transition from the ground state to an excited one *i:*

$$R_{0i} = \mu_{0i} \cdot m_{0i}$$

EQ. 9

Symmetry restrictions imply that *R* may be non-negligible only for molecules belonging to symmetry groups devoid of roto-reflection elements, i.e., of inversion centers and symmetry planes. Therefore, only *chiral* systems may exhibit CD. The integral of a CD band allied with a single electronic transition is related to the rotational strength through the relation in Eq. 10

$$R_i = C \int_v \frac{\Delta \varepsilon_i(v)}{v} dv$$

EQ. 10

where *C* is a numerical constant equal to $2.296 \cdot 10^{-39}$ in cgs units. Conversely, a CD spectrum may be thought to amount to a sum of Gaussian bands with intensity proportional to the rotational strength defined at the discrete frequencies corresponding to the 0→*i* electronic transitions:

$$\Delta \varepsilon(v) = \frac{1}{\sqrt{\pi} C} \sum_i \Gamma_i v_i R_i$$

EQ. 11

where Γ_i is the appropriate Gaussian band-shape function centered at ν_i

1.2.1.2 Exciton Coupling : Shape and Information of ECD spectra

For a better comprehension of the processes giving rise to CD we can hint at some relevant aspects by a simple model, which accounts for only one (although important) of the possible situations and provides the best description possible for the case of conjugated polymers: the so-called *exciton coupling*. We start considering an isolated achiral chromophore: it gives rise to absorption, corresponding to the formation of an oscillating transition electric dipole moment. When an electromagnetic radiation meets the oscillator, it is absorbed only if its frequency matches the oscillator's. In this case left and right circularly polarized light behave exactly the same. Let's introduce a second oscillator in the close neighborhood of the first one. They couple to each other because of through-space dipolar interaction. For the sake of simplicity, let's suppose that the two oscillators share the same resonance frequencies (degenerate coupling). If they oscillate in-phase, charges of the same sign are brought near to each other, leading to an unfavorable, high-energy coupling mode; in-antiphase they avoid close contact (as one approaches, the other one goes away), leading to a low energy mode.[57] In-phase mode leads to a higher resonance frequency than in antiphase-coupled oscillation. This reasoning can be extended to different chromophores (non-degenerate coupling) and the strength of the coupling decreases with increasing difference in resonance frequencies.
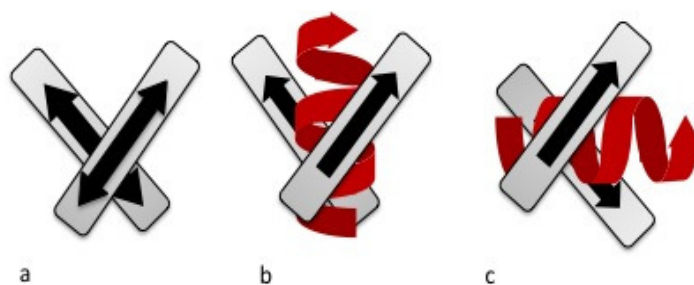
FIGURE 10 A) COUPLED OSCILLATORS, B) IN-PHASE, HIGH ENERGY COUPLING, RIGHT HANDED HELIX C) ANTIPHASE LOW ENERGY COUPLING, LEFT HANDED HELIX.

The two coupling modes for a skew arrangement of the two oscillators (chromophores) define helical paths of opposite signs, as shown Figure 10: for a given chiral arrangement of the two oscillators we notice that one defines a right-handed screw sense, the other a left-handed one. It won't be surprising that the interaction between left and right circularly polarized light with such chiral systems will be different. Indeed, it has been shown that a positive screw sense will be associated with a positive circular dichroism, while a negative screw leads to negative CD. Therefore, the CD spectrum of skewed coupled oscillators will consist of two bands with different maximum wavelengths and opposite sign, namely, a *CD couplet.* (Figure 11)
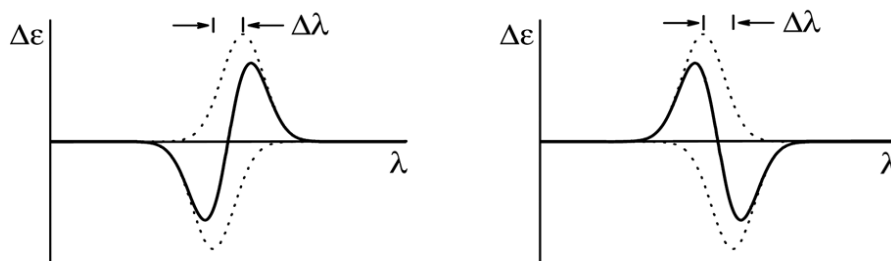
FIGURE 11: POSITIVE CD COUPLET ON THE LEFT AND NEGATIVE CD COUPLET ON THE RIGHT

The exciton-coupled CD spectrum is determined by the reciprocal arrangement of the two coupling dipoles. The sign of a couplet is defined as the sign of its long-wavelength component (positive: Figure 11 on the left, negative: Figure 11 on the right) and it may be inferred watching the two dipoles along the line corresponding to their distance vector. If the dipole in the front can be brought onto that in the back by means of a clock-wise rotation, they define a positive chirality. Similarly, an anti-clockwise rotation defines a negative chirality as in Figure 10. The exciton chirality rule states that a positive chirality corresponds to a positive exciton couplet, and *viceversa*. It's very important to observe that the coupling (especially degenerate) as described in section 1.1.2.2 (either considering the H and J aggregate or not) leads to a split band (one component for each coupling mode), which in some particular cases

can be observed also in absorption spectrum but which is systematically detectable with circular dichroism (on condition that a skewness is originated by the involved dipoles).

1.3 Chirality – Conjugated Materials: a Charming Marriage

In 1967 Ciardelli *et al.* prepared the first chiral poly-acetylene derivative by carrying out the polymerization of (S)-4-methyl-1-hexyne in presence of Fe(acac)$_3$/Al(i-C$_4$H$_9$) as catalyst. [58] However, compared to the extensive work made in conjugate polymers field and despite the history of the control of chirality in polymers, the research on conjugated chiral derivatives seems to be still embryonic.

As demonstrated in previous sections the electronic and optoelectronic properties of conjugated polymers (CPs) can be modified and tuned by controlling the conformation, arrangement, and alignment of the main chains. This control means that not only the primary structure but also the higher-order structures of CPs are indispensable factors to be accounted for in achieving advanced optoelectronic properties and functions. Moreover self-assembly is one of the most reliable ways to construct higher-order and even super-hierarchical structures in CPs. The forces driving self-assembly processes are discussed above in section 1.1.2. It is clear in this context how the capability to easily modify, control and characterize these superstructures is of outstanding importance. A possible answer to all these requests could be given by chirality. In fact the introduction of a chiral modifier along the backbone of the polymer may be used to tune the efficiency of π overlaps through a directional, opportune and specific interactions Moreover the added chiral dopant can introduce a particular geometric distortion in the supramolecular aggregates that is easily detectable using chiroptical spectroscopic techniques, which make access to a range of structural information otherwise hidden or not observable with common techniques. Moreover chiral supramolecular architectures may provide materials with new particular applications such as circularly polarized emitters, phototransistors

switchable only with the appropriate circularly polarized light, and sensors capable to discriminate enantiomers.

1.3.1   Chirality Introduction and Expression

The introduction of chirality in supramolecular conjugated systems has been achieved following two principal approaches. The first way is based in the introduction of well defined chiral moieties (such as binaphtol derivatives) directly into the backbone of the polymers.[59] This approach generates a completely different class of materials with new intrinsic and specific properties. An example of derivative obtained this way is shown in Figure 12.
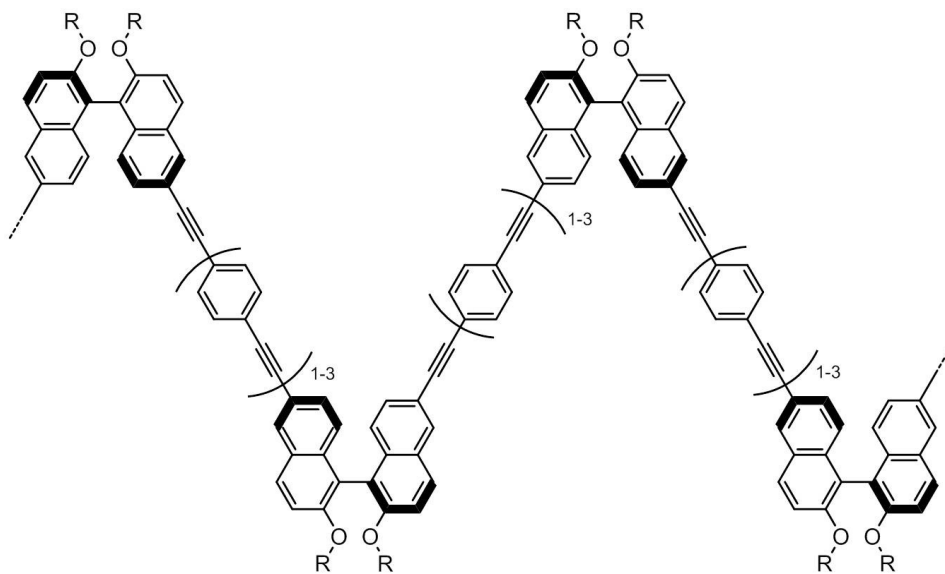
FIGURE 12

As conjugated polymers typically contain solubilizing alkyl groups, the most straightforward way to introduce chirality is to attach chiral substituents to generate chiral homopolymers. In this way, a plethora of conjugated polymers, with different backbones and substituents, has been prepared and their (chiral) properties have been investigated. Alternatively, a chiral functionalized monomer can be reacted with an achiral functionalized monomer in a polycondensations reaction, resulting in

alternating copolymers. However, according to their molecular structure, they can be regarded as homopolymers, comprised of AB repeating units. As a consequence, both approaches result in "one component systems". Moreover chiral and achiral units can be randomly distributed along the polymer chain. However in this work we shall focus only on the second type of materials, and further we'll discuss the implication of such chirality introduction.

The introduced chirality in polymer molecules can be expressed principally through two ways: either strong intrachain interactions are present and so the molecule adopts a chiral conformation itself, for instance a one-handed helix, or interchain interactions are preferred and many molecules, which typically adopt a planar, achiral conformation, stack in a chiral (one-handed helical) way. Examples of conjugated polymers that can adopt a helical conformation are poly(3,6-carbazole)s, [60] oxazoline-functionalized poly(thiophene)s, [61] poly-(3,6-polyphenanthrene)s. [62] If chiral side-chains are implanted, one helical sense can be discriminated and will prevail.

However, most conjugated polymers show a clear tendency to aggregate. Typically, the polymers adopt a more planar conformation and π-interactions promote stacking of the polymer chains. If the polymers are substituted with chiral side-chains, the asymmetric branching may result in a nonparallel orientation of the stacked polymer chains. The use of enantiomerically pure chiral substituents can again result in a preferred helical sense. (Figure 13) A typical example of such polymers is chirally substituted regioregular head-to-tail coupled poly–(3-alkythiophene)s. [63] In a good solvent, the polymer adopts a random-coil conformation, in which chirality is not expressed. In poor solvents or films, however, the polymer chains planarize and stack; strong Cotton effects become visible, reflecting the (supramolecular) chirality.
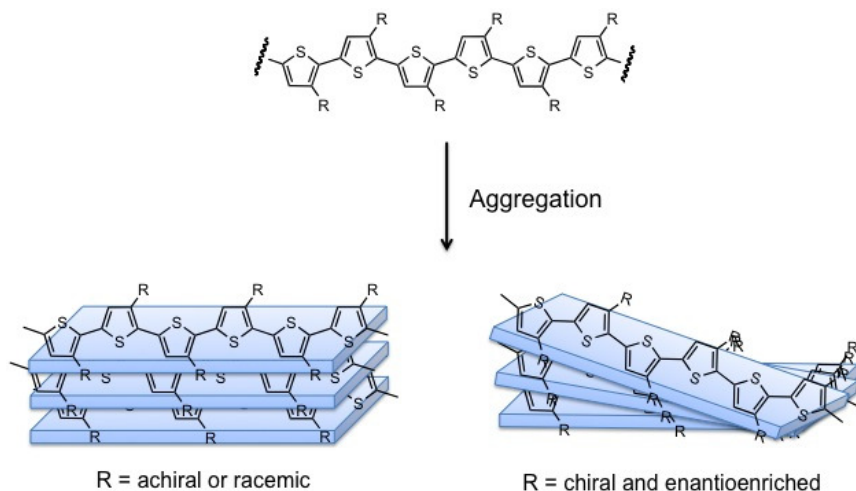
FIGURE 13

1.3.1.1   Intrachain Helicity

The formation of helical structure due to strong intrachain interactions is subjected to the presence two factors: the first geometrical and the second energetic. In fact, *condicio sine qua non* for helix formation is the capability of the polymer backbone to wrap on itself, and this is possible only in presence of overall bond angles between two monomers less than 180 degrees. Not surprisingly this class of compounds is characterized by the presence of *cis* double bonds, five-membered rings, and *ortho* and *meta* functionalized phenylenes. Moreover, most attempts to create synthetic polymers with helical structures have involved the introduction of hydrogen-bonded moieties into the main chains. Moore *et al.* demonstrated that the conjugated backbone of oligo-(*meta*-phenylene-ethynylene) (OmPE) derivatives spontaneously acquires a stable helical conformation that is stabilized only by solvophobic π – π interactions.[64] Introducing polar tri(ethylene glycol) groups into the side chains of the aromatic backbone OmPE forms conformationally well-defined helices in acetonitrile, which is a poor solvent for the conjugated backbone. This helical conformation changes to disordered random coils upon increasing the temperature or decreasing the polarity of the solvent. This change in conformation indicates that solvophobic effects are the driving force for the formation of a helical

conformation. In addition, it was demonstrated that with a longer conjugated backbone (n > 8), a stable helical conformation can be achieved. These results provide significant knowledge about the formation of intrachain helicity in CPs. Thus, it is only essential to use the solvophobic and $\pi - \pi$ interactions, as well as the sufficient length of the conjugated backbone, for forming the intrachain helical conformation of the OmPE derivative, but it is not necessary to consider selective and directionally specific interactions, such as hydrogen bonds. After the above-mentioned study, Schanze *et al.* synthesised a poly-(*meta*-phenylene ethynylene) (PmPE) derivative with L-alanine sodium salt groups into the side chains.[65](Figure 14 - a)
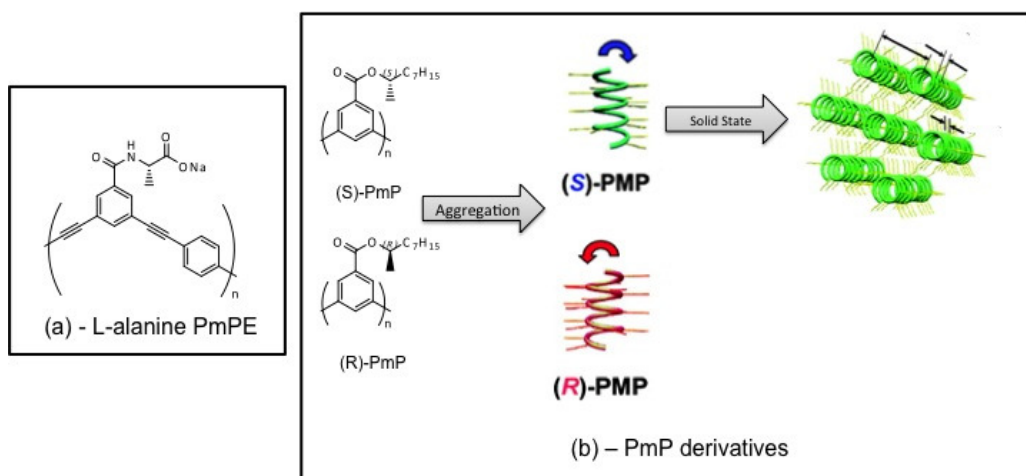
FIGURE 14: (a) L-ALANINE FUNCTIONALIZED PmPE DERIVATIVE PREPARED BY SCHANZE *et al*. (b) PmP DERIVATIVES PREPARED BY AKAGI AND SUDA

This system adopts random-coil conformation in methanol (a good solvent) and a helical conformation in water. A Van't Hoff plot indicated that helix formation was favoured by enthalpy due to $\pi - \pi$ interactions in the helix but disfavoured by entropy due to the loss of conformational freedom accompanying the helical transition. The chirality of side chains induces a symmetry selection leading to the formation of a left-handed helix in polar mixed solvent of water–methanol. In this case the intrachain helical structure is stabilized not only by solvophobic $\pi - \pi$ interactions but also by intramolecular hydrogen bonds between the proximal amide units of the helix. Akagi

and Suda reported that a poly-(*meta*-phenylene) (PmP) derivative, modified with chiral alkyl side chains, forms a one-handed helical structure.[66] Helical conformation is shown even in a good solvent, such as chloroform, without forming intramolecular hydrogen-bonding interactions. This behavior is due to the rigid main chain structure, which prevents the transition to a random-coil conformation, even in a good solvent. X-ray diffraction analysis showed the presence of whisker of self assembled polymers in an annealed film. Such whisker are composed by hexagonal columnar packed structure in turn consisting of intrachain one-handed helices.(Figure 14 -b)

1.3.1.2   Interchain Helicity

Polythiophene Derivatives. A pioneering study on the origin and the effects of the interchain helicity in CPs aggregates was conducted by Meijer *et al.*[67] They investigated a chiral polythiophene (PT) derivative (Scheme 7 a,b) characterized by a perfect head-to-tail (HT) alternation. This study was inspired from the work made by Lemaire and co-workers in 1988.[68] They synthesized the first chiral polythiophene (Scheme 7 a,b) *via* the electrochemical polymerization of the corresponding monomers in nitrobenzene. Macromolecular chirality was induced by the presence of enantiomeric (S)- and (R)-2-methyl butyl groups on the thiophene ring, from which they were separated by a propyloxy spacer to decrease steric hindrance in the polymerization. Unfortunately, however, the non-regiospecificity of this polymer made the supramolecular characterization very difficult, and resulted in an intrinsically inhomogeneous system. Regioregularity was than achieved by using a synthetic route developed by McCullough *et al* [69] which furnishes a consecutive HT couplings > 98%. Spectroscopic measurements on head-to-tail derivative indicated that it exists in a chiral aggregated state with a highly ordered structure at low temperature or in a poor solvent. This implied the formation of an interchain helical structure driven by both solvophobic and intermolecular $\pi - \pi$ interaction. Its CD spectrum exhibited a strong bisignate Cotton effect (exciton couplet) with a large dissymmetry factor, resulting from exciton coupling among the PT conjugated

backbones, which indicates the formation of helical aggregates through interchain interactions.
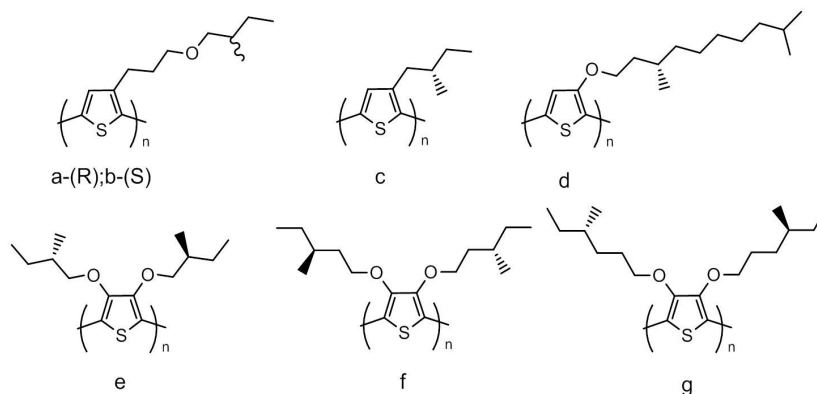
SCHEME 7: EXAMPLES OF SOME PREPARED AND STUDIED CHIRAL PT DERIVATIVES

Interestingly, studies have revealed a non-linear relationship between the *g value* and the optical purity of the chiral substituent,[70] a phenomenon referred as "majority rule effect". The above synthetic route and its modifications have been used to synthesize several PT chiral derivatives (Scheme 7). Strong optical activity was also reported by Meijer and co-workers [71] for the related regioregular polythiophene in Scheme 7-c (bearing a short (S)-2-methylbutyl substituent).

Regioregular chiral poly(3-alkoxythiophenes) such as in Scheme 7-d (R = 3,7-dimethyloctyloxy) have also been recently prepared by Koeckelberghs and coworkers.[72] The CD spectrum of a spun-cast film from the last compound exhibited a large bisignate Cotton effect associated with the $\pi - \pi^*$ absorption band. Reynolds and co-workers [73] have similarly used a modified "MacCullogh route" to prepare systems in Scheme 7-e,f,g bearing two chiral groups in position 3 and 4. These branched PTs again exhibit very strong optical activity. The highest one was reported for the bulkier Scheme 7-g with a chiral anisotropy factor $g = 1.8 \cdot 10^{-2}$ in xylene/DMF solution, and even higher ($g = 2.9 \cdot 10^{-2}$) when spray-coated from toluene.

PPV Derivatives. The same approach described above was used on almost every class of conjugated polymers, such as polyfluorenes, PPVs and PPEs; and the introduction of chiral pendants, in order to promote the formation of chiral supramolecular aggregates, led to the preparation of new very interesting species. Meijer in 1997 prepared the first CPLED (Circularly Polarized Light Emitting Device) based on the first chiral stereodefined PPV derivative. [74] This system is still used today as a standard to evaluate the properties of a circularly polarized polymeric emitter. After that a series of chiral enantio-pure or -enriched PPV systems were prepared, some of which are shown in Scheme 8.

Studies on the effect of regioregularity on macroscopic properties of these compounds revealed strong chiroptical behavior associated with an exciton-coupled CD.[75] This phenomenon, as in previous cases, results from a twisted cofacial packing of the polymer chains due to aggregation. Moreover, the regularity of the substitution pattern of PPV derivatives has a strong influence on their chiroptical properties in thin films.
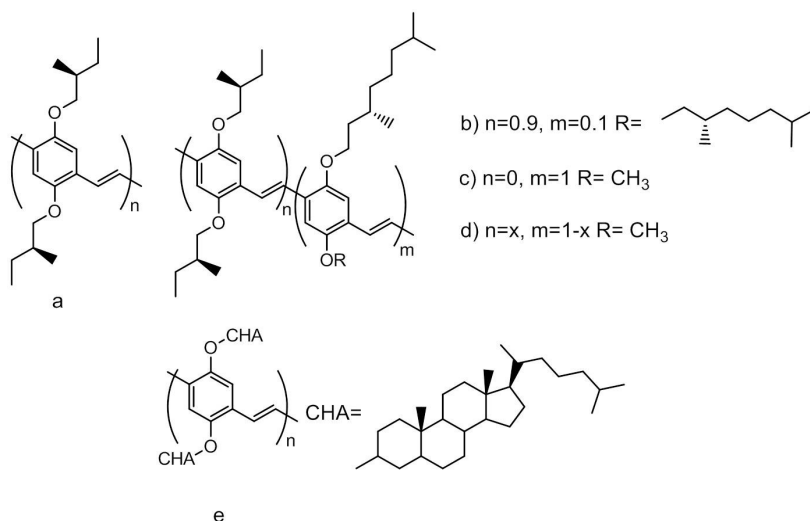
SCHEME 8: EXAMPLES OF SOME PREPARED AND STUDIED CHIRAL PPV DERIVATIVES

A non-linear behavior of circular polarization with respect to the amount of irregularities is observed. So, a regioregular substitution pattern of the side chains along the PPV backbone facilitates the ordering of the polymer chains in well-defined chiral superstructures and results in a high degree of circular polarization in absorption. A small degree of regio-irregularity, up to 20% (polymer Scheme 8-d), appears not to disturb the formation of chiral aggregates, since no significant decrease of g value is observed. For copolymers with more than 60% of irregularities, the degree of circular polarization becomes very low proving that high amounts of irregularities preclude well-defined ordering of the polymer chains. The degree of interchain order of conjugated polymers in aggregated phases depends on the regularity of the substitution pattern of side chains on the polymer backbone. This resembles the well-known dependence of crystallinity on tacticity, as in the case *e.g.* polypropylene. Very small changes in stereochemistry can yield significant effects on macroscopic properties as a result of morphological features.

PPE Derivatives. Very interesting results in this field were obtained also by studying PPE derivatives. The first optically active PPE (Scheme 9 -a) was prepared by Fiesel and Scherf [76] in 1998 in analogy with the work of Meijer on PPVs. Even in this case the chiroptical activity of Scheme 9-a in poor solvents, *e.g.* 1-decanol, or in solvent/non-solvent mixtures like chloroform/methanol, unambiguously points at an intermolecular aggregation phenomenon of individual polymer chains. The results obtained in this work led to the preparation of a plethora of PPEs some of which are summarized in Scheme 9.

A really interesting behavior was evidenced by Swager and coworkers.[77] For polymer in Scheme 9-b, consistently with previous studies, at low concentration of poor solvent, the appearance was observed in the Uv/Vis spectrum of the typical band of aggregation corresponding to an exciton-coupled CD.
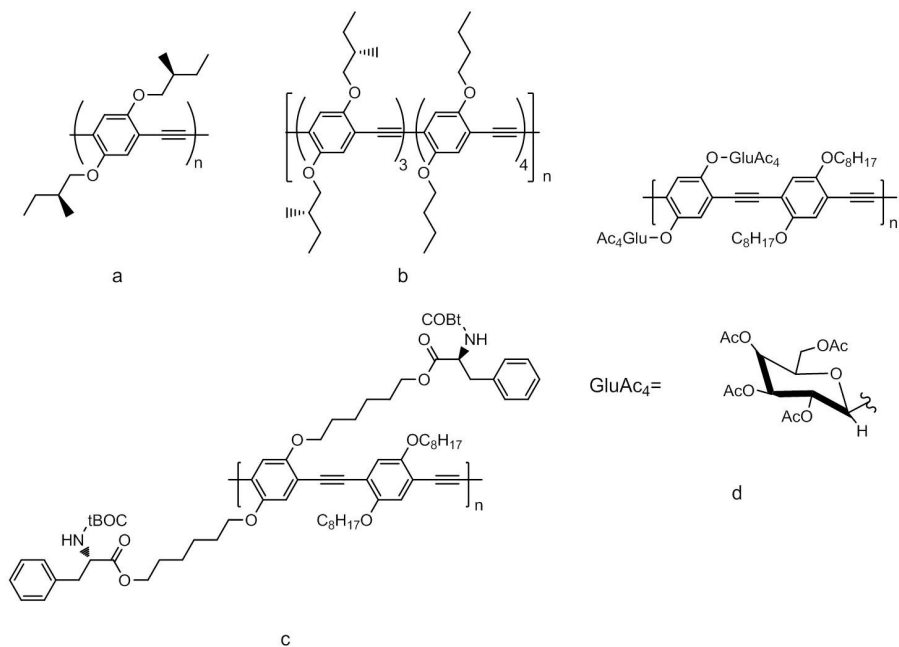
SCHEME 9: EXAMPLES OF SOME PREPARED AND STUDIED CHIRAL PPE DERIVATIVES

The most striking feature in the behavior of this polymer is that above methanol concentrations of 50% the CD dropped off dramatically, while the aggregate peak continued to grow (UV/Vis). This effect can be understood as shown schematically in Figure 15.
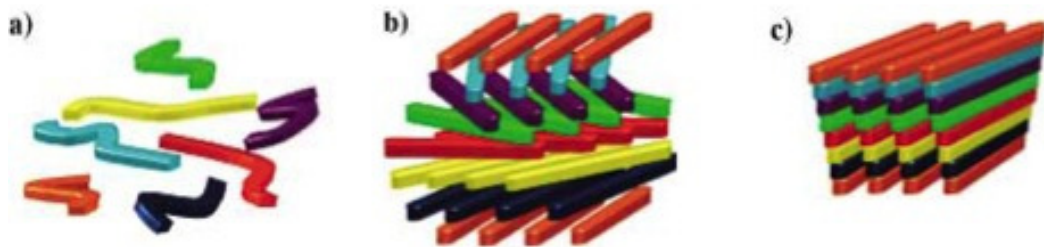
FIGURE 15[77] : A) POLYMERYC CHAINS IN SOLUTION B) CHIRAL AGGREGATE FORMED IN PRESENCE OF A SMALL AMOUNT OF NON-SOLVENT C) ALMOST ACHIRAL AGGREGATE OBSERVED IN PRESENCE OF LARGER AMOUNTS OF NON-SOLVENT

Initially a chiral aggregate forms with a small angle between polymer chains to give an organization reminiscent of a cholesteric liquid crystal. However, the polymer ultimately favors a more densely packed aggregate structure with alignment of polymer chains and the helical structure is lost.

A key factor able to favor and control the structure of aggregated chiral and emissive organization of polymers is the presence of functionalized chiral pendant capable of establishing ancillary intermolecular interactions in the aggregates. Two PPE derivatives, one functionalized with phenylalanine and the other with glucose were synthesized by Farinola and coworkers, and their chiroptical properties were fully investigated (Scheme 9-c,d).[36c,d] Absorption, CD, fluorescence, and CPL spectra demonstrate that phenylalanine-appended polymer undergoes extensive aggregation in solvent/nonsolvent. A more pronounced tendency to form supramolecular aggregates than simple alkoxy-PPEs was observed, induced by amino acid side groups. This is reasonably due to stronger intermolecular interactions between polar protected amino acid moieties. Moreover, a red-shifted CD-active transition is present. This is distinctive of aggregates of phenylalanine derivative and arises from strongly interacting polymer chains packed in a fashion endowed with supramolecular handedness. A pictorial representation of stacked layers of polymer chains compatible with this reasoning is shown in Figure 16.

However even in the most non-solvent rich samples, as it is in thin films, fluorescence is not completely quenched, instead, it is reduced to about 30% intensity compared to the non-aggregated sample in solution. Also for glucose-substituted PPE (Scheme 9-d) the formation of aggregates was early detected by absorption, CD, luminescence and CPL. A so-called aggregate absorption band emerges at 470 nm due to the planarization of the conjugated backbone forced by aggregation, which also quenches the fluorescence.
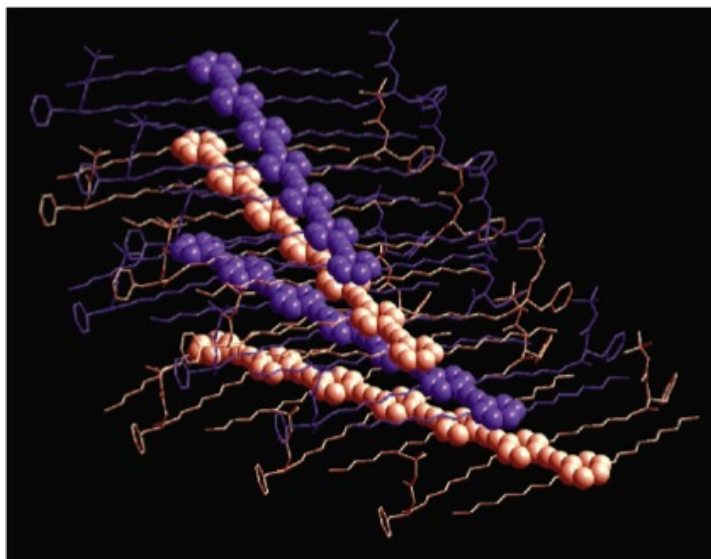
FIGURE 16: PICTORIAL MODEL OF AGGREGATED CHAINS EVIDENCING SUPRAMOLECULAR CHIRALITY ADOPTED BY THE POLYMER BACKBONES (REPRESENTED WITH SPHERES)

The spectroscopic effects of aggregation are most striking in the CD spectra, which show a series of intense bands with alternating sign. The most red-shifted CD signal is observed at 470–473 nm (nearly corresponding to the Abs planarization band) and attains a $g = 10^{-2}$, with a remarkable 1000-fold increase with respect to the solvated species. This large value is allied with strong interactions between distinct polymeric chains close to each other in the aggregates. Glucose groups introduce some rigidity even in the isolated polymer chains, and prevent an effective aggregation. The copolymer chains are essentially planar and are arranged in a cofacial and quasi-parallel fashion with a small negative twist between chains, and lateral interdigitation between alkyl groups.

2 Results and Discussions

2.1 Stereospecific MEH-PPV

Poly-p(phenylenevinylene) and its derivatives are probably the most studied semiconducting polymers, both theoretically and experimentally, because of their excellent properties for organic electronics applications. The parent compound, PPV, exhibits a good fluorescence band in the green region of the electromagnetic spectrum but it is practically insoluble in most common organic solvents. For this reason films of this material have to be prepared by thermal conversion of a soluble non-conjugated polymeric precursor. Most commonly, in order to improve the processability of this system, PPV was modified by inserting two alkoxyde groups at positions 2 and 5 of the phenylene ring. The alkoxy-substituted derivatives are more soluble than PPV and show a reduction of the HOMO-LUMO band gap of 0.3/0.4 eV. The 2-(2-etylhexyloxy)-5-methoxy-p-polyphenylene-vinylene (MEH-PPV) is probably its most important derivative; it presents very interesting absorption properties with a maximum in absorbance near to 500 nm, and, as every PPV described in the previous sections, forms cofacially aggregated moieties in the solid-state, despite the steric hindrance provided ethylhexyloxy group. The aggregation provides strongly coupled π-systems of the polymeric chains and results in a significant quenching of photo- and electroluminescence.

Structure – properties relationship for this system has been very intensively investigated. In literature it's very easy to find a description of optical properties as a function of polymer length, number of defects along the chain, solvent of origin, techniques of deposition etc.[78] On the other hand, the presence of the stereogenic

center on the ethylhexyloxy substituent has been completely overlooked. In fact, all previous analyses and applications have concerned the non-stereoregular polymer, that is, the polymer prepared from chiral compounds in their racemic form. For this reason, with the aim to clarify if, and to what extent, the introduction of dissymmetry influences the structure and the properties of the MEH-PPV aggregates, we decided to prepare and study MEH-PPV carrying all stereogenic centers in (R) configuration ((R)-MEH-PPV). The aggregation properties of the prepared (R)-MEH-PPV systems have been evaluated in comparison with a non-stereoregular system obtained and treated in the same conditions.

2.1.1   Synthesis of *(R)*-MEH-PPV

2.1.1.1   *MEH-PPV and (R)-MEH-PPV via Gilch Polymerization*

Focusing on the potential application of this system, we decided to start our investigation from the polymer obtained in the most common way. A typical system or device based on MEH-PPV as active layer uses medium-high molecular weight polymer classically obtained by Gilch route of synthesis.[79] To this end, it was necessary to develop a synthetic pathway that allows the insertion of the chiral non-racemic unit and which terminates with Gilch polymerization. Moreover the synthetic approach needed to consider the cost and availability of enantiopure (2R)-ethylhexyl building block. A screening of literature revealed that the most convenient source of the chiral moiety is offered by (2R)-ethylhexanol, which can be obtained in its enantio-enriched form by enzymatic resolution of the racemate.[80] A sample of ca. 3 g of (2R)-ethylhexanol, 99 e.e. (HPLC), was kindly provided by Prof. Zdenko Hameršak from the Department of Organic Chemistry and Biochemistry, Ruder Boskovic Institute, Zagreb. So the chosen synthetic pathway (Scheme 10) was a modification of the method used by Neef and Ferraris [43] taking into account the requirements expressed above. In fact, with respect to the publis

hed route, we decided to use as the first step a Mitsunobu-type reaction between 4-methoxyphenol and 2-ethylhexanol, instead of the more common

Williamson synthesis of ethers, which would employ a bromo-derivative of the alkyl group. This way we avoided a preliminary bromination step and obtained sensibly higher conversion with respect to 2-ethylhexanol.
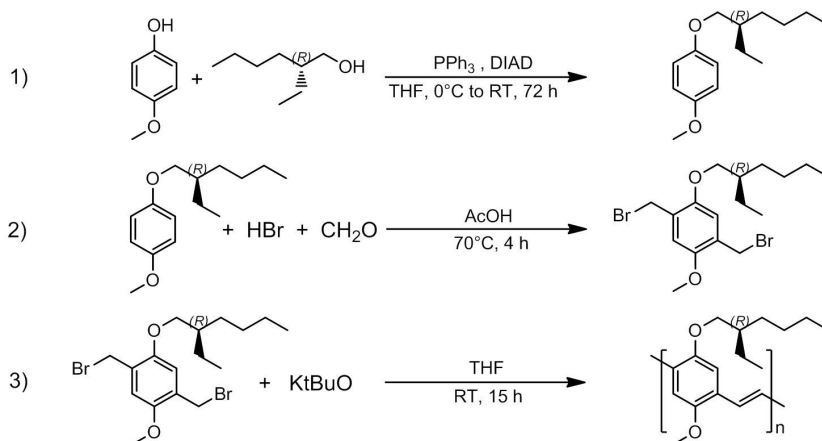
SCHEME 10 : SYNTHETIC PATHWAY FOR THE SYNTHESIS OF MEH-PPV AND (R)-MEH-PPV EMPLOYING GILCH POLYMERIZATION ROUTE

We observed an unexpected strong variability of the reaction yield, ranging from 60 to 97%, depending on the temperature and the relative concentrations of reactants. These parameters were optimized on the racemic derivative and, employing 3 equivalents of phenol and cooling the system to 0 °C during the addiction of DIAD, we finally obtained for step 1 a 97% yield for both racemic and enantiopure alcohol. The second step consisted in a typical dibromomethylation of the aromatic ring performed with formaldehyde and hydrobromic acid. The crucial step of polymerization was performed following what reported in the previously mentioned work.[43] Considering our purpose to observe the effects of chirality in the most in the most easily achievable and less controlled polymeric system, we operated in simplest reaction conditions, *i.e.* in absence of any chain initiator or stopper. The resulting polymers (stereoregular and random) had $M_n \approx 400 \ kDa$ with a polydispersity index (PDI) of 1.84 for MEH-PPV and 1.87 for *(R)*-MEH-PPV, and a structure without particular defects giving us a useful system to start our investigation. Both polymers

were obtained with about 65% yield of polymerization and a 47% overall yield and were characterized with absorption, fluorescence and ECD (of course only for *(R)*-MEH-PPV) spectra in different conditions of aggregation. These measurements will be discussed in section 2.1.2.1.

2.1.1.2 MEH-PPV and (R)-MEH-PPV via Horner Polycondensation

In some contrast to our expectations, chiroptical properties of *(R)*-MEH-PPV did not indicate any particular order of the polymeric chains in the aggregates (see below). We interpreted this fact, we starts from the considered that a 400 kDa polymer is composed by more than 1000 units, and the chains may be too long to give rise to a chiral arrangement in supramolecular architectures. In other words, the excessive length of the backbone might hamper the observation of a preferential chirality in the supramolecular structures, because the (controlled) stereocenter constitutes only a small perturbation with respect to the extremely large polymeric rodlike molecules. In fact, such a long covalent system will naturally show a remarkable tendency to form random aggregates: a random arrangement is more easily achieved with respect to a cofacially well-oriented superstructure. For this reason we decided to move our investigation on systems with at least one order of magnitude shorter chains. Of course, the introduction of the chiral modifier in such a system needed to be subjected to the same restrictions adopted in the previous case. A shorter MEH-PPV was reported for Horner polycondensation reaction. The synthetic pathway is reported in Scheme 11 and, except for the first step, which was already discussed, it is based on the route proposed by Hörhold and coworkers (Section 1.1.3.1).[48] Employing this route we obtained about 60% yield of polymerization, for both stereorandom and stereoregular systems, and an overall yield of about 30%. The polymers obtained following this procedure had $M_n \approx 10\ kDa$ with a polydispersity index of *1.52* for MEH-PPV and *1.50* for *(R)*-MEH-PPV.

Despite Hörhold reported that Horner polycondensation prevents the formation of *cis* double bonds, ^{1}H-NMR characterization showed some prominent

signals between 6.5 and 6.9 ppm which are associated to protons on *cis*-vinylene linkages. Their amount was extimated by integration of NMR signals and resulted almost the 25% of the double bonds.
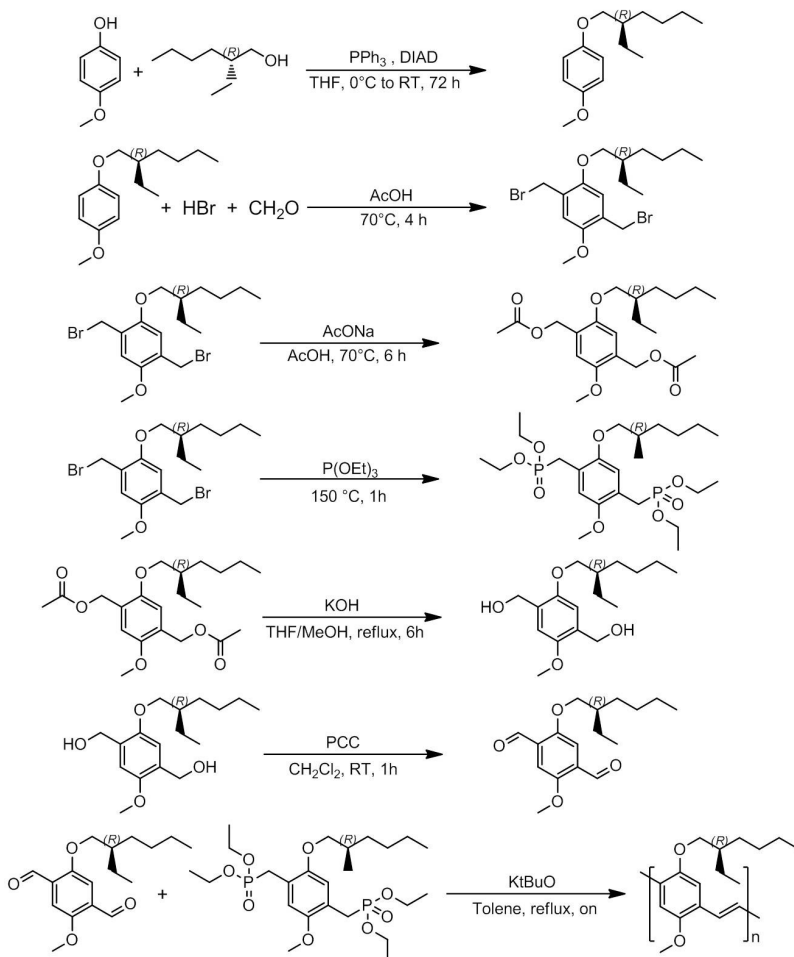
SCHEME 11: SYNTHETIC PATHWAY FOR THE SYNTHESIS OF MEH-PPV AND (R)-MEH-PPV EMPLOYING HORNER POLYCONDENSATION ROUTE

We considered undesirable the presence of these imperfections, which also makes the analysis of such materials more complicated. In order to reduce the extent of *cis* double bonds along the backbone we treated a sample of the analyzed polymer with UV irradiation. In fact, it was reported that through photochemical conversion it is possible to achieve the complete isomerization of *cis* to *trans* double bonds. A sample

of *(R)*-MEH-PPV was dissolved in THF (2 mg/mL) and irradiated with a 125 W medium pressure arc mercury lamp. The *cis*/*trans* conversion was monitored by UV/Vis spectroscopy checking the shift of the absorption maximum. After about 30 min the system reached an equilibrium value with the absorption maximum passed from 473 to 484 nm and even after further UV irradiation we didn't observe any more modifications in *cis*/*trans* ratio. ^{1}H-NMR characterization of the new specie showed a *cis*/*trans* ratio lower than 1:9. Absorption, fluorescence and ECD spectra in different conditions of aggregation were recorded for every system evaluating also the incidence of *cis* double bond densities along the chains.

2.1.2 Spectroscopic Characterization of *(R)*-MEH-PPV

Optical measurements on MEH-PPV samples were conducted monitoring the polymers properties in different conditions of aggregation. This effect was achieved starting from a solution of the polymer in $CHCl_3$ and gradually increasing the amount of methanol, which is a poor solvent for alkoxy-substituted PPVs. The presence of increasing amounts of non-solvent favors intermolecular interactions and gives rise to the formation of small aggregates, which -in our hypothesis- mimic the supramolecular disposition in the solid state or in thin films. The obtained profiles offer a sort of step-by-step image of the aggregation process useful to clarify the nature and the dynamics of these species. Absorption, fluorescence and ECD spectra in different conditions of aggregation were recorded for every system discussed above and they showed interesting behaviors especially in terms of comparison of the stereorandom and the stereospecific systems.

2.1.2.1 Optical Properties of "Gilch" MEH-PPV and (R)-MEH-PPV

As said above, the obtained "Gilch" MEH-PPVs were characterized by very high molecular weight and, for the non-stereospecific system, absorption properties are well established and reported. Optical characterization was performed employing chloroform/methanol mixtures that ranged from 0 to 90% of methanol. The

absorption spectra for both stereospecific and stereorandom MEH-PPV are reported in Figure 17.

FIGURE 17: ABSORPTION SPECTRA REGISTERED WITH INCREASING AMOUNT OF METHANOL FOR HIGH MOLECULAR WEIGHT MEH-PPV AND (R)-MEH-PPV RESPECTIVELY

These spectra shows only negligible differences between the two species. In fact, going from 30 to 50% of methanol we observe for both polymers a significant transformation of the absorption band characterized by a reduction of molar extinction and a bathochromic shift of the maximum, due to the formation of a so-called aggregation-band at higher wavelengths. A similar result was found by

comparing fluorescence spectra recorded in the same conditions: in both cases a 20% of MeOH didn't affect fluorescence properties; but starting from 30% a dramatic quenching of fluorescence take place, and luminescence almost completely disappeared at 90%. This result seemed to prove that for this kind of system the specificity of a chiral substituent along the backbone affects to a very minor extent (if at all) the macromolecular arrangement of the polymer chains. Moreover, ECD spectra (Figure 18) recorded on *(R)*-MEH-PPV showed only very weak signals and no evident trend or explicit relationship could be found observing the profile of spectra compared with the increasing concentration of methanol.
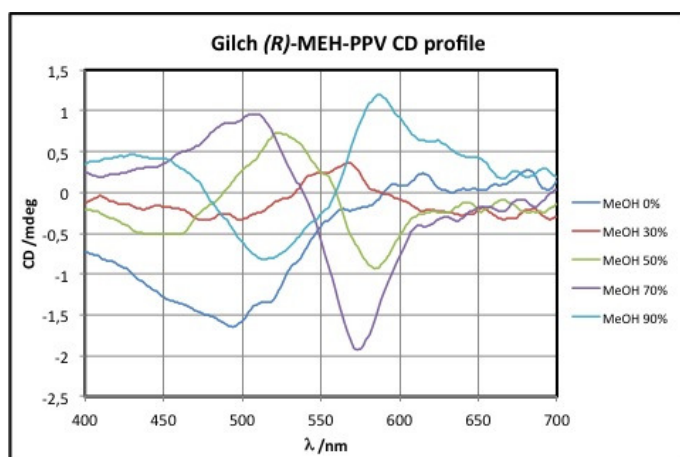
FIGURE 18: ECD SPECTRA IN DIFFERENT AGGREGATION CONDITIONS FOR HIGH MOLECULAR WEIGHT *(R)*-MEH-PPV

The latter result unambiguously demonstrates that there isn't any particularly chiral arrangement for this species; the difference between a butyl and an ethyl group constituting the chiral modifier results, even controlling the geometry of the stereogenic center, uneffective compared to length of the backbone: the skewness possibly induced by the stereocenter constitutes only a small perturbation with respect to the extremely large polymeric rodlike molecules.

2.1.2.2 Optical Properties of "Horner" MEH-PPV and (R)-MEH-PPV

The derivatives obtained by Horner polycondensation were investigated in similar way as "Gilch" MEH-PPVs. In Figure 19 the absorption spectra collected for the stereorandom and the stereospecific Horner MEH-PPV derivatives are shown.
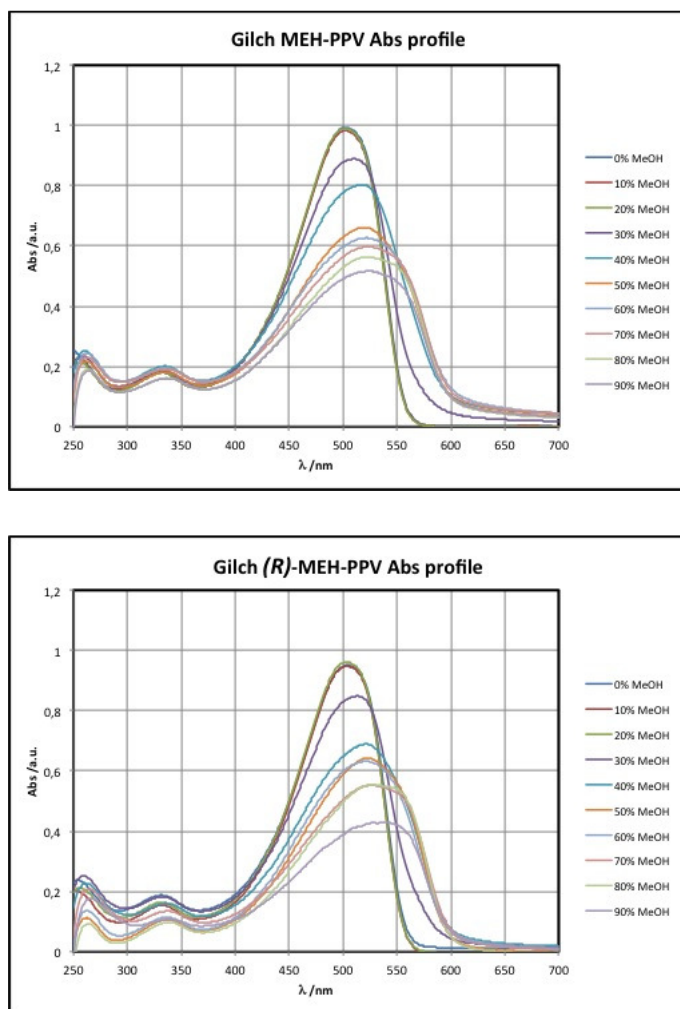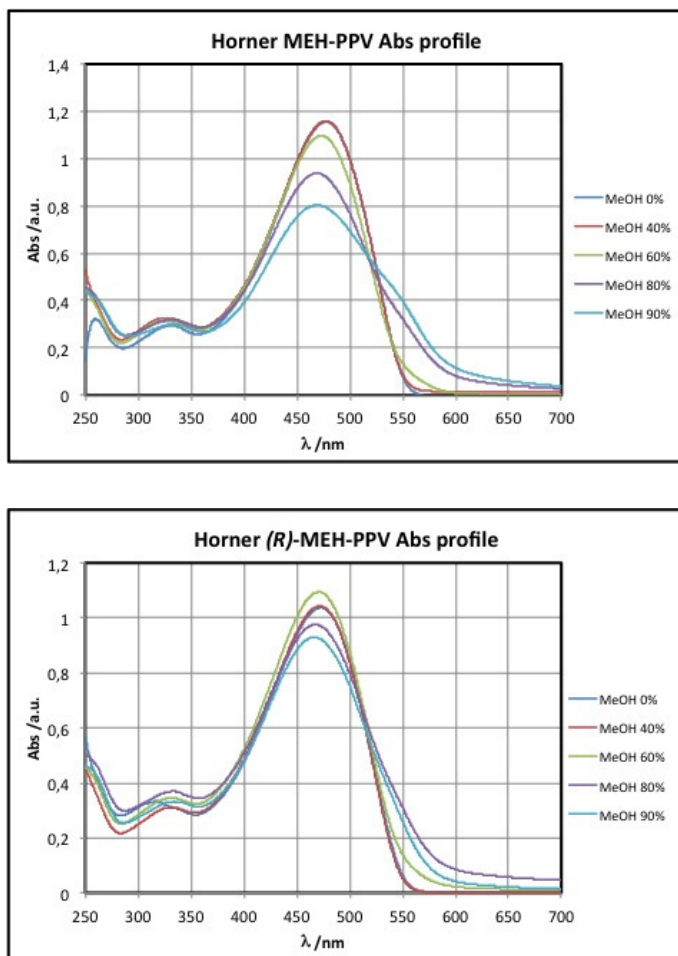

FIGURE 19: ABSORPTION SPECTRA REGISTERED WITH INCREASING AMOUNT OF METHANOL FOR LOW MOLECULAR WEIGHT MEH-PPV AND *(R)*-MEH-PPV RESPECTIVELY

First of all we, observed for both systems a substantially lower tendency toward aggregation. In fact while for "Gilch" MEH-PPVs a 30% concentration of methanol was sufficient to promote aggregation, for "Horner" MEH-PPVs no particular effects were observed until 60% of non-solvent was present. Moreover, with respect to "Gilch" MEH-PPV the absorption spectra registered for both non-aggregated species showed a maximum at 473 nm, about 25 nm lower than the value reported in literature. This phenomenon, on the basis of what had been observed by ^{1}H-NMR characterization, was assigned to the unexpected presence of *cis* linkages inside the backbone. In fact, the presence of *cis* double bonds, even in an overall *transoid* conformation, results in a closer arrangement of the bulkier groups so introducing a torsional disorder and a consequent less efficient π-conjugation. The *cis/trans* double bonds ratio was estimated to be about 1:3 and the decrease of absorption wavelength is consistent with literature data about the behavior of MEH-PPV as function of variable amounts of *cis* linkages.[81] Moreover, in this case the comparison between the absorbance profile for the two polymers showed considerable differences in the behavior between "Horner" MEH-PPVs. For the stereorandom derivative we observed the appearance of a shoulder at lower energies clearly indicating the formation of an aggregate. Instead, for *(R)*-MEH-PPV there's only a small progressive band broadending. This result led us to speculate that, stereoregularity may somehow hinder the process of aggregation and modify the nature of aggregates themselves. An empirical observation of this phenomenon was given by time evolution of the prepared samples. In Figure 20 six samples of MEH-PPVs are divided into three pairs prepared with increasing concentrations of methanol (respectively 60, 80 and 90%). Samples on the left of each pair were prepared with *(R)*-MEH-PPV and samples on the right with MEH-PPV at the same concentration. The image depicts the samples 18 h after their preparation. As evident for MEH-PPV the aggregation processes led to the formation of a visible precipitate. For *(R)*-MEH-PPV this was observed only after 48 h confirming the difference between the two systems.

FIGURE 20: SAMPLES OF LOW MOLECULAR WEIGHT *(R)*-MEH-PPV (ON THE LEFT OF EACH PAIRS) AND MEH-PPV (ON THE RIGHT) WITH INCREASING AMONTS OF NON-SOLVENT, 18 HOURS THEIR PREPARATION

The difference in the nature of the two aggregates prepared by the Gilch and Horner procedures was very efficiently proved by ECD measurement. In fact as shown in Figure 21 until the 60% of methanol was reached *(R)*-MEH-PPV exhibited only a weak negative CD band centered at *470 nm* allied to the electric-dipole allowed transition of the π-conjugated chromophore perturbed by chiral groups at a remote position. After 60%, when aggregation starts, the ECD spectra showed a significant response to aggregation, definitely clearer than what observed in absorption spectra,
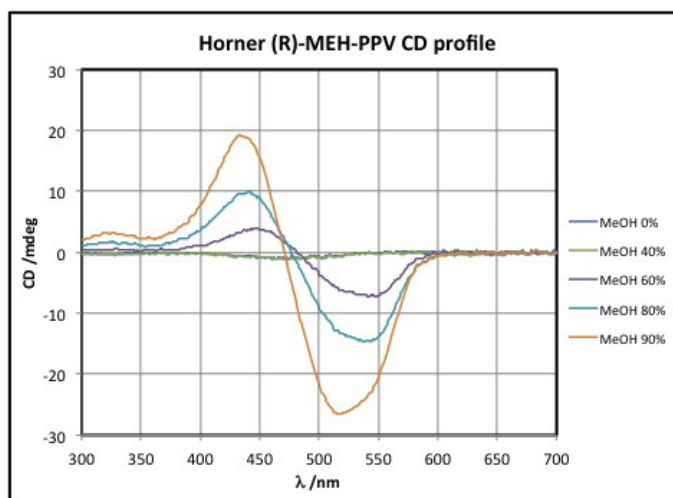
FIGURE 21: ECD SPECTRA IN DIFFERENT AGGREGATION CONDITIONS FOR LOW MOLECULAR WEIGHT *(R)*-MEH-PPV

In fact a strong bisignate Cotton effect is observed in the CD spectrum at the position of the π - π* band allied to the formation of a chiral supramolecule with an extended structure characterized by a defined dihedral angle between polymeric chains. The shape and the intensity of the signal are consistent with a negative exciton coupled CD which proves the existence of strong interchain interactions and a supramolecular negative helicity assumed by the aggregate. A fluorescence study on the stereorandom and stereoregular MEH-PPV demonstrated that the observed differences in their aggregation behavior doesn't reflect the photoluminescence properties of these systems. In fact *(R)*-MEH-PPV and MEH-PPV evidenced almost the same fluorescence profile, both showing a dramatic quenching corresponding to aggregation.

Finally, the sample obtained by UV irradiation of *(R)*-MEH-PPV (see above) was investigated by the same techniques. Optical characterization of the UV-irradiated polymer showed no particular difference in the absorption profile with respect to non-irradiated sample and the same behavior was observed also for circular dichroism. The latter results evidenced how for this system, within certain limits, the amount of *cis* imperfections doesn't affect dramatically the aggregation properties and above all the chiral arrangement imposed by the stereogenic center is almost completely preserved.

Although the photoluminescence properties weren't improved the observations obtained for "Horner" MEH-PPVs show how the controlled chirality on this very common polymer can be envisaged as a good way to modulate the aggregation. In fact, the aggregates of MEH-PPV and *(R)*-MEH-PPV were found to be profoundly different: the stereospecific system showed a remarkably lower tendency toward aggregation, and the formed aggregates are intrinsically different. Moreover the formation of the aggregates, and their different nature too, were barely observable in the absorption spectra, while they resulted unambiguously by CD

spectra, evidencing the importance of this technique to monitor the presence of chiral aggregates and to study their structure.

2.2 Stereoregular MEH-PPE

The structurally closest relatives to PPVs, the poly-p-(phenylene-ethynynelene)s, have attracted relatively less attention in the polymer community, despite their fascinating properties. In fact, for instance the groups of Swager[82], Müllen[83] and Wede[84] demonstrated that PPEs with their unique property profile are exceptional materials in such different areas as explosive detection[77] molecular wires in bridging nanogapsand polarizers for LC displays. [85]

Early attempts to prepare the parent PPE led to the formation of infusible, insoluble, very low-molecular weight oligomers.[86] The first success in preparing soluble PPE derivatives was achieved by Giesa.[87] The attachment of long alkoxy groups to the linear, rigid PPE backbone was expected to endow polymers with increased solubility. The choice of alkoxy groups was based on the simplicity of the synthetic access to the corresponding monomers, and dialkoxy-substituted PPEs are the most easily synthesized representatives of the PPE class. Dialkoxy substituted PPEs in solution have λ_{max} values that are reported to range from 410[87] to 453 nm.[88] Preferred solvents are THF or chloroform. It is important to notice that the absorption spectra of many dialkoxy-substituted PPEs have been investigated in thin films. While Scherf's chiral dialkoxy PPE does not show any bathochromic shift when the solution spectra are compared to the solid-state spectra, Le Moigne's dialkoxy-PPEs show a bathochromic shift of 25-28 nm when measured in the solid state.[88] Wrighton carefully examined PPE films and found in annealed films (thermal treatment) bathochromic shifts ranging from 35 to 50 nm. In addition to the bathochromic shift, the corresponding absorption bands tend to get much sharper in the solid state after annealing, suggesting a higher order in these films. [89]

The morphological and supramolecular control constitutes also for PPEs a primary goal. We decided therefore to approach this matter starting from our previous experience with PPVs synthesizing the correspondent PPE derivative. MEH-PPE was prepared also in this case keeping all stereogenic centers in *(R)* configuration (*(R)*-MEH-PPE), and it was compared with a non-stereoregular system obtained and treated in the same conditions.

2.2.1 Synthesis and Optical Characterization of *(R)*-MEH-PPE

2.2.1.1 Preparation of MEH-PPE and (R)-MEH-PPE

As already discussed in section 1.1.3.2 the principal route for the preparation of PPEs is a Cassar-Heck-Sonogashira polymerization, i.e. the polycoupling of an aryldiyne with dibromo or diiodoarenes, the latter being much more reactive. In our case the preparation of the enantiopure monomeric unit followed the same reasoning made for the preparation of *(R)*-MEH-PPV. The chosen synthetic pathway is depicted in Scheme 12.Apart from the already discussed first step, the synthetic pathway follows the route published by Weder and coworkers in 2000.[90] The polymerization step was performed in a mixture of toluene and iPr$_2$NH at 80 °C and stirred for 20 h. The isolated polymer appeared as a bright yellow powder and it was obtained with a yield of polymerization of about 76 %. The overall yield for the process was 42% and the major limit to the overall reaction yield was given by second step (64% conversion).

The obtained MEH-PPE and *(R)*-MEH-PPE were characterized by GPC measurements and we observed a $M_n \approx 15\ kDa$ for both polymers with a PDI of 1.81 for MEH-PPE and 1.78 for *(R)*-MEH-PPE.
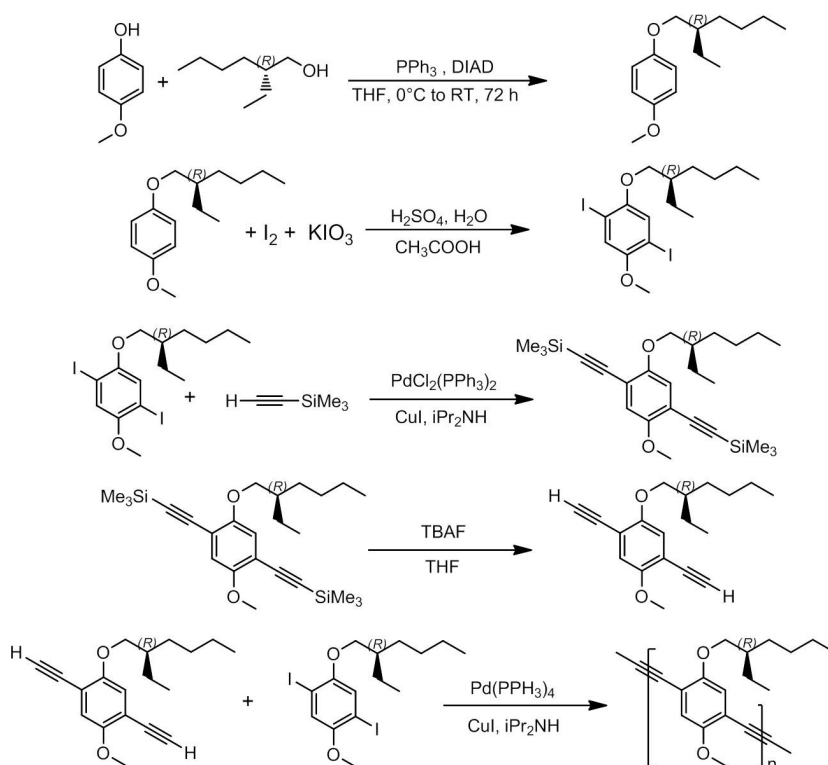
SCHEME 12: SYNTHETIC PATHWAY FOR THE SYNTHESIS OF MEH-PPE AND (R)-MEH-PPE

As expected, they resulted soluble in CH_2Cl_2, THF and $CHCl_3$, only slightly soluble in Et_2O and acetone, and almost completely insoluble in alcohols, water and hydrocarbons, so also in this case $CHCl_3$/methanol was adopted as a good-solvent/non-solvent mixture to evaluate aggregation properties.

2.2.1.2   *Optical Characterization of MEH-PPE and (R)-MEH-PPE*

Optical characterization of MEH-PPEs as usual started from the idea to observe a progressive step-by-step aggregation increasing the amount of methanol in the solvent mixture. Absorption profiles for MEH-PPEs and *(R)*-MEH-PPEs in different conditions of aggregation are shown in Figure 22 and as for the case of "Horner" MEH-PPVs they showed some interesting differences.
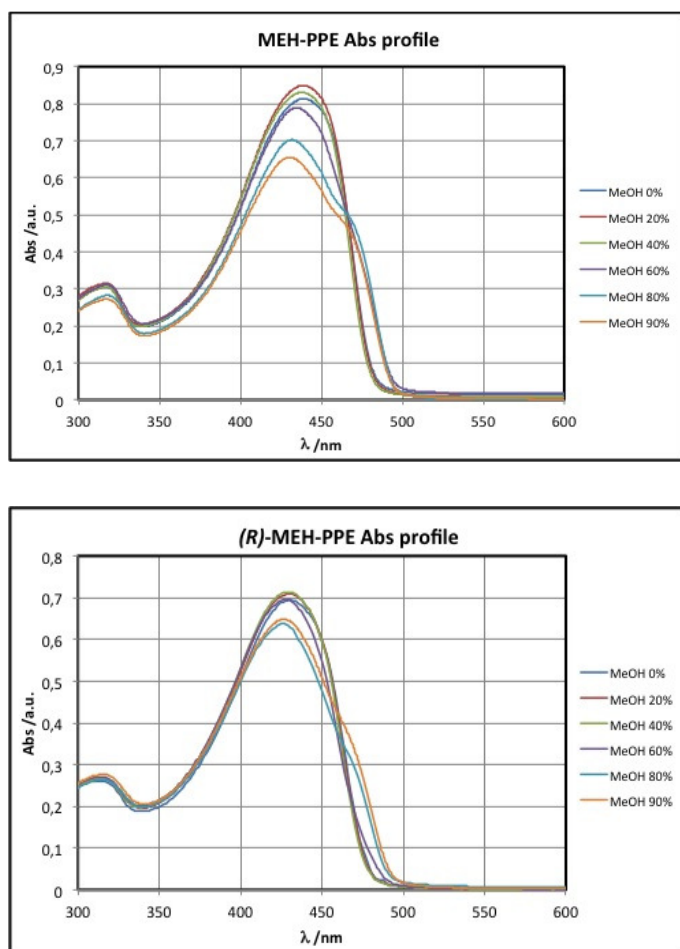
FIGURE 22: ABSORPTION SPECTRA REGISTERED WITH INCREASING AMOUNT OF METHANOL FOR MEH-PPE AND (R)-MEH-PPE RESPECTIVELY

First of all the spectra collected in absence of methanol showed a λ_{max} = 440 nm for MEH-PPE, which is consistent with the data reported in literature, and for *(R)*-MEH-PPE a λ_{max} = 435 nm. This difference between the two species could be allied to the stereoregularity of the second system. In fact it was conjectured that the presence of stereogenic centers sharing the same configuration along the whole backbone could impart a very small systematic deviation from planarity, making the conjugation less effective. Moreover aggregation seemed progressed differently. In fact for both systems until 50% of methanol no process was observed. Aggregation started in presence of 60% of methanol and while for MEH-PPE the process was

reflected immediately in the spectrum, by showing at lower energies a shoulder on the edge of the principal absorption band, for *(R)*-MEH-PPE a well defined aggregation peak appeared only in presence of the 80% of non-solvent, before showing just a little broadening of the main band.

This behavior seemed to reflect the one observed for "Horner" MEH-PPV, and also in this case florescence spectra showed no particular differences passing from MEH-PPE to *(R)*-MEH-PPE. However a very interesting observation was made starting from ECD measurements. In fact as shown in Figure 23 going on with increasing the concentration of non-solvent didn't produce any particular modification in the ECD spectrum. Despite our hypothesis the latter evidence demonstrated that aggregation proceeded without any chiral response, and the spectra reflected in all cases only the effects of central chirality of the substituents. Apparently, in this case the chiral perturbation wasn't sufficient to impart any kind of helicity to the supramolecular system. We conclude that a discrimination based only on different steric hindrances of the ethyl and butyl groups at the chiral center was not able to compete with the stabilization allied with the complete and symmetric superimposition of π clouds. In addition, for this system, the effect of the chirality of the side groups could be nullified by the non-regioregularity of the polymeric backbone.
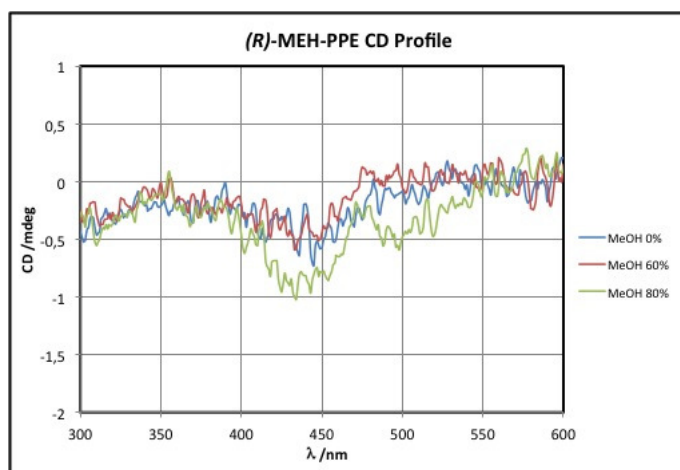
FIGURE 23: ECD SPECTRA IN DIFFERENT AGGREGATION CONDITIONS FOR *(R)*-MEH-PPE

Head-to-head and head-to-tail coupling occurs in this polymer randomly, and this phenomenon could strongly affect the geometrical features of the entire system. For these reasons we decided to investigate systems characterized by symmetrically substituted monomers containing a chiral modifier which could stabilize chiral aggregates by means of stronger ancillary interactions, such as hydrogen bonding.

2.3 PPE Functionalized with Aminoacid Derivatives

The interest in obtaining PPE derivatives able to break the symmetry of aggregates by preventing the formation of perfect cofacial architectures, led us to focus on various chiral pendants. The observation made in the previous section for MEH-PPEs about the features needed to induce a controlled twist in the aggregates, prompted us to look for a pendant group able to stabilize chiral superstructures by interactions different from the simple steric hindrance. Moreover enantiopure alkyl or alkoxy derivatives such as *(2R)*-ethylhexanol are typically expensive and difficult to obtain so a large-scale application which exploits these molecules is not really conceivable.

In this respect, some biological molecules represent easily available sources of enantiopure compounds. Indeed, PPEs functionalized with biomolecules such as monosaccharides[91], oligonucleotides[92], and biotine[93] have been reported in the literature, as potential semiconducting or highly fluorescent active materials in biosensing applications. Natural α-aminoacids (and their derivatives) have found widespread applications in the field of molecular recognition, owing to their ability to form multiple labile interactions, often responsible for stereodiscriminating structures.[94] Their introduction in PPEs, which are polymers with a strong tendency to autoaggregation, would represent a step toward novel complex molecular architectures, whose order may be modulated through the judicious choice within the variety of this class of chiral modifiers. Moreover, this passage may be further elaborated with the development of PPEs bearing many types of biological enantioenriched derivatives. α-Aminoacids derivatives also provide the possibility to

"transmit" the asymmetry to the entire system through hydrogen bonding interactions. The presence of these additional interactions makes α-aminoacids derivatives very attractive: hydrogen bonds are highly selective and directional, and their strength in a macromolecular architecture depends largely on the solvent, number, relative position and geometry, granting a fine modulation and control of the aggregation properties so bestowing to the system a high tunability.

Considering all these properties, also in light of the experience on phenylalanine-functionalized PPE gained in the group wherewith this research was conducted,[36] we moved our investigation on a new series of aminoacidic derivatives of PPE, functionalized by linking the aminoacidic moieties (more properly the methyl ester derivatives) as an amide to the PPE skeleton through an oxaalkyl chain of suitable length. Several different materials, a homopolymer and some copolymers, of this type were prepared and their properties were characterized by means of optical and chiroptical techniques.

2.3.1 Synthesis and Characterization of Leucine Functionalized PPE

Our development of this new class of compounds was founded on the assumption that a fruitful investigation should start from a proper molecular design. Two choices needed to be made at this point: what aminoacidic derivative should be used and how it had to be connected to the PPE backbone. The criteria for the selection of an appropriate aminoacidic derivative consisted principally in two observations: the chosen derivative should present on the stereogenic center a group with pronounced steric hindrance, and, moreover, that group shouldn't carry itself any kind of functionalities, in order to prevent any interaction different from the π-stacking and the hydrogen bonding promoted by the amide group. Following these statements our choice fell on leucine. On the other hand, in our idea, the connection between the chiral moiety and the backbone would have to be such that the distance between the two portions should be large enough to not hamper the backbone but not too large to preclude the chiral interactions. For these reasons, and because of

what observed in the case of phenylalanine-functionalized PPE[36], we chose a linear six carbon atoms alkoxy chain as linker (6-oxyhexanoic acid derivative). The resulting material is the final product depicted in Scheme 13.

2.3.1.1   Preparation of Leucine Functionalized PPE (LeuHex-PPE)

The approach to the synthesis of this new material was the same adopted in case of MEH-PPEs. The synthetic pathway is fully depicted in Scheme 13. The first intermediate, 1,4-di(ethyl6-oxyhexanoate)benzene (step 1), was synthesized via the nucleophilic substitution between hydroquinone and ethyl 6-bromohexanoate. Impressively, this reaction gave a yield of about 83 % and no complicated purification was required. Afterwards, the electrophilic substitution of 1,4-di(ethyl6-oxyhexanoate)benzene by iodine was carried out, this step was performed in classic conditions, that is, acetic acid as solvent in the presence of sulphuric acid and water at 75 °C, in order to obtain at the same time two acidic functionalities at the end of the oxalkylic chains. At this point we tried to directly functionalize the obtained derivative with aminoacidic moieties by reaction with the methyl ester derivative of the aminoacid in presence of DMAP and EDC, but unfortunately only a 35% yield was achieved. So we decided to employ a different approach: we passed through the acidic chloride by reaction with $SOCl_2$ and a catalytic amount of DMF, and then compound obtained from step 3 was treated with two equivalents of aminoester. Following this route we obtained a 72% yield for the two steps. Polymerization was performed with a classic Cassar-Heck-Sonogashira reaction between a diodo- and a diethynyl- derivative of the monomeric unit. Thus the LeuHex-PPE was obtained as a yellow-orange powder with a 76% polymerization yield and was characterized by GPC measurements showing a $M_n \approx 9000$ (about 15 monomeric units) and a *PDI = 1.72*. The obtained polymer resulted as expected soluble in chlorinated solvents, but interestingly it is just slightly less soluble in methanol and ethanol. On the contrary it resulted only slightly soluble in acetone and THF and completely insoluble in diethyl ether, water and hydrocarbons. This peculiarity of LeuHex-PPE with respect to the other systems discussed above is addressable to the presence of the amidic
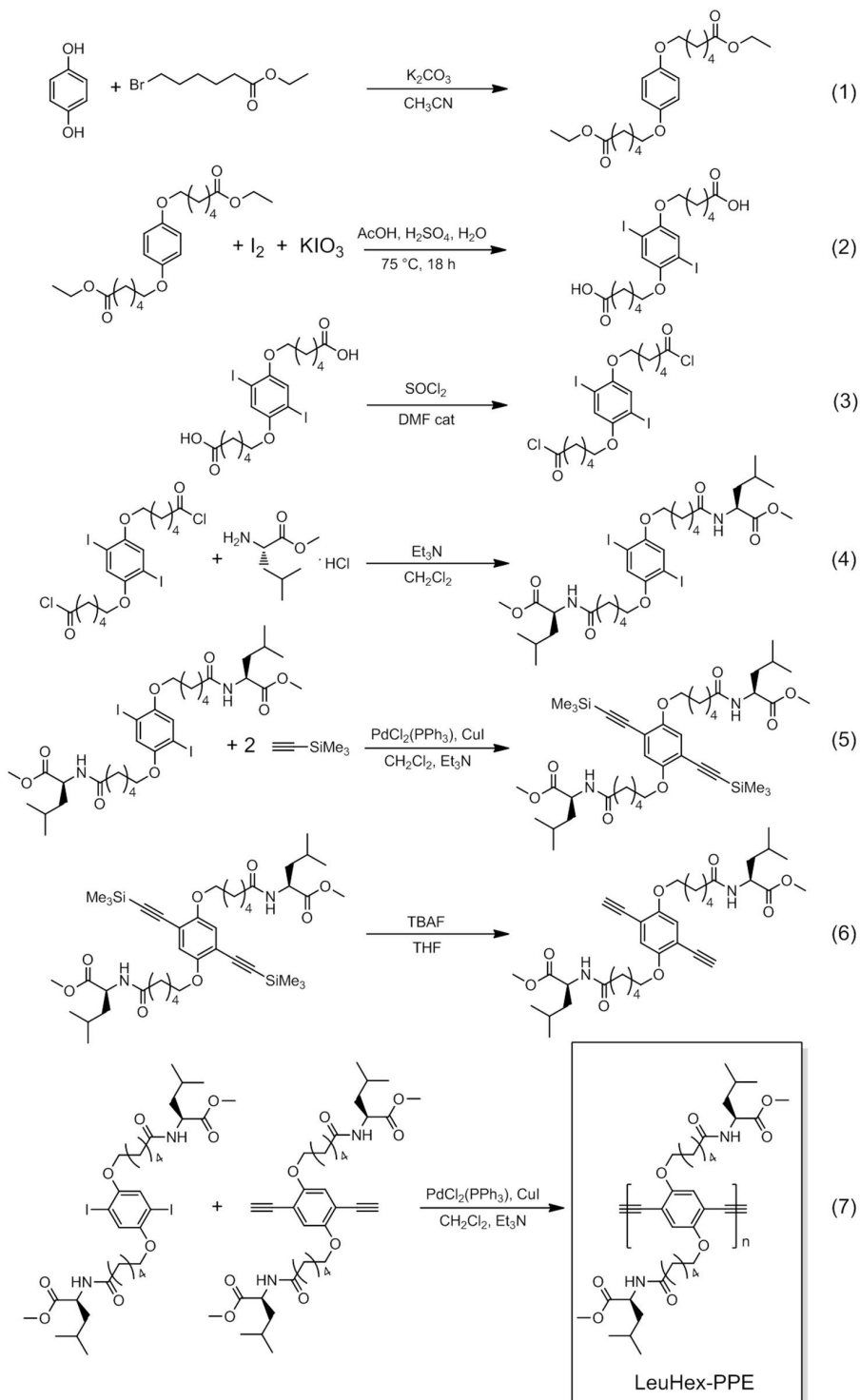
SCHEME 13 : SYNTHETIC PATHWAY FOR THE SYNTHESIS OF LeuHex-PPE

functionalities and so to the capability to form hydrogen bonds with alcoholic solvents.

2.3.1.2 *Chiroptical Characterization of LeuHex-PPE*

According to the solubility of LeuHex-PPE, optical and chiroptical properties of such a system were investigated employing variable solvent/non solvent mixtures composed by CH_2Cl_2 and Et_2O. The absorption spectrum of LeuHex-PPE in CH_2Cl_2 shows a broad π - π^* conjugation band with maximum at 440 nm (Figure 24), in keeping with other dialkoxy-substituted PPEs.
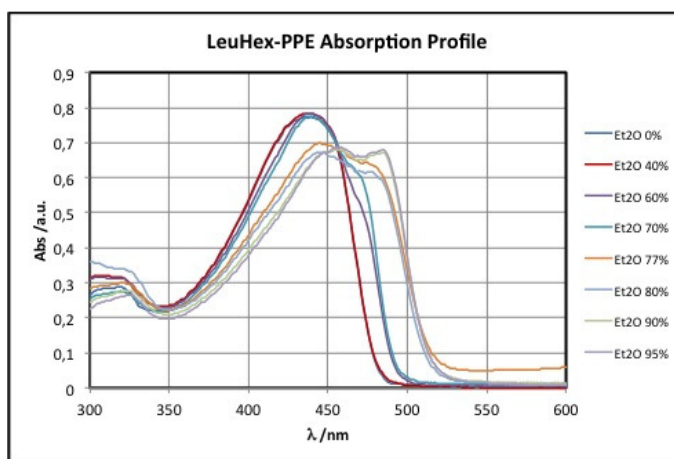
FIGURE 24: ABSORPTION SPECTRA IN DIFFERENT AGGREGATION CONDITIONS FOR LeuHex-PPE

Upon addition of Et_2O as nonsolvent, a solvatochromism is observed: the main band is reduced and red-shifted; moreover, a new band progressively appeared at 480 nm which may be assigned to aggregated species dispersed in solution. The consequences of nonsolvent-promoted aggregation are especially evident in the CD spectra. Remarkably, circular dichroism didn't show a simple progressive behavior with respect to the amount of diethyl ether (Figure 25): in dichloromethane, LeuHex-PPE exhibited only a very weak negative CD band (g = -2.5·10^{-5}) centered at 450 nm that descends from the transition of π-conjugated chromophore in presence of the chiral modifier.
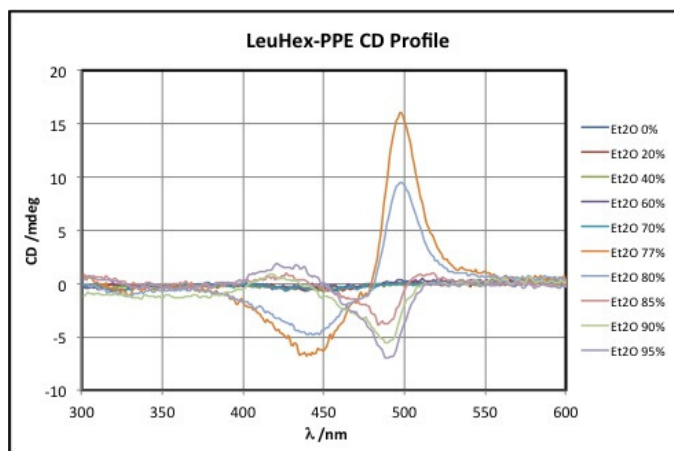
FIGURE 25: ECD SPECTRA IN DIFFERENT AGGREGATION CONDITIONS FOR LeuHex-PPE

Upon aggregation, between 70 and 80% of non-solvent, this weak mono-signed CD was replaced by a stronger bisignate Cotton effect showing a maximum at 495 nm and a zero-point around 480 nm in correspondence with the so-called aggregation peak. It attained for its most red-shifted band a maximum g-value of $1.6 \cdot 10^{-3}$, about 70-fold larger with respect to the non-aggregated system. This value is allied with a chiral interaction between distinct polymeric chains close to each other in the aggregates. Despite in absorption spectra only a small increase of the aggregation peak is observed passing from 77 to 95% of Et_2O, circular dichroism measurements revealed a dramatic difference in the nature of the formed aggregate. In fact, going further with the fraction of non-solvent resulted first in a weaker signal (80% Et_2O) and successively the CD spectrum completely changed and showed a negative CD couplet with a minimum at 495 nm coincident with the aggregation peak, and an inflection at 448 nm in correspondence with the maximum in the absorption spectrum (Figure 24: 85, 90, 95% Et_2O). The estimated g value for this system is -$3.3 \cdot 10^{-4}$, about 5-fold less intense than the one observed at lower concentrations of Et_2O. This fact proved that this system may lead to two different aggregates, depending on the solvent. This behavior recalls the one observed by Swager and coworkers.[77] Initially a chiral aggregate is formed with a small angle between polymer chains. However, in more drastic solvent conditions, polymer chains arrange in a

completely different way and ultimately yield a different aggregate structure, probably with opposite helicity and a more parallel alignment of polymer backbones. This causes the lower g value, and the different shape of the CD spectrum.

Chiroptical measurements were crucial to understand the behavior of LeuHex-PPE. Their analysis revealed that in this case the formation of a strong chiral aggregate is somehow prevented. Probably the steric hindrance provided by the long alkoxy chain terminating with leucine on every phenylene unit makes interchain interactions more difficult, destabilizing chiral aggregation germs. In presence of larger amounts of non-solvent, aggregation becomes more effective, preventing the formation and the growth of chiral superstructure, and furnishing aggregates with better alignment of polymeric backbones.

2.3.2   Aminoacid Methyl Ester Functionalized PPE Copolymers.

In order to stabilize a twisted aggregate organization, and in agreement with the results reported for Phenylalanine functionalized PPE,[36] we decided to *dilute* the content of chiral modifiers along the backbone by alternating them to a small achiral substituent. Such unit was chosen with the idea of introducing a group that was the least interacting and bulky as possible. Considering this, a dimethoxy derivative appeared to be the most proper choice. Furthermore, we also decided to evaluate the effects of different bulkiness on the aminoacid moiety on the aggregation. To this end, several aminoacid functionalized copolymers were prepared and their optical and chiroptical properties were evaluated both as aggregates in solution and as thin films. The effect of aminoacidic chirality was also determined by comparing the prepared systems with similar polymer without chiral elements, i.e. based on glycine. The structures of analyzed systems are shown in Scheme 14.

Prepared Copolymers

achiral   *chiral*
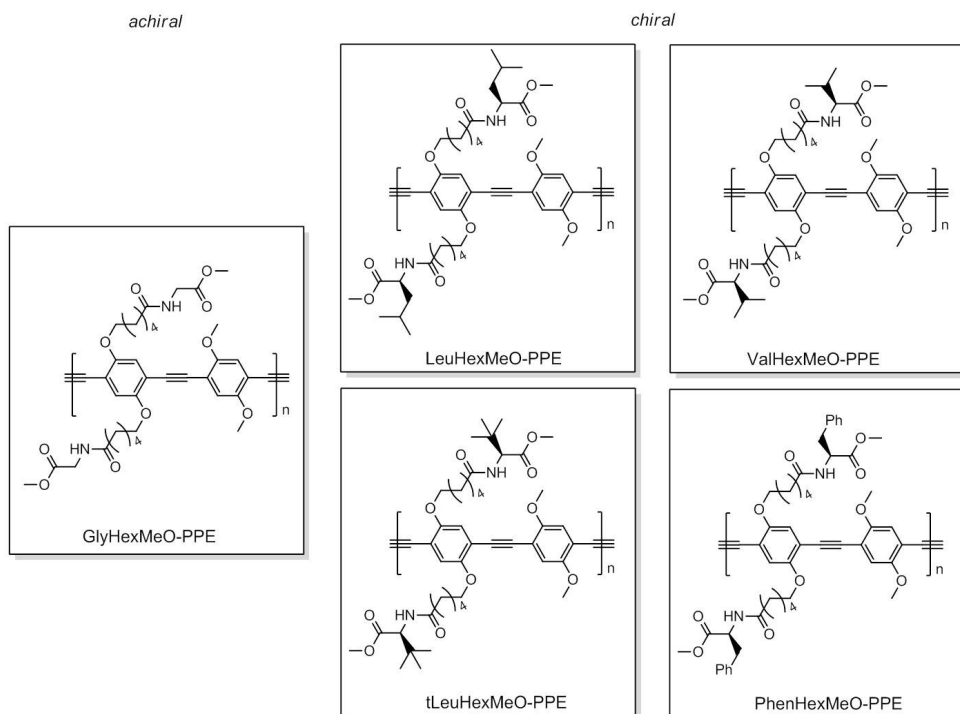
SCHEME 14: PREPARED AMINOACID METHYL ESTER FUNCTIONALIZED PPE COPOLYMERS

2.3.2.1 *Synthesis of Aminoacid Methyl Ester Functionalized PPE Copolymers*

The synthesis of these new derivatives was achieved following the same synthetic approach adopted for LeuHex-PPE. Scheme 15 reports the complete synthetic pathway.

The synthesis of these systems was performed by Pd-catalyzed cross-coupling reaction of 1,4 diethynyl-2,5-dimethoxybenzene with the respective aminoacid-functionalized diiodoarene, furnishing all the derivatives as yellow-orange powders. Polymers were characterized by ^{1}H and ^{13}C-NMR spectra. Peak integration confirmed that the structural units derived from the two monomers are present in a 1:1 ratio.

2.3.2 - Aminoacid Methyl Ester Functionalized PPE Copolymers.

R = H, *i*Pr, *t*Bu, Bn, *i*Bu
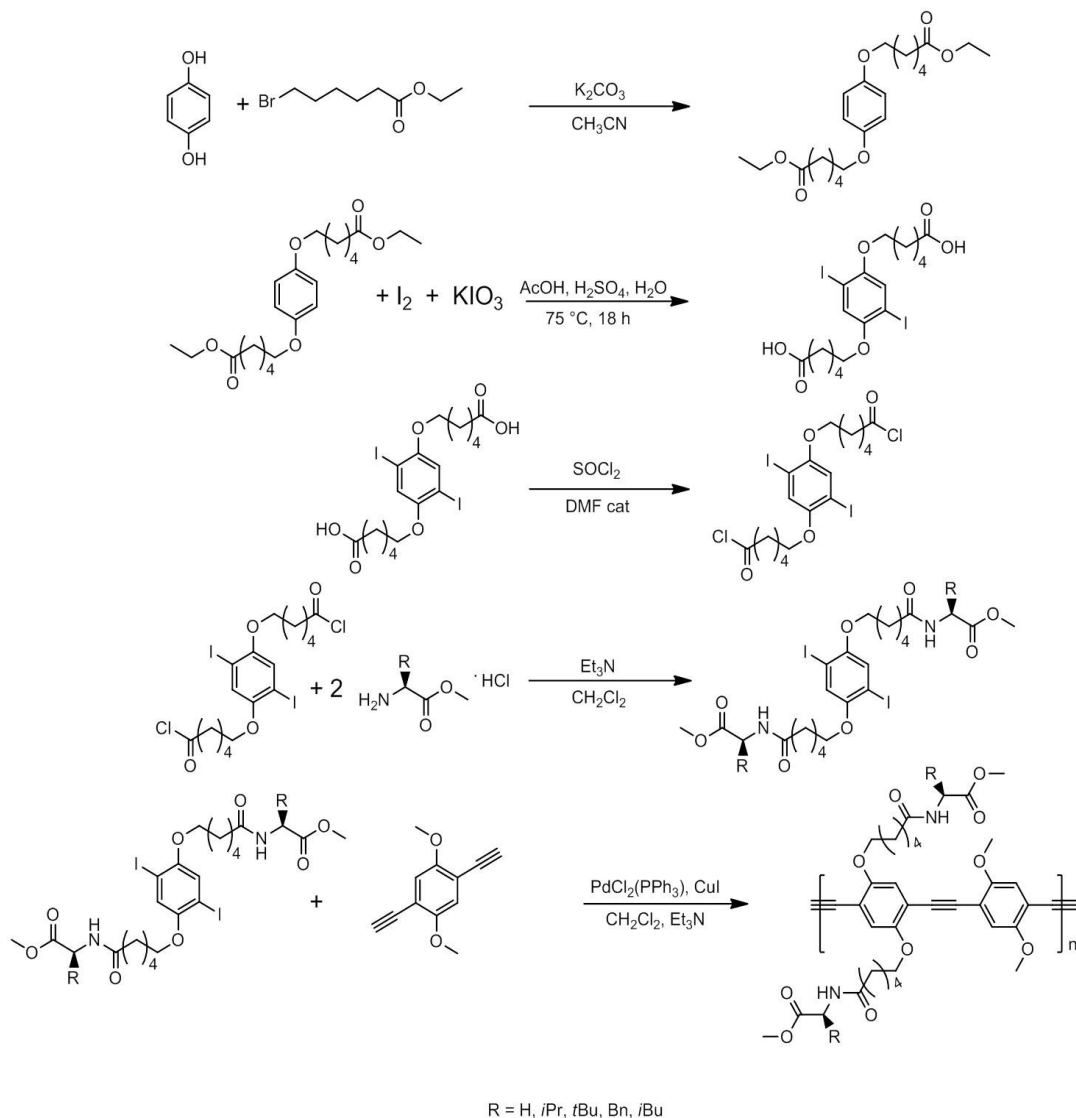
SCHEME 15: SYNTHETIC PATHWAY EMPLOYED FOR THE PREPARATION AMINOACID FUNCTIONALIZED PPE COPOLYMERS

Furthermore, the ^{13}C resonances of butadiyne carbon atoms at about 80 ppm are absent. Systems were characterized also by DOSY experiments in order to get some information about their diffusion coefficients and so to have a rough idea of their dimensions. Molecular weights, polymerization yields and diffusion coefficients for every polymer are reported in Table 2.

TABLE 2:

Polymer	Yield /%	M_n(GPC) /kDa	PDI	D(CDCl$_3$,25 °C) /10^{-10}m^{2}s^{-1}
GlyHexMeO-PPE	32	-	-	0.38[a]
LeuHexMeO-PPE	78	10.1	1.81	1.23
ValHexMeO-PPE	77	9.1	1.62	1.38
PhenHexMeO-PPE	70	9.2	1.86	1.45
tLeuHexMeO-PPE	78	-	-	1.42

[a] registered in DMSO-d^6

GPC data on glycine and *tert*-leucine derivatives aren't yet available. However an indication on their dimension is obtainable by comparing their diffusion coefficients with the ones measured for LeuHexMeO-PPE, ValHexMeO-PPE and PhenHexMeO-PPE. From this comparison it is reasonable to assume that the sizes of these polymers roughly match the values reported for the other systems. Considering the molecular weights of monomeric units, the observed GPC values are consistent with species constituted of about 25 phenylene units. Interestingly, a marked difference in the solubility properties of chiral and achiral derivatives was observed. In fact, similarly to LeuHex-PPE, all chiral systems were found to be soluble in chlorinated solvents, just slightly less soluble in methanol and ethanol, only slightly soluble in acetone and THF, and completely insoluble in diethyl ether, water and hydrocarbons. On the contrary the glycine derivative resulted soluble in DMSO, only partially soluble in chloroform and almost completely insoluble in other common solvents. This phenomenon preliminarily gives some ideas of the aggregate, letting us reasonably assume the existence of much stronger interactions for the achiral system than for chiral ones.

The efficiency and the importance of hydrogen bonding in these systems were evaluated by investigating the N-methylated derivative of the leucine-functionalized

copolymer. The synthesis of such a compound was achieved by treating the Leucine diiodo-derivative with NaH and CH$_3$I in DMF (Scheme 16).
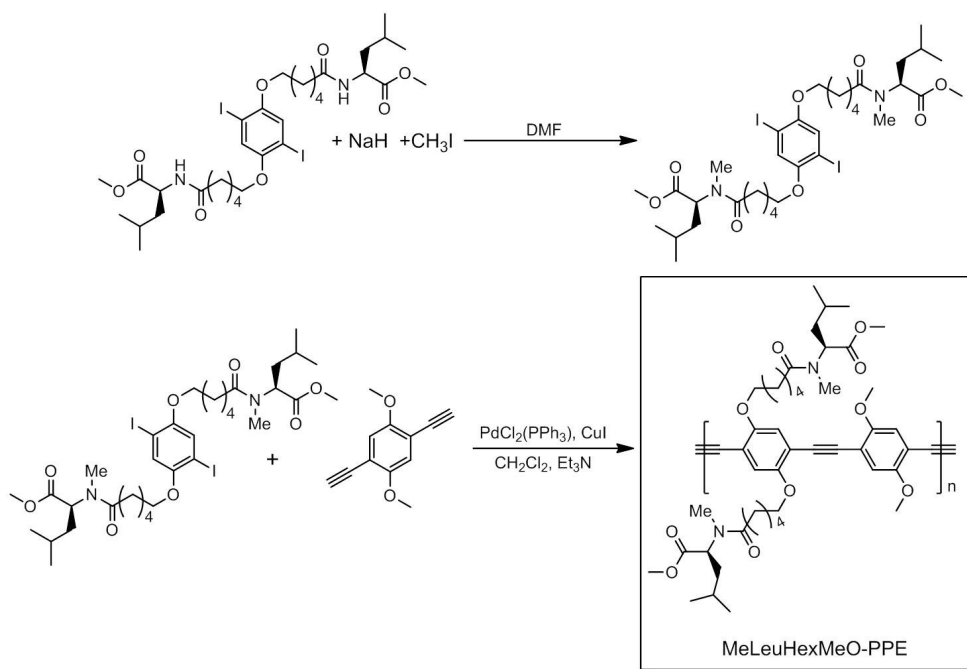
SCHEME 16: PREPARATION OF N-METHYLLEUCINE FUNCTIONALIZED COPOLYMER

The polymerization was carried out in standard conditions affording a 75% yield and furnishing MeLeuHexMeO-PPE as yellow-orange powder. Peak integration confirmed that the structural units derived from the two monomers are present in a 1:1 ratio and by GPC analysis we measured $M_n \approx$ *19 kDa* and PDI = 1.5. A preliminary indication of the importance of hydrogen bonding for the formation of aggregates was given by the comparison of solubility properties of the latter substrate with its non-methylated homologous. In fact, MeLeuHexMeO-PPE - differently from LeuHexMeO-PPE - resulted completely soluble in chlorinated solvents, THF, acetone and diethyl ether, and almost completely insoluble in water, methanol, ethanol and hydrocarbons. This information constitutes a preliminary proof that the absence of hydrogen bonding sites makes this system behave as a simple dialkoxy substituted PPE.

2.3.2.2 Optical and Chiroptical characterization of Aminoacid methyl ester Functionalized PPE copolymers

The optical characterization of these systems led to highlight a profound difference toward aggregation between the chiral and the achiral substrates. Figure 26 shows the absorption spectra of GlyHexMeO-PPE and LeuHexMeO-PPE recorded in chloroform at the same concentration (0.026 mg/mL).
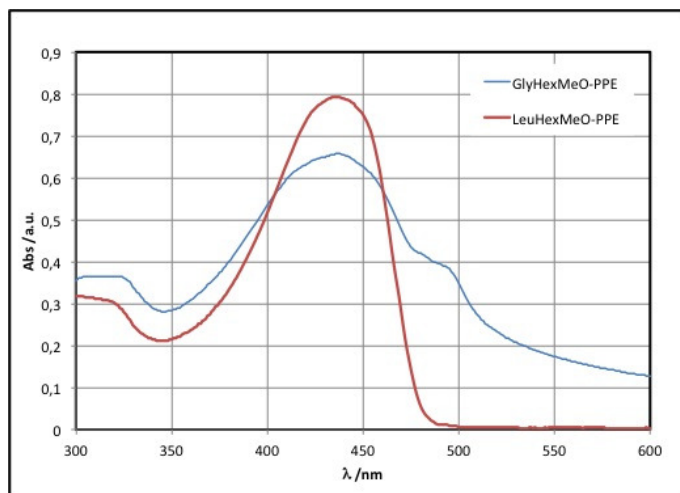
FIGURE 26: COMPARISON OF ABSORPTION SPECTRA IN CHCl₃ FOR LeuHexMeO-PPE (IN RED) AND GlyHexMeO-PPE (IN BLUE)

These spectra evidenced a common maximum in absorbance centered at 438 nm, which depends only from the nature of the chromophore and is in agreement with previously studied alkoxy substituted PPE. For glycine derivative a band at 490 nm is also present attesting the existence of aggregates even in these conditions.

The spectra of ValHexMeO-PPE, tLeuHexMeO-PPE and PheHexMeO-PPE collected in the same conditions resulted practically superimposable to the one of LeuHexMeO-PPE. This observation proved a greater tendency toward aggregation of the achiral system than the chiral ones. This phenomenon could depend on the reduced steric hindrance provided by glycine, but also, for systems carrying chiral modifiers, on the formation of chiral supramolecules. In fact for achiral substrates a

perfectly cofacial arrangement which maximize $\pi - \pi$ interaction is conceivable and can result in stronger aggregates.

Step-by-step aggregation measurements for LeuHexMeO-PPE were conducted employing CH_2Cl_2/Et_2O as solvent/non-solvent mixture. The absorption profiles in different phases of aggregation are shown in Figure 27.
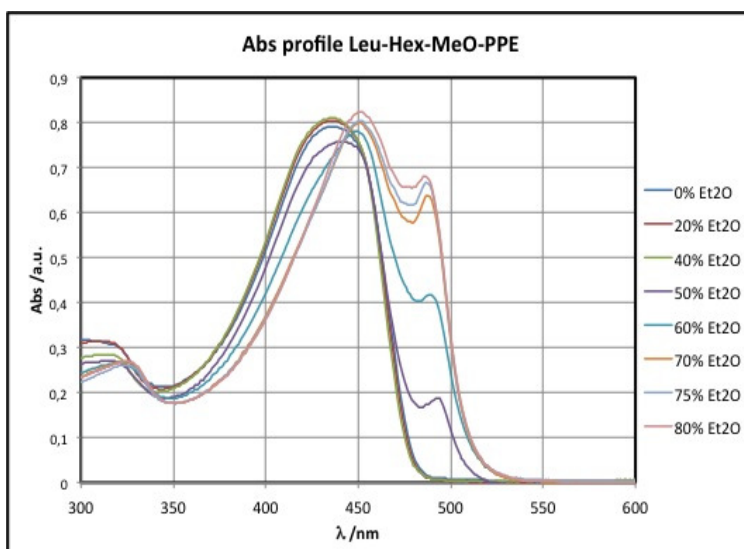
FIGURE 27: ABSORPTION SPECTRA IN PRESENCE OF DIFFERENT AMOUNT OF NON-SOLVENT FOR LeuHexMeO-PPE

Upon addition of diethyl ether as a nonsolvent, a clear solvatochromism is observed: the main band is red-shifted, and its shape becomes sharper; moreover, a new, narrow band appears at 490 - 493 nm which may be assigned to aggregates dispersed in solution. Switching from Et_2O to different non-solvents such as cyclohexane resulted in similar absorption spectra and a minimum amount 10% CH_2Cl_2 is needed in every case to maintain the aggregates in solution.

The spectroscopic effects of aggregation are most striking in the CD spectra (Figure 28): LeuHexMeO-PPE in CH_2Cl_2 exhibited only the classic weak negative band centered at 445 nm with a g value of $1.2 \cdot 10^{-5}$ due to the perturbation induced by the chiral group far from the chromophore.
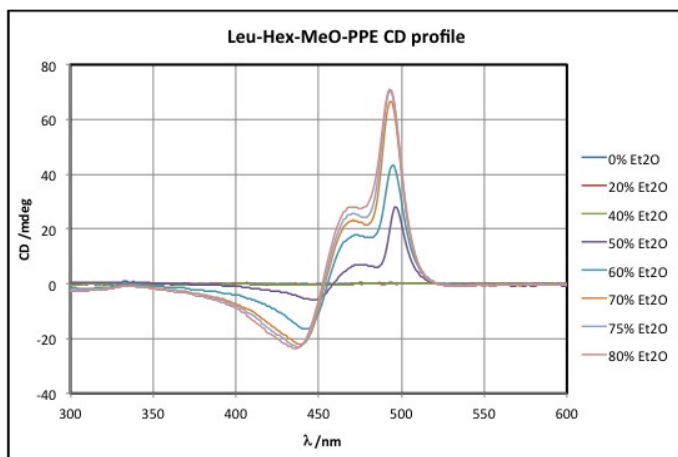
FIGURE 28: ECD SPECTRA IN PRESENCE OF DIFFERENT AMOUNT OF NON-SOLVENT FOR LeuHexMeO-PPE

Upon addition of Et_2O, this weak mono-signed band was replaced by a complex, asymmetric and positive CD couplet which attained a maximum g = $5.5^.10^{-3}$ (almost 500-fold larger with respect to the solvated species). This large g value is allied with strong interactions between distinct polymeric chains close one to each other in the aggregates, and the sign of the couplet describes a relative orientation between the chains associated with a right-handed helicity. It is noteworthy that the g value at 490 nm reached its maximum already for the 50:50 mixture, where only a small shoulder is visible in absorption spectrum. In these conditions the few aggregates formed have already a well-defined structure which is preserved upon further aggregation. The intense CD spectra with g values close to 10^{-2} typical of PPE aggregates call for strong interactions between polymer chains, allowing for an effective exciton-coupled CD mechanism (ECCD). The atypical shape of the observed CD profiles with respect to the standard ECCD expectations is the result of a strong vibronic coupling, as it has been demonstrated for glucose functionalized PPE.[36d] When exciton coupling occurs between vibronic transitions, rather than purely electronic ones, the resulting CD profile may strongly differ from a typical CD couplet.[95]

In our hypothesis, the overall superstructure is stabilized by a hydrogen bonds framework. The role played by hydrogen bonding was investigated by comparing the

aggregation properties of LeuHexMeO-PPE and MeLeuHexMeO-PPE. Absorption and circular dichroism profiles for MeLeuHexMeO-PPE are reported in Figure 29.
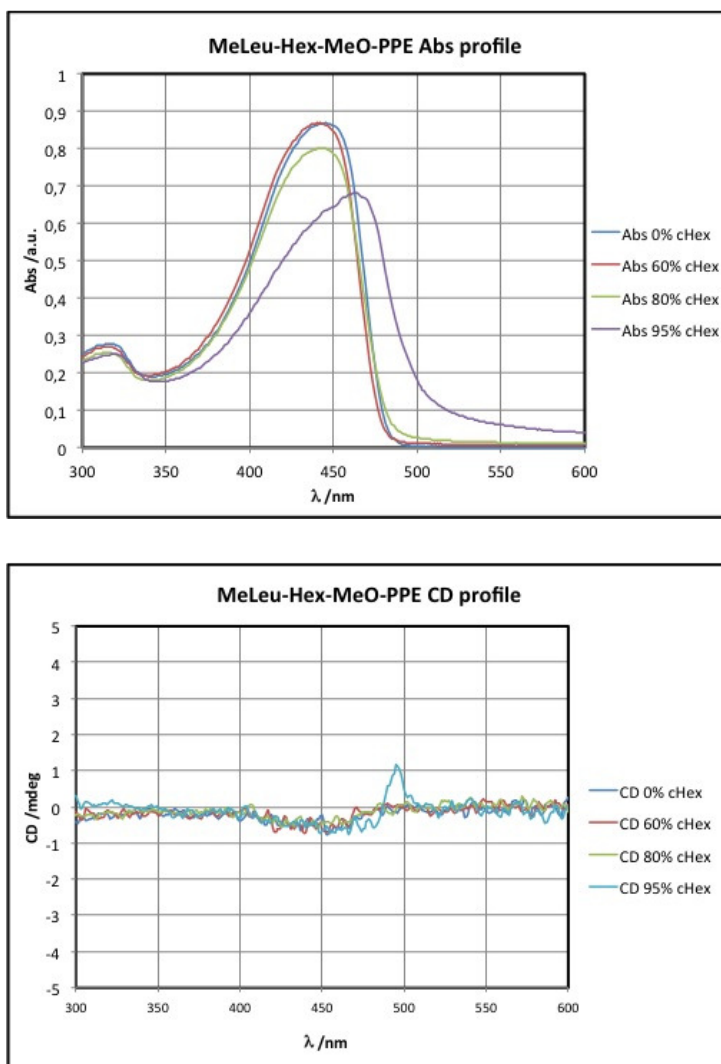
FIGURE 29: ABSORPTION AND ECD SPECTRA IN PRESENCE OF DIFFERENT AMOUNT OF NON-SOLVENT FOR MeLeuHexMeO-PPE

Due to its solubility these spectra were collected using cyclohexane as nonsolvent, and we started to observe aggregation only when at least an 80% of cyclohexane was present. Aggregation was found to be extremely less efficient for MeLeuHexMeO-PPE than for LeuHexMeO-PPE and CD spectra revealed, even with the

95% of cyclohexane, the formation of no particular chiral superstructure. The last result unambiguously demonstrates the importance of hydrogen bonding for these systems, whose role resulted crucial to produce stable chiral aggregates.

A pictorial model of aggregated chains of LueHexMeO-PPE evidencing supramolecular chirality adopted by the polymer backbones (in yellow), the relative dispositions of side chains and the directions of hydrogen bonds is shown in Figure 30. Due to the symmetry properties of the monomeric units, the two carbonyl groups attached to the same ring are pointing toward the same direction (downwards in Figure 30), while the two NH groups are both pointing upwards. Thus, the hydrogen bond network established in our supramolecular aggregates resembles the one observed in parallel beta sheets of polypeptides.
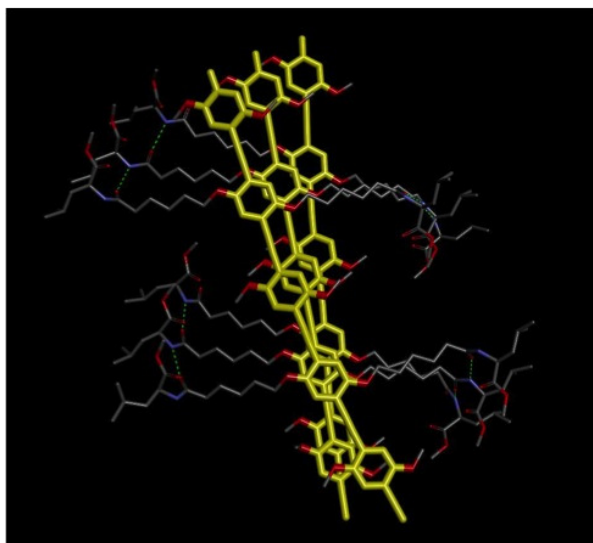
FIGURE 30: PICTORIAL MODEL SHOWING THE SUPRAMOLECULAR CHIRALITY, THE RELATIVE DISPOSITION OF SIDE CHAINS AND THE DIRECTION OF HYDROGEN BONDS.

Interesting results were observed also modifying the aminoacidic derivative linked to the polymeric backbone. In fact, beyond our expectations, together with hydrogen bonds, pronounced effects on the aggregation properties of these systems are ascribable to the substituent on the aminoacidic fragments. These effects were

investigated by studying the optical and chiroptical properties of ValHexMeO-PPE, tLeuHexMeO-PPE and PheHexMeO-PPE. A preliminary indication of a different behavior of these substrates with respect to LeuHexMeO-PPE was revealed by the examination of the absorption profiles. All the spectra were recorded at the same concentration (0.026 mg/mL) and employing the same solvent/non-solvent mixture (CH_2Cl_2/Et_2O). As can be seen from Figure 31 each of these systems presents highly specific characteristics. First of all the fraction of solvent necessary to promote aggregation is specific for every system: if for PheHexMeO-PPE 40% Et_2O is sufficient to observe a small aggregation peak at 490nm, 55% is needed by ValHexMeO-PPE and 60% by the *tert*-leucine derivative.
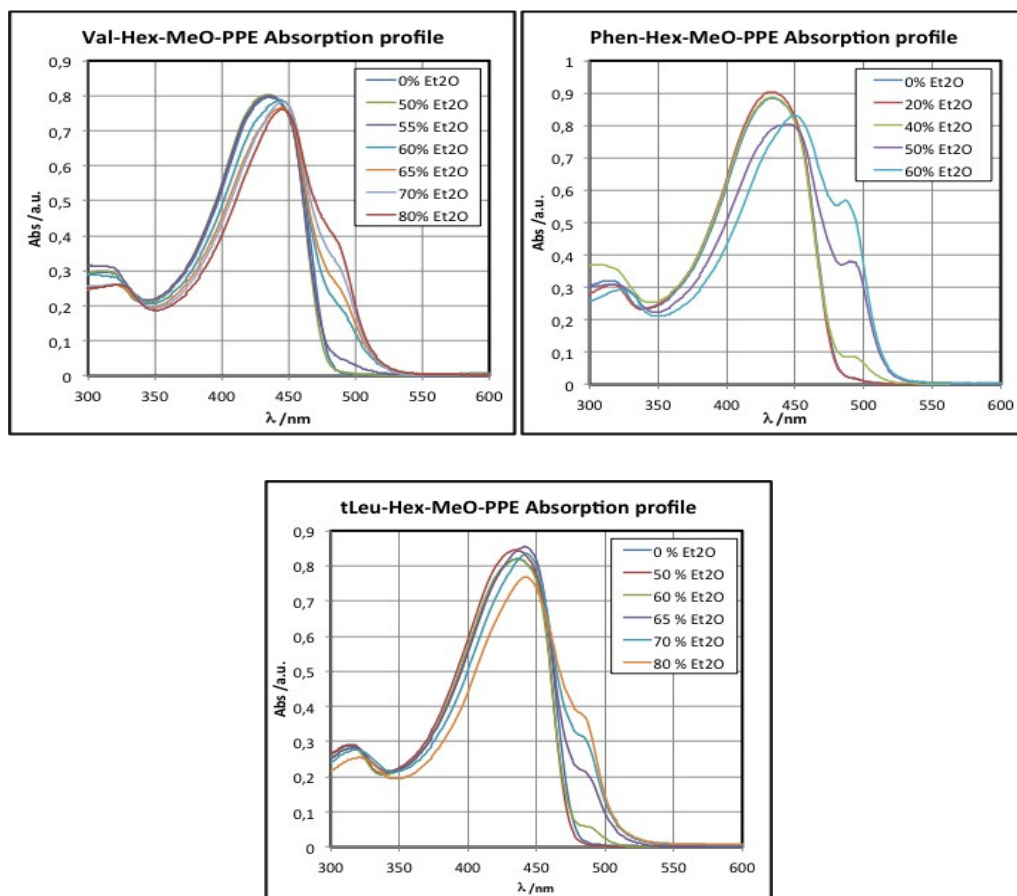
FIGURE 31: ABSORPTION PROFILES FOR ValHexMeOPPE, PhenHexMeOPPE AND tLeuHexMeOPPE

Moreover, also the concentration limit of nonsolvent to avoid precipitation showed the smallest value (60% Et_2O) for Phenylalanine against the 80% of ValHexMeO-PPE and tLeuHexMeO-PPE. More information is provided by the relative intensities and by the shapes of the aggregation peaks. In fact, also in this case, PheHexMeO-PPE exhibited a behavior similar to LeuHexMeO-PPE: increasing with the amount of non-solvent a neat aggregation peak at 490 nm is formed and the main band shifted to the red passing from 440 to 450 nm. Instead, for valine and *tert*-leucine derivatives, the aggregation peak appeared as a shoulder on the main band and the observed red shift resulted smaller. All these observations let us to identify the following trend with respect to the tendency towards aggregation:

LeuHexMeO-PPE ≈ PheHexMeO-PPE > tLeuHexMeO-PPE ≈ ValHexMeO-PPE

This trend seems in first approximation to be consistent with the bulkiness of the substituents on the aminoacidic fragments. However, very interesting and unexpected results about the nature of these aggregates were provided by CD measurements (Figure 32). For PheHexMeO-PPE the aggregation produced an asymmetric positive couplet-like CD feature which attained a *g* value of $4.7^{.}10^{-3}$ at 495 nm. Interestingly, the maximum *g* value was reached when the concentration of the non-solvent was only 40%, and further increasing the fraction of Et_2O resulted in a lowering of the dissymmetry factor.

An explanation of this phenomenon can be provided by an accurate observation of the shapes of the CD bands. In fact, although on a first sight, the CD spectra of PheHexMeO-PPE recorded in presence of amounts of nonsolvent larger than 40%, resembled those of LeuHexMeO-PPE (Figure 28), various differences emerge at a deeper analysis. The different relative intensities of the bands, the absence of an isodichroic point and a progressive pronounced band broadening, together with a blue-shift of the zero-point upon aggregation, make these spectra not describable as a simple ECCD, even considering the vibronic progression. The most likely hypothesis is that, in this case, the formation of a second type of aggregate is

involved, stabilized by larger amounts of nonsolvent. Therefore, the observed CD spectra are in fact the superposition of at least two different set of spectra, allied with distinct aggregation modes.

A comparable behavior was observed also in the case of tLeuHexMeO-PPE. When aggregation started, at 60% of Et$_2$O, a positive ECCD similar to the one of leucine derivative arose, allied with a g value of $5\cdot10^{-3}$, consistent with the formation of chiral supramolecule. Upon further aggregation, as for PhenHexMeO-PPE, the shape of CD spectra changed highlighting also in this case the formation of a second type of aggregate.
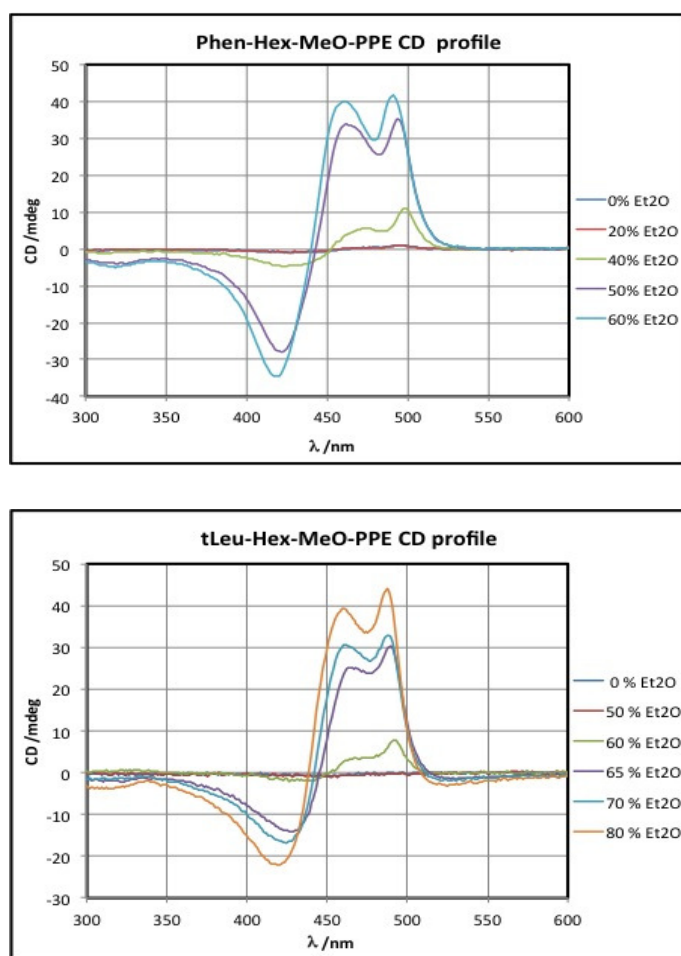
FIGURE 32: ECD PROFILES PhenHexMeOPPE AND tLeuHexMeOPPE

On the basis of the absorption profiles and considering the structural similarities between *tert*-leucine and valine, it was expected for both tLeuHexMeO-PPE and ValHexMeO-PPE an analogous behavior toward aggregation. On the contrary, CD measurements on valine derivative revealed for such species some striking and unforeseen peculiarities (Figure 33). First of all, upon aggregation, we observed a negative CD couplet (g = - 4.7$\cdot$10^{-3} measured at solvent/non-solvent ratio of 40/60) instead of the positive one observed for tLeuHexMeO-PPE and for the other analyzed systems.
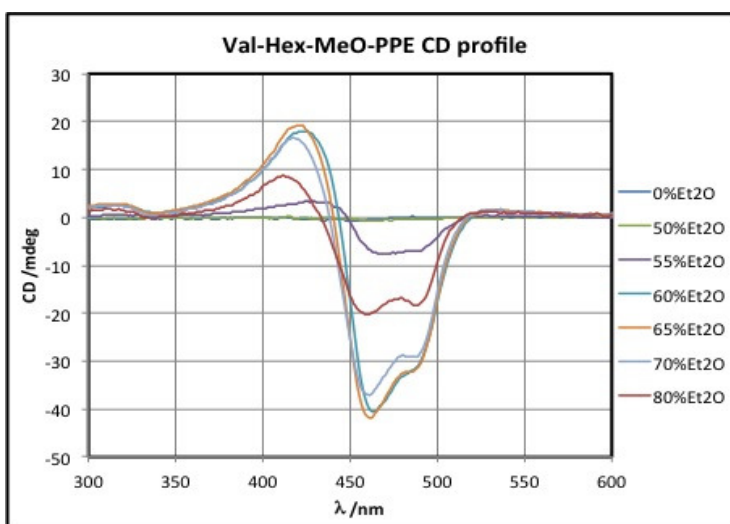
FIGURE 33: ECD PROFILE FOR ValHexMeOPPE

Moreover for ValHexMeO-PPE, even in the early stages of aggregation (i.e. when 60% of diethyl ether was present), the shape of the CD signal looked already different from the one of LeuHexMeO-PPE and addressable to the contemporary presence of two different aggregates. As in the cases of PheHexMeO-PPE and tLeuHexMeO-PPE, further aggregation modified the CD spectra blue-shifting the zero-point and showing a marked band broadening. This interpretation corroborates our hypothesis about the involvement of another kind of aggregate to account for the appearance of ValHexMeO-PPE, PhenHexMeO-PPE and tLeuHexMeO-PPE circular dichroism profiles.

An experimental evidence confirming our hypothesis was supplied by CD spectra collected for all the four described chiral substrates as thin films. Thin films of these materials were prepared by deposition of about 400 µL of a solution in CH_2Cl_2 (1 mg/mL) on a quartz plate and slow evaporation of the solvent in a controlled atmosphere saturated with CH_2Cl_2 vapors.

Thin film obtained with LeuHexMeO-PPE showed an absorption spectrum (Figure 34) similar, apart from some differences in the relative intensities of the two main bands, to the one observed for aggregates dispersed in a non-solvent rich mixture. In the same vein, also PhenHexMeO-PPE's films absorption spectra resemble those of the solution aggregates.
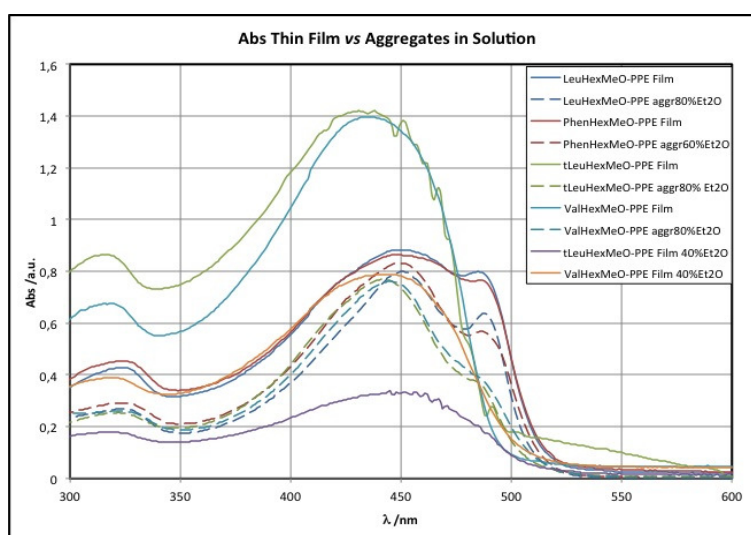
FIGURE 34: COMPARISON BETWEEN ABSORPTION SPECTRA OF LeuHexMeO-PPE, ValHexMeOPPE, PhenHexMeOPPE AND tLeuHexMeOPPE AS THIN FILMS (SOLID LINES) (OBTAINED BY SLOW EVAPORATION OF A CH_2Cl_2 SOLUTION) OR AS AGGREGATES IN SOLUTION (DASHED LINES). ORANGE AND PURPLE LINES SHOW THE ABSORPTION SPECTRA OF FILMS OF ValHexMeOPPE AND tLeuHexMeOPPE PREPARED USING A SOLUTION CONTAINING THE 40% OF NON-SOLVENT

This observation could not be extended to valine and *tert*-leucine derivatives. In fact absorption spectra of their films showed a behavior more comparable to that of

free chains in solution than to that of aggregate species. A different effect was observed when the film of tLeuHexMeO-PPE or ValHexMeO-PPE was prepared starting from a solution which already contains some aggregates. In fact measurements conduced on tLeuHexMeO-PPE and ValHexMeO-PPE films obtained evaporating a solution where 40% of ether was present, exhibited absorption spectra closer to the one of aggregated species in solution.

Moving to ECD characterization, films of LeuHexMeO-PPE prepared from methylene chloride almost perfectly matched the behavior of the aggregates in solution (Figure 35).
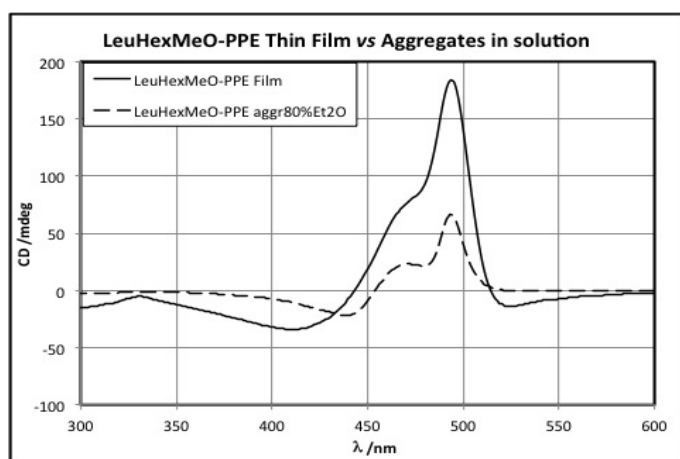
FIGURE 35: COMPARISON BETWEEN ECD SPECTRA OF LeuHexMeO-PPE AS THIN FILM (SOLID LINE) AND AS AGGRREGATE IN SOLUTION (DASHED LINE)

This observation suggests that intermolecular interactions leading to aggregate formation in solvent/nonsolvent mixtures are similarly at work also in the thin films from CH_2Cl_2. As already discussed in section 1.3.1 this behavior is reported in literature to be typical of these materials, justifying the study of aggregation properties in solvent/non-solvent mixtures. Interestingly, the observed g-value for this system resulted to be $9.3 \cdot 10^{-3}$, about 2-fold larger than the one recorded in solution, proving a more efficient coupling of the polymer chains in the solid state.

Films of tLeuHexMeO-PPE and ValHexMeO-PPE casted from CH$_2$Cl$_2$ showed no CD bands confirming the apparent solvated-like nature of the polymer chains in these films. Instead, tLeuHexMeO-PPE and ValHexMeO-PPE films prepared starting from a 60:40 CH$_2$Cl$_2$/ Et$_2$O solvent mixture, as well as PheHexMeO-PPE ones, turned out to be much more interesting. In fact, all the systems showed non-vanishing CD spectra attaining g values of 1.3$\cdot$10^{-3} for PheHexMeO-PPE, 2.5$\cdot$10^{-3} for tLeuHexMeO-PPE and -2.5.10^{-3} for ValHexMeO-PPE. Even though the reported values are about half the ones observed for solution dispersed aggregates, a striking observation arises from the comparison of the shapes of these CD spectra with their homologous in solvent/non-solvent mixtures (Figure 36). In fact, the CD spectra of thin films don't match their correspondent in solution, but resemble the ones obtained for LeuHexMeO-PPE.
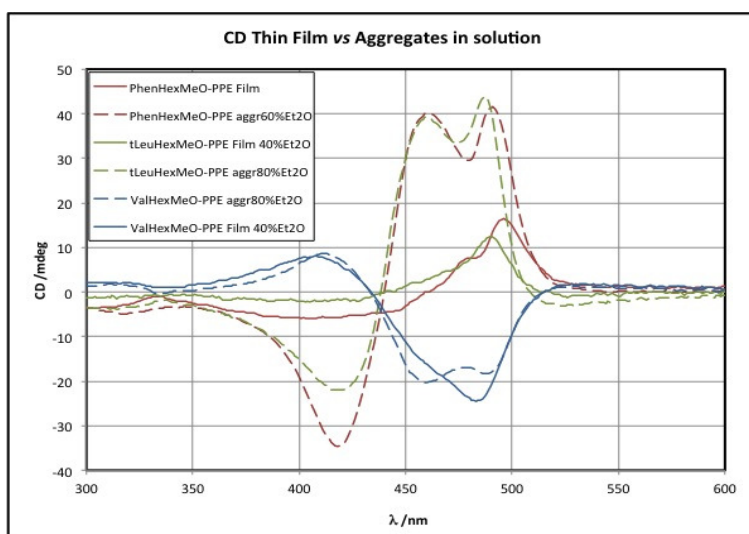
FIGURE 36: COMPARISON BETWEEN ECD SPECTRA OF ValHexMeOPPE, PhenHexMeOPPE AND tLeuHexMeOPPE AS THIN FILMS (SOLID LINES) AND AS AGGRREGATE IN SOLUTION (DASHED LINE). FOR ValHexMeOPPE AND tLeuHexMeOPPE ARE SHOWN ONLY FILMS OBTAINED IN PRESENCE OF NON SOLVENT.

This phenomenon supports the hypothesis based on the coexistence of two different aggregates in nonsolvent rich mixtures and suggests that the interactions responsible for aggregation in the thin films work as observed for the leucine derivative and produce preferentially only one of the two possible aggregates. Thus it

is also reasonable to think that these aggregates roughly possess the same geometrical features of LeuHexMeO-PPE aggregates (apart from the opposite twist observed for the valine derivative). Moreover, it is noteworthy how, passing from valine to *tert*-leucine derivatives (i.e. discriminating between an isopropyl and a *tert*-butyl group), thin films obtained in presence of the same amount of Et$_2$O show practically mirror-image CD spectra (same |g| value, opposite sign, practically identical shape) suggesting supramolecules with almost identical geometrical feature and opposite helicity.
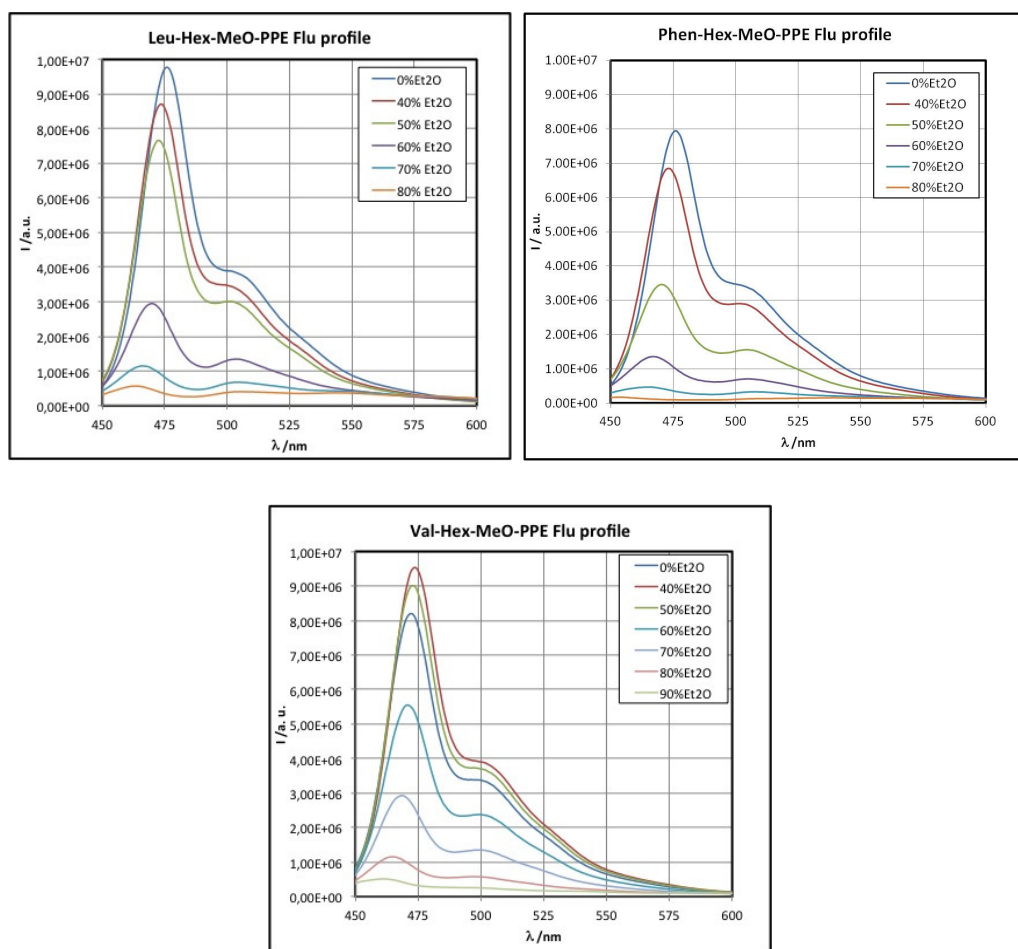
FIGURE 37: FLUORESCENCE PROFILES FOR LeuHexMeOPPE, PhenHexMeOPPE AND ValHexMeOPPE

The aggregation processes in solution for leucine, phenylalanine and valine derivatives were also monitored by photoluminescence experiments. No particular differences were observed in the fluorescence profiles for the three substrates. Upon excitation at 435 nm LeuHexMeO-PPE, PhenHexMeO-PPE and ValHexMeO-PPE (Figure 37) display in dichloromethane a main emission band at about 475 nm with a long-wavelength (probably vibronic) shoulder. The observed Stokes shift with respect to the main absorption band was 35 nm. Increasing the fraction of Et$_2$O caused principally hypochromism and a progressive small blue-shift of the main emission band down to 467 nm (27 nm Stokes shift). When aggregation started, a new band appeared at 504-505 nm (less evident for ValHexMeO-PPE, resembling the behavior observed for absorption spectra) probably due to the formation of the aggregated species. Together with the concentration of Et$_2$O, also the relative intensity of the two bands slightly changes in favor of the 505 nm one, because of the increased relative concentration of the aggregated form, while the non-aggregate band is progressively blue-shifted according to a concentration-dependent shift. The most effective result of nonsolvent addition was however a marked depression of the overall fluorescence intensity (almost completely quenched for the most nonsolvent-rich mixtures), due to the well-known quenching side-effect of aggregation of conjugated polymers.

Summarizing, in the last section it has been presented the synthesis of five aminoacid functionalized PPE copolymers, four chiral and one achiral, through a simple organometallic methodology. These systems were investigated in detail in presence of solvent/non-solvent mixtures and as thin films showing very interesting aggregation properties. First of all, we observed a different behavior toward aggregation between achiral and chiral derivatives. Moreover by means of circular dichroism spectroscopy we were able to obtain precious information about the structural organization of aggregated LeuHexMeO-PPE. The aggregation properties of ValHexMeO-PPE, PheHexMeO-PPE and tLeuHexMeO-PPE with respect to leucine derivative have also been elucidated: two different types of aggregates were observed for these copolymers when dispersed in solution, and only the one of these

was detected in thin films. Finally, for these systems the role of hydrogen bonding interactions was evaluated, demonstrating that they are essential to stabilize chiral superstructure.

3 Final Remarks

Organic conjugated polymers are by far the most promising functional materials in view of applications in inexpensive and flexible electronic devices. Several prototypes of field-effect transistors (OFETs), light-emitting diodes (OLEDs), photovoltaic cells[96], and related devices based on organic materials have already been fabricated, and the first commercial LED based on polymer technology was produced by Philips in 2002. At molecular level, the performances of such devices, depend on polymers' primary structure, but to an even larger extent on their supramolecular organization. Therefore, the characterization and the control of the supramolecular arrangement of these systems constitute a crucial challenge in achieving advanced properties and functions of optoelectronic devices.

The work presented in this thesis moved from the fact that introduction of stereodefinite chiral elements in conjugated polymers has been exploited as a structural modification able, to generate a regular intermolecular chiral orientation of the rigid polymer chains during aggregation processes. In this context, several PPVs and PPEs functionalized with chiral groups with controlled stereochemistry, were prepared and characterized. ECD spectroscopy has proved to be an optimal technique to study these systems, as it allowed, due to its high sensitivity to the presence of chiral aggregated species, to investigate aggregation properties both in the solid state and in solution.

First of all, we focused our investigation on well known systems such as MEH-PPV and MEH-PPE. The aggregation properties of these systems have been extensively investigated in the literature, but on the other hand, the presence of the stereogenic center on the ethylhexyloxy substituent has been completely overlooked.

Therefore we synthesized, respectively *via* Gilch and Horner route of polymerization, a high and a medium-low molecular weight stereospecific MEH-PPV with all stereogenic centers in *(R)* configuration. Aggregation properties of these systems were evaluated in comparison to their non-stereospecific homologous. High molecular weight *(R)*-MEH-PPV showed no particular chiral arrangement in the aggregate. Instead, the observations obtained for low molecular weight derivatives evidenced different behaviors between the aggregates of MEH-PPV and *(R)*-MEH-PPV: the stereospecific system showed a remarkably lower tendency toward aggregation and impressively and the formed aggregates are characterized by strong interchain interactions and a supramolecular negative helicity. The comparison between high and low molecular weight polymers highlights how, also the molecular weight plays a fundamental role indicating that the structure of the aggregates is the result of the balance of weak intermolecular forces.

The same idea led us to the preparation of the stereospecific MEH-PPE. For *(R)*-MEH-PPE aggregation proceeded without any chiral response, and the CD spectra reflected in all cases only the effects of central chirality of the substituents. We conclude that a discrimination based only on different steric hindrances of the ethyl and butyl groups at the chiral center, which is sufficient in the case of low molecular weight *(R)*-MEH-PPV, in this case is not able to compete with the stabilization allied with the complete and symmetric superimposition of π clouds. For these reason we moved our investigation on PPE containing a chiral modifier which could stabilize chiral aggregates by means of stronger ancillary interactions, such as hydrogen bonding.

In this context several novel different PPEs functionalized with α-aminoacids were prepared, through a simple organometallic method, and fully investigated. Chiroptical measurements on the homopolymer LeuHex-PPE revealed that in that case the formation of a stable chiral aggregate is somehow prevented. More stable

chiral aggregates were instead observed in the case of copolymers By means of circular dichroism spectroscopy we obtained precious informations about LeuHexMeO-PPE, ValHexMeO-PPE, PhenHexMeO-PPE and tLeuHexMeO-PPE as aggregates dispersed in solution and as thin films. For these systems, the role of hydrogen bonding resulted to be essential to stabilize chiral superstructure, leading, together with the steric hinderance proper of the aminoacid, to different aggregates as function of the aminoacidic fragment. These observations together with the fact that these products are relatively easy to prepare, not expensive and functionalizable with any aminoacidic derivates make this class of materials suitable for further investigations and, at least in principle, highly tunable.

4 Experimental Section

4.1 General Remarks

All the operations under inert atmosphere were carried out according standard Schlenk technique and employing dried and prepurified nitrogen. When strict anhydrous conditions were required the reaction vessels were oven dried at 120 °C for 12 h prior to use. Thin layer chromatographies were performed using 0.20 mm precoated aluminum silica gel plates purchased by Machery-Nagel GmbH & Co. Flash chromatographies were conduced following standard conditions[97] and using Merck 60 (0.04 – 0.06 mm) silica gel as stationary phase.

4.1.1 Solvents and Reagents

Commercial grade solvents were purified by employing conventional procedures,[98] and stored over activated molecular sieves under nitrogen atmosphere. Purification methods are listed below:

- Acetonitrile(Sigma-Aldrich) and triethylamine (J. T. Baker) were dried by refluxing for 6 hours over CaH_2 and then distilled.

- N,N-dimethylformamide (DMF) (Fluka) was shaken for 72 h with $CaSO_4$ and then distilled under reduced pressure.

- Diisopropylamine (Sigma-Aldrich) was distilled from NaOH.

- n-Hexane and toluene (Sigma-Aldrich) were refluxed for 6 h over Na and then distilled.

- Tetrahydrofuran (THF) (Sigma-Aldrich) was refluxed for 6 h over Na, distilled, refluxed again for 3 h over $LiAlH_4$ and then distilled.

- Dichloromethane (Sigma-Aldrich) was refluxed for 6 h over P_2O_5 and distilled.

When anhydrous conditions weren't strictly required the solvents listed above were employed at commercial grade purity. Petroleum ether b.p. 40 – 60 °C, ethyl acetate, diethyl ether, chloroform (Sigma-Aldrich), acetic acid (Carlo Erba) were used without any further purification. Chloroform, methanol, dichloromethane, diethyl ether (Sigma-Aldrich) and ciclohexane (Carlo Erba) for spectrophotometric and GPC analysis were used at HPLC purity grade.

(2R)-ethylhexanol, 99% e.e. (HPLC), was kindly provided by Prof. Zdenko Hameršak from the Department of Organic Chemistry and Biochemistry, Ruder Boskovic Institute, Zagreb. All the other reagents were purchased from Sigma-Aldrich and employed without further purifications.

4.1.2 Instrumentation

All spectrophotometric experiments were performed at room temperature. Ultraviolet-visible (Uv/Vis) spectra were recorded using a Jasco V-650 spectrophotometer with a 1 cm path length cylindrical quartz cuvette. Electronic Circular Dichroism spectra were recorded using a Jasco J-710 spectropolarimeter with a 1 cm path length cylindrical quartz cuvette registering at least four accumulations. CD measurements on thin films were repeated rotating the sample at 90 and 180° checking the absence of signals due to linear dichroism. Fluorescence experiments were performed employing a Fluorolog Horiba Jobin Yvon fluorimeter employing a 1 cm path length quartz cell. ^{1}H-NMR and ^{13}C-NMR characterization was performed by using a Varian Gemini 600 spectrometer operating at 600 MHz in $CDCl_3$ and in DMSO d[6]; all chemical shifts are reported in the standard δ notations using the peak of the residual proton and of the carbon of CDCl3 and DMSO-d[6] as internal reference. Gel Permeation Chromatography (GPC) analysis was performed by employing a Jasco HPLC system equipped with a PU 2089 pump and a thermostated CO 2065plus column employing IR 2031plus and UV 2077plus as refractive index and spectrophotometric revelator and the calibration was performed with standard uniform polystyrene.

4.1.3 Samples Preparation

Samples for spectrophotometric characterization were prepared by diluting with adequate amounts of solvent and non-solvent a concentrated solution of the desired polymer and tested. Final concentrations were 0.01 mg/mL for high molecular weight MEH-PPV and *(R)*-MEH-PPV, 0,016 mg/mL for low molecular weight MEH-PPV and *(R)*-MEH-PPV, 0,022 mg/mL for MEH-PPE and *(R)*-MEH-PPE and 0,026 mg/mL for each aminoacidic derivative. Thin films of aminoacid functionalized PPEs were prepared by depositing a 400 µL of a 1 mg/mL dichloromethane solution of the desired polymer on a bordered quartz plate, and keeping it in a chamber almost saturated with dichloromethane vapors until the solvent was completely evaporated. Time needed for complete evaporation of the solvent was estimated to be about 2 h. For valine and *tert*-leucine derivative films were prepared also by slow evaporation of 700 µL of a 0.6 mg/mL solution of the desired polymer in a 60:40 CH_2Cl_2/Et_2O mixture.

4.2 Synthetic Procedures

4.2.1 *(R)*-MEH-PPV and MEH-PPV via Gilch Polymerization.

The synthetic pathway is summarized in Scheme 17. For MEH-PPV and *(R)*-MEH-PPV was followed the same synthetic procedure.
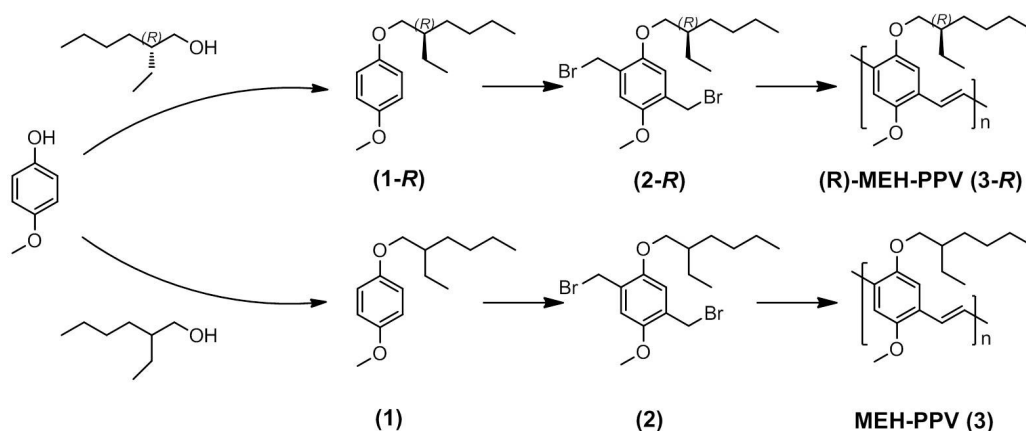
SCHEME 17: PREPARATION OF *(R)*-MEH-PPV AND MEH-PPV *via* GILCH POLYMERIZATION

4.2.1.1 Synthesis of (R)-1-((2-ethylhexyl)oxy)-4-methoxybenzene (1-R)

In a oven dried 100 mL flask, equipped with a dropping funnel, were added under nitrogen atmosphere 2.74 g of 4-methoxyphenol (22.1 mmol), 2.55g of triphenylphosphine (9.7 mmol), 20 mL of dry THF and 1.2 mL of *(R)*-2-ethylhexanol (7.67 mmol). The obtained solution was cooled to 0 °C, and at the same time was prepared in the funnel a solution with 10 mL of dry THF and 1.9 mL of DIAD (9.7 mmol). This solution was dropped in 30 min. The system was allowed to reach room temperature and then stirred for 72 h. The solvent was removed under vacuum and the obtained mixture was separated by flash chromatography on silica gel (petroleum ether/ethyl acetate 9:1 as eluent) affording 1.76 g (7.43 mmol, 97% yield) of **(1-R)** as a colorless liquid. ^{1}H NMR (CDCl$_3$, 298 K), δ (ppm): 6.86 (s, 4H), 3.86 (m, 5H), 1.8-0.8(m, 15H). ^{13}C NMR (CDCl$_3$, 298 K), δ (ppm): 151.15, 151.08, 115.04, 114.80, 72.05, 56.30, 39.68, 30.72, 29.19, 24.10, 23.12, 14.17, 11.30.

4.2.1.2 Synthesis of (R)-1,4-bis(bromomethyl)-2-((2-ethylhexyl)oxy)-5-methoxybenzene (2-R)

To a round-bottom flask were added under N$_2$ atmosphere **(1-R)** (1.74 g, 7.35 mmol), paraformaldehyde (1 g, 33 mmol), acetic acid (4 mL), and 33% HBr in acetic acid (4 mL). The reaction was heated to 70 °C for 4 h. After allowing the reaction to cool to room temperature, the reaction was diluted with chloroform followed by extraction with water and NaHCO$_3$(aq). The chloroform solution was dried over Na$_2$SO$_4$ followed by removal of the chloroform under reduced pressure. Purification by recrystallization from hexane afforded 2.31 g (5.47 mmol, 74.5%yield) of **(2)** as a white powder. ^{1}H NMR (CDCl$_3$, 298 K), δ (ppm): 6.86 (s, 2H), 4.61 (s, 4H), 3.86 (m, 5H), 1.8-0.8(m, 15H). ^{13}C NMR (CDCl$_3$, 298 K), δ (ppm): 151.50, 151.18, 128.03, 127.56, 115.00, 114.70, 72.05, 56.30, 39.68, 30.72, 29.70, 29.19, 24.10, 23.12, 14.17, 11.30

4.2.1.3 Synthesis of (R)-MEH-PPV (3-R) via Gilch Polymerization

To a round-bottom flask, under nitrogen atmosphere, equipped with a mechanical stirrer and a dropping funnel, were added **(2-R)** (2.24 g, 5.3 mmol), and

dry THF (110 mL). A solution of potassium *tert*-butoxide in dry THF (23 mL, 1.0 M) was then dropped down in 30 min. After complete addition of the base, the reaction was stirred for an additional 16 h. The reaction was poured into 300 ml of rapidly stirred methanol, and the resulting polymer was collected by suction filtration. The polymer was then purified by dissolution into 120 mL of CHCl$_3$ and subsequent precipitation into 300 mL of rapidly stirred methanol. The polymer was isolated by suction filtration and dried under reduced pressure to give 0.90 g (65% yield) of **(3-R)** as a bright red powder. Mol. Wt.: M$_n$= 401.203 kDa (PDI) of 1.87 determined by GPC with uniform polystyrene standards in CHCl$_3$. ^{1}H NMR (CDCl$_3$, 298 K), δ (ppm): 7.5-7.1 (bm, 2H), 6.9(bs, 2H), 3.9 (bs, 5H), 1.8-0.8 (bm, 15H). ^{13}C NMR gave no significant signals because of high polymer dimensions.

4.2.1.4   Synthesis of 1-((2-ethylhexyl)oxy)-4-methoxybenzene (1)

For this preparation was followed exactly the same procedure described in 4.2.1.1 using racemic 2-ethylhexanol instead of *(R)*-2hetylhexanol.Also in this case were obtained 1.75 g (7.43 mmol, 97% yield) of **(1)** as a colorless liquid. ^{1}H NMR (CDCl$_3$, 298 K) and ^{13}C NMR (CDCl$_3$, 298 K) were completely superimposable to those of **(1-R).**

4.2.1.5   Synthesis of 1,4-bis(bromomethyl)-2-((2-ethylhexyl)oxy)-5-methoxy-benzene (2)

For this preparation was followed exactly the same procedure described in 4.2.1.2 using **(1)** instead of **(1-R)**. Also in this case were obtained 2.35 g (5.48 mmol, 75% yield) of **(2)** as white powder. ^{1}H NMR (CDCl$_3$, 298 K) and ^{13}C NMR (CDCl$_3$, 298 K) were completely superimposable to those of **(2-R)**.

4.2.1.6   Synthesis of MEH-PPV (3) via Gilch Polymerization

For this preparation was followed exactly the same procedure described in 4.2.1.3 using **(2)** instead of **(2-R)**. 0.92 g (65% yield) of **(3)** were obtained as a bright red solid. Mol. Wt. determined by GPC with uniform polystyrene standards was found

to be M_n = 400.251 kDa with a (PDI) of 1.84. ^{1}H NMR (CDCl$_3$, 298 K) was completely superimposable to those of **(3-R)**.

4.2.2 *(R)*-MEH-PPV and MEH-PPV via Horner Polycondensation

The synthetic pathway is summarized in Scheme 18. For MEH-PPV and *(R)*-MEH-PPV was followed the same synthetic procedure.

4.2.2.1 Synthesis of (R)-2-methoxy-5-(2-ethylhexyloxy)-1,4-xylylene-bis(diethylphosphonate) (4-R)

In a 25 mL round-bottom flask it was prepared a mixture of triethyl phosphite (3 mL, 2.907 g; 17.4 mmol) and **(2-R)** (0.85 g; 2.01 mmol) it was heated slowly to a temperature of 150 °C, and the evolving ethyl bromide distilled off simultaneously. After 2 h, vacuum was applied for another 15 min at 180 °C. The obtained bright yellow oil was then allowed to cool to room temperature. Upon addition of 10 mL of petroleum ether **(4-R)** crystallized yielding 0.95 g (1.77 mmol, 88% yield) of white crystals. ^{1}H NMR (CDCl$_3$, 298 K), δ (ppm): 6.93 (s, 1H), 6.87 (s, 1H), 3.99 (m, 8H), 3.78(m, 5H), 3.18 (dd, 4H), 1.91 (quint, 1H), 1.73-0.81 (m, 26H). ^{13}C NMR (CDCl$_3$, 298 K) δ (ppm): 151.32, 150.61, 120.61, 119.85, 114.83, 114.05, 71.21, 61.82, 61.75, 56.11, 39.75, 38.91, 38.45, 29.12, 27.42, 23.91, 23.01, 16.35, 16.28, 14.02, 11.12.
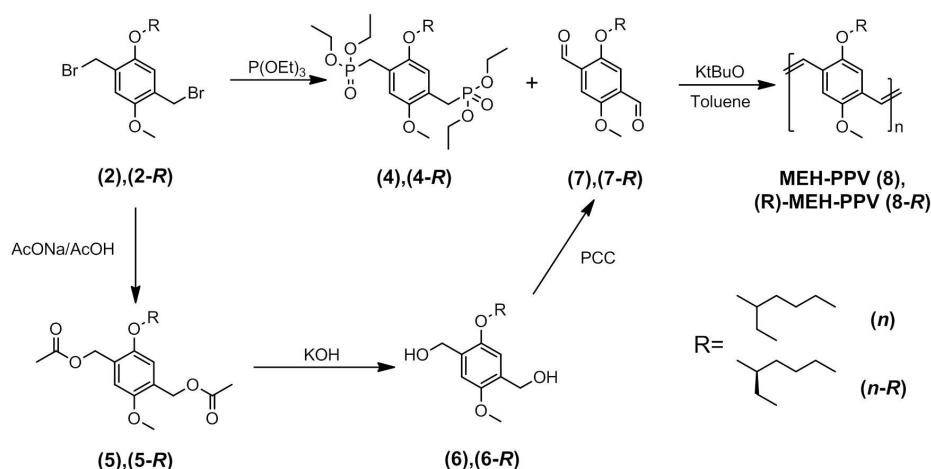
SCHEME 18: PREPARATION OF *(R)*-MEH-PPV AND MEH-PPV *via* HORNER POLYCONDENSATION

4.2.2.2 Synthesis of (R)-1,4-bis-(acetoxymethyl)-2-methoxy-5-(2-ethylhexyloxy)-benzene (5-R)

A stirred suspension of **(2-R)** (1 g; 2.35 mmol) and sodium acetate (600 mg; 7.2 mmol) in glacial acetic acid (15 mL) was heated at reflux for 6 h. The reaction mixture was filtered and concentrated under reduced pressure. Water was added and the mixture was extracted with chloroform. The organic layer was washed with water, dried over Na_2SO_4, and the solvent removed to give 0.87 g (2.28 mmol, 97% yield) of **(5-R)** as a colorless oil. ^{1}H NMR (CDCl$_3$, 298 K), δ (ppm): 6.87 (bs, 2H), 5.12 (s, 4H), 3.82 (m, 2H), 3.79 (s, 3H), 2.07 (d, 6H), 1.68 (hept, 1H), 1.5-1.2 (m, 8H), 0.89 (m 6H).

4.2.2.3 Synthesis of (R)- 1,4-bis(hydroxymethyl)-2-methoxy-5-(2-ethylhexyloxy)-benzene (6-R)

To a solution of **(5-R)** (0.85 g; 2.23 mmol) in a 1:1 mixture of THF and CH$_3$OH (6 mL) was added dropwise a 10% KOH solution in methanol (0.7 mL). The reaction mixture was heated at reflux for 6 h. After allowing the mixture to cool, chloroform was added, and the obtained mixture was washed three times with water, dried over Na$_2$SO$_4$ and the solvent was evaporated under reduced pressure to afford 0.60 g (2.03 mmol, 91% yield) of **(6-R)** as yellowish oil. ^{1}H NMR (CDCl$_3$, 298 K), δ (ppm): 6.85 (s, 2H), 4.65 (d, 4H), 3.8 (dd, 2H), 3.7 (s; 3H), 2.14 (bs,2H, OH), 1.7 (hept, 1H), 1,50-1,20(m, 8H), 0.89 (m, 6H).

4.2.2.4 Synthesis of (R)-2-((2-ethylhexyl)oxy)-5-methoxyterephthalaldehyde (7-R)

A stirred suspension of **(6-R)** (0.59 g; 2 mmol) and PCC (1.38 g; 6.39 mmol) in 20 mL of dichloromethane was refluxed for 2 h. The obtained black precipitate was filtered off and the solution was concentrated under vacuum. The crude product was purified by flash chromatography over silica gel with dichloromethane as eluent yielding 506 mg (1.73 mmol 86% yield) of bright yellow crystals of **(7-R)**. ^{1}H NMR (CDCl$_3$, 298 K), δ (ppm): 10.49 (d,2H), 7.42 (bs, 2H), 3.96 (dd, 2H), 3.92 (s, 3H), 1.76 (hept, 1H), 1.50-1.20 (m, 8H), 0.89 (m,6H). ^{13}C NMR (CDCl$_3$, 298 K) δ (ppm): 191.05,

152.72, 151.89, 131.61, 130.82, 115.6, 114.7, 74.91, 55.82, 40.31, 29.93, 28.62, 23.82, 23.05, 14.35, 11.65.

4.2.2.5   Synthesis of (R)-MEH-PPV (8-R) via Horner Polycodensation

Under nitrogen atmosphere **(7-R)** (500 mg, 1.7 mmol) and **(4-R)** (900 mg; 1.7 mmol) were dissolved in dry toluene (25 mL) whilst stirring and heating at reflux. To this solution was added solid potassium *tert*-butoxide (570 mg; 5.2 mmol) in one portion. The solution immediately turned to red. After 5 h at reflux the reaction mixture was allowed to reach room temperature, diluted with additional toluene and quenched with HCl (aq) (15 mL). The organic layer was then separated, washed several times with distilled water, and dried with Na_2SO_4. The resulting toluene solution was filtered, concentrated to about 20 mL, and precipitated into rapidly stirred methanol (100 mL). The polymer was separated by centrifugation, dissolved in chloroform and precipitated again with methanol. The obtained solid was collected by centrifugation and dried under vacuum affording 560 mg (60% yield) of bright red fibers. Mol. Wt.: M_n = 10200 Da, PDI = 1.50 determined by GPC with uniform polystyrene standards in $CHCl_3$.^{1}H NMR ($CDCl_3$, 298 K), δ (ppm): 7.5-7.1 (bm, 1.5H), 6.9(bs, 2H), 6.5-6.8 (bm, 0.5H) 3.9 (bm, 5H), 1.8-0.8 (bm, 15H).

4.2.2.6   Photoisomerization of (R)-MEH-PPV (8-R)
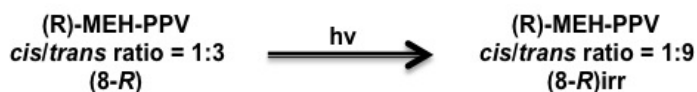
SCHEME 19

In a 25 mL Schlenk tube, under nitrogen atmosphere, 20 mg of **(8-R)** were dissolved in 10 mL of dry and degassed THF. The system was then irradiated by a 125 W medium pressure arc mercury lamp. The reaction was monitored by UV/Vis spectroscopy checking the shift of the absorption maximum. After about *30 min* the absorption maximum passed from 473 to 484 nm. Further UV irradiation didn't produce any

modifications. The solution was then concentrated at about 3 mL and poured into 15 mL of rapidly stirred methanol. The obtained red solid was collected by centrifugation and dried under vacuum affording **(8-R)irr** almost quantitatively. ^{1}H NMR (CDCl$_3$, 298 K), δ (ppm): 7.5-7.1 (bm, 1.8H), 6.9(bs, 2H), 6.5-6.8 (bm, 0.2H) 3.9 (bm, 5H), 1.8-0.8 (bm, 15H).

4.2.2.7 *Synthesis of MEH-PPV (8) via Horner Polycodensation*

All the intermediates **(4)**, **(5)**, **(6)**, **(7)** were prepared following exactly the same procedure adopted for **(4-R)**, **(5-R)**, **(6-R)**, **(7-R)** starting from **(2)** instead of **(2-R).** For these systems NMR spectra were completely superimposable to those of their homologous. Reaction yields for the preparation of each intermediate are reported in Table 3

TABLE 3

	(4)	**(5)**	**(6)**	**(7)**
Reaction yield %	86	96	91	83

Also **MEH-PPV (8)** was prepared as described in section 4.2.2.5 for **(R)-MEH-PPV (8-R).** 573 mg (62% yield) of **(8)** were obtained as a bright red solid. Mol. Wt.: M_n = 10050 Da, PDI = 1.52. ^{1}H NMR and ^{13}C NMR were equal to those reported for **(8-R)**.

4.2.3 Preparation of *(R)*-MEH-PPE and MEH-PPE

The complete synthetic pathway is summarized in Scheme 20.

4.2.3.1 *Synthesis of (R)-2,5-diiodo-4-((2-ethylhexyl)oxy)methoxybenzene (9-R)*

Compound **(1-R)** (1.6 g, 7.2 mmol), KIO$_3$ (0.62 g, 2.9 mmol) and I$_2$ (2 g, 8 mmol) were added to a stirred solution of acetic acid (45 mL), 96% H$_2$SO$_4$ (1 mL) and H$_2$O (3.5 mL). The reaction mixture was heated to reflux under stirring for 16 h and then cooled to room temperature. Aqueous Na$_2$S$_2$O$_4$ (20%) was added until the brown color of

iodine disappeared and the reaction mixture was dilute with dichloromethane and extracted with NaOH (aq, 10%) and brine.

(1-R),(1)   **(9-R),(9)**   **(11-R),(11)**   **(12-R),(12)**

(10-R),(10)
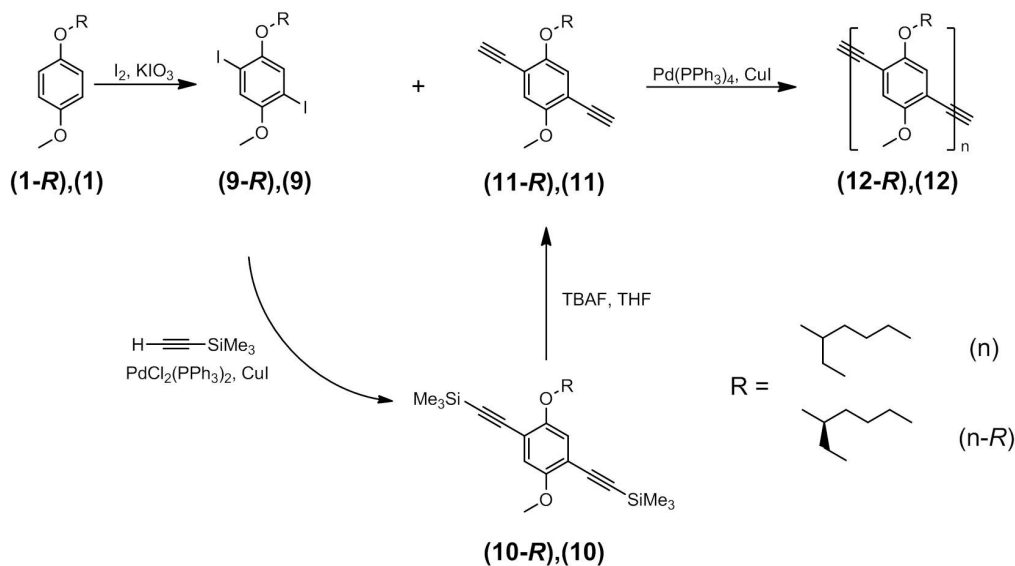
SCHEME 20: PREPARATION OF *(R)*-MEH-PPE AND MEH-PPE

The organic layers were dried over Na_2SO_4 and the solvent was evaporated to yield an orange oil. The crude product was purified by flash chromatography on silica gel with petroleum ether/AcOEt 8:2 affording (2.25 g, 4.6 mmol, 64% yield) pure **(9-R)** as a colorless oil. ^{1}H NMR (CDCl$_3$, 298 K) δ (ppm): 7.17(s, 1H), 7.15 (s,1H), 3.80 (m, 5H), 1.71 (hept, 1H), 1.6-1.4 (m, 6H), O.91 (m, 8H). ^{13}C NMR (CDCl$_3$, 298 K) δ (ppm): 153.20, 153.13, 122.48, 121.54, 86.12, 85.55, 72.53, 56.67, 39.47, 30.52, 29.05, 23.95, 23.01, 14.32, 11.52.

4.2.3.2 Synthesis of (R)- 2,5-bis-(trimethylsilyl)ethynyl-4-((2-ethylhexyl)oxy)methoxybenzene (10-R)

Compound **(9-R)** (1 g, 2.1 mmol), PdCl$_2$(PPh$_3$)$_2$ (70 mg, 100 μmol) and CuI (20 mg, 100 μmol) were dissolved in 7 mL of diisopropylamine under nitrogen atmosphere. Thus, trimethylsilylacetylene (610 μL, 420 mg, 4.27 mmol) was added at room temperature over the course of 10 min to the vigorously stirred solution; during the addition a white precipitate formed. After the addition was complete, the

reaction mixture was heated to reflux under stirring for 1 h. After cooling to room temperature, toluene (5 mL) was added and the white precipitate was filtered off. The solution was concentrated and passed through a chromatography column (silica gel) using toluene as eluent. Evaporation of the solvent led to **(10-R)** as an orange oil (768 mg, 1.87 mmol, 88.7% yield), which crystallized upon standing at 0 °C. ^{1}H NMR (CDCl$_3$, 298 K), δ (ppm): 6.88 (s,1H), 6.87 (s,1H), 3.85 (m, 2H), 3.81(s, 3H) 1.17 (hept, 1H), 1.6-1.4 (m, 6H), 0.91 (m, 8H), 0.21 (s, 18H). ^{13}C NMR (CDCl$_3$, 298 K) δ (ppm): 154.43, 154.12, 117.42, 115.79, 114.03, 113.45, 101.12, 101.03, 100.24, 100.16, 71.78 , 56.51, 39.74 , 30.59, 29.20, 23.99, 23.13 , 14.15, 11.35 , 0.08.

4.2.3.3 Synthesis of 2,5-diethynyl-4-((2-ethylhexyl)oxy)methoxybenzene (11-R)

A solution of 1.5 g (4.75 mmol) of tetrabutylammonium fluoride trihydrate in 5 mL of THF was added dropwise to 13 mL of THF containing 760 mg (1.85 mmol) of **(10-R).** The obtained dark mixture was stirred overnight. The reaction was quenched by adding 50 mL of water and extracted three times with dichloromethane. The organic phase was dried over Na$_2$SO$_4$ and the solvent was evaporated under vacuum. The crude product was purified by flash chromatography (hexane/AcOEt 9:1 as eluent) affording 451 mg of **(11-R)** (1.66 mmol, 89% yield) as an orange oil. ^{1}H NMR (CDCl$_3$, 298 K), δ (ppm): 6.94 (s, 1H), 6.93 (s, 1H), 3.83 (m, 5H), 3.33 (m, 2H), 1.71 (hept, 1H), 1.6-1.4 (m, 6H), 0.91 (m, 8H). ^{13}C NMR (CDCl$_3$, 298 K) δ (ppm): 154.44, 154.29 , 117.82, 116.00 , 113.44, 112.55 , 82.52, 82.48, 79.77, 79.71 , 72.19 ,56.42 , 39.40 , 30.51, 29.05, 23.90, 23.02 , 14.04, 11.14 .

4.2.3.4 Synthesis of (R)-MEH-PPE (12-R)

Under inert atmosphere Pd(PPh$_3$)$_4$ (70 mg, 62 μmol) and CuI (10 mg, 62 μmol) were added to a solution of **(9-R)** (660 mg, 1.39 mmol) and **(11-R)** (450 mg, 1.66 mmol) in 30 mL of toluene an 14 mL of diisopropylamine, in presence of 37 μL (0.32 mmol) of iodobenzene as chain terminator. The reaction mixture was stirred at 75 °C; ammonium iodide salts were formed immediately after the start of the reaction and

the mixture became highly fluorescent. After a reaction time of 20 h, the reaction mixture was cooled to room temperature and added dropwise to rapidly stirred methanol (600 mL). The precipitate was collected by suction filtration and re-precipitated from CHCl$_3$/methanol. The polymer **(12-R)** was isolated and dried under vacuum to yield 630 mg, (76%yield) as a bright yellow solid. Mol. Wt.: M$_n$ = 14820 Da PDI = 1.78 determined by GPC with uniform polystyrene standards in CHCl$_3$. ^{1}H NMR (CDCl$_3$, 298 K), δ (ppm): 7.05 (bm, 2H), 3.89 (bm, 5H), 1.71 (bm, 1H), 1.6-1.4 (bm, 6H), 0.91(bm, 8H).

4.2.3.5   Synthesis of MEH-PPE (12)

All the intermediates **(9)**, **(10)** and **(11)** were prepared following exactly the same procedure adopted for **(9-R)**, **(10-R)** and **(11-R)** starting from **(1)** instead of **(1-R).** For these systems NMR spectra were completely superimposable to those of their homologous. Reaction yields for the preparation of each intermediate are reported in Table 4

TABLE 4

	(9)	(10)	(11)
Reaction yield %	66	87	89

Also **MEH-PPE (12)** was prepared as described in section 4.2.3.4 for *(R)-*MEH-PPE **(12-R).** 620 mg (73% yield) of **(8)** were obtained as a bright yellow solid. Mol. Wt.: M$_n$ = 15050 Da, PDI = 1.81. ^{1}H NMR and ^{13}C NMR showed the same resonances observed for **(12-R)**.

4.2.4   Preparation of LeuHex-PPE

The synthetic pathway is shown in Scheme 21
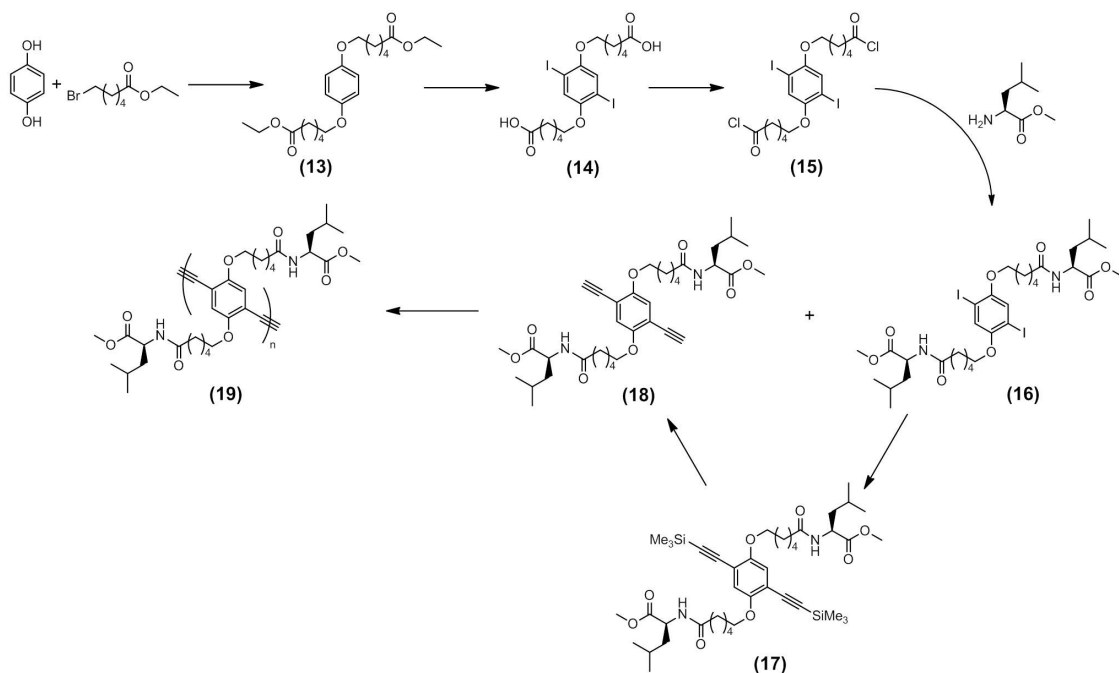
SCHEME 21: PREPARATION OF LeuHex-PPE

4.2.4.1 *Synthesis of diethyl 6,6'-(1,4-phenylenebis(oxy))dihexanoate (13)*

1,4-Hydroquinone (2 g, 18 mmol) was added to a stirred suspension of anhydrous potassium carbonate (24.5 g) in dry acetonitrile (160 ml). Ethyl-6-bromohexanoate (8.67 g, 39 mmol) was then added. The reaction was stirred under nitrogen and refluxed for 4 days. Since the reaction had gone to completion, it was then filtered and the residue was washed with DCM. The solvent was then evaporated under reduced pressure. The resulting product was then redissolved in DCM and washed with water. The organic layer was then dried with Na_2SO_4, filtered and evaporated affording **(13)** 5.89 g (14.85 mmol 83% yield) as white powder. ^{1}H NMR (CDCl$_3$, 298 K), δ (ppm): 6.99 (s, 4H), 4.11 (quar, 4H), 3.89 (t, 4H), 2.32 (t, 4H), 1,75 (quint, 4H), 1.67 (quint, 4H), 1.47 (quint, 4H), 1.24 (t, 6H). ^{13}C NMR (CDCl$_3$, 298 K) δ (ppm):173.55, 151.92, 114.83, 68.75, 59.33, 36.41, 28.95, 25.23, 24.90, 14.13.

4.2.4.2 Synthesis of 6,6'-(2,5-diiodo-1,4-phenylene)bis(oxy)dihexanoic acid (14)

KIO$_3$ (1.5 g, 7.18 mmol) and I$_2$ (3.95 g, 15.5 mmol) were dissolved in a mixture of acetic acid (118 mL), H$_2$SO$_4$ (3.5 mL) and water (10 mL), and then compound **(13)** (5.85 g, 14.75 mmol) was added. The resulting mixture was stirred at 75 °C for 24 h. After cooled in ice-water bath, the reaction mixture was filtered and washed several times with cold ethanol. The final product was collected and dried under vacuum affording 5.92 g (10.02 mmol 68% yield) as white powder. ^{1}H NMR (DMSO, 298 K), δ (ppm): 7.28 (s, 2H), 3.91 (t, 4H), 2.18 (t, 4H), 1.65 (quint, 4H), 1.52 (quint, 4H), 1.42 (quint, 4H).

4.2.4.3 Synthesis of 6,6'-(2,5-diiodo-1,4-phenylene)bis(oxy)dihexanoyl chloride (15)

1.7 g (2.88 mmol) of **(14)** were suspended in 8 mL of SOCl$_2$. Then two drops of DMF were added and the system was refluxed for two hours until complete dissolution of the solid was observed. The excess of SOCl$_2$ was then removed under vacuum affording a brown viscous oil which crystallized upon standing at 0 °C. The crude product was then recrystallized from 40 mL of a 10:1 mixture of heptane/toluene, affording 1.58 g (2.53 mmol 88% yield) of **(15)** as a pearl white crystalline solid extremely sensitive to atmospheric humidity. ^{1}H NMR (CDCl$_3$, 298 K), δ (ppm): 7.15(s, 2H), 3.92 (t, 4H), 2.95 (t, 4H), 1,79 (m, 8H), 1.58 (m, 4H).

4.2.4.4 Synthesis of leucine functionalized diiodoarene derivative (16)

In strict anhydrous conditions leucine methyl ester hydrochloride (1.01 g, 5.6 mmol), 4 mL of Et$_3$N and 35 ml of dry CH$_2$Cl$_2$ were placed in a round bottom flask and cooled with an ice/water bath. Then compound **(15)** (1.58 g, 2.53 mmol) in 25 mL of CH$_2$Cl$_2$ was added. After 2 hours, the reaction mixture was allowed to warm to room temperature and further stirred for 24 hours. The solvent was removed under vacuum and the crude product was purified by flash chromatography (silica gel, CH$_2$Cl$_2$/AcOEt 4:1) to give 1.75 g (2.07 mmol, 82% yield) of **(16)** as a white solid. [1]H

NMR (CDCl$_3$, 298 K), δ (ppm): 7.14 (s, 2H), 5.81 (d, 2H), 4.63 (td, 2H), 3.90 (t, 4H), 3.71 (s, 6H), 2.25 (t, 4H), 1.80 (quint, 4H), 1.71 (quint, 4H), 1.63 (m, 5H), 1.52 (m, 5H), 0.92 (t, 12H). ^{13}C NMR (CDCl$_3$, 298 K) δ (ppm): 173.80, 172.83, 151.45, 123.10, 89.15. 69.61, 52.32, 50.65, 41.95, 36.55, 28.96, 25.60, 25.32, 24.93, 22.76, 21.92.

4.2.4.5 Synthesis of leucine functionalized bis-trimethylsilil arildiyne derivative (17)

Compound **(16)** (1 g, 1.2 mmol), PdCl$_2$(PPh$_3$)$_2$ (70 mg, 100 μmol) and CuI (20 mg, 100 μmol) were dissolved in 10 mL of CH$_2$Cl$_2$ and 15 mL of Et$_3$N under nitrogen atmosphere. Thus, trimethylsilylacetylene (185 μL, 268 mg, 2.7 mmol) was added. After the addition was complete, the reaction mixture was heated to reflux and stirred for 2 h. After cooling to room temperature, the white precipitate was filtered off and the solvent was evaporated under vacuum. The crude product was purified by flash chromatography (silica gel, CH$_2$Cl$_2$/AcOEt 5:1 as eluent) affording 838 mg (1.07 mmol, 89% yield) of **(17)** as a yellowish solid. ^{1}H NMR (CDCl$_3$, 298 K), δ (ppm): 6.85 (s, 2H), 5.77 (d, 2H), 4.62 (td, 2H), 3.92 (t, 4H), 3.70 (s, 6H), 2.22 (t, 4H), 1.79 (quint, 4H), 1.69 (quint, 4H), 1.62 (m, 5H), 1.51 (m, 5H), 0.91 (t, 12H), 0.21 (s, 18H). ^{13}C NMR (CDCl$_3$, 298 K) δ (ppm): 173.69, 172.63, 153.99, 117.17, 114.14, 101.11, 100.35, 69.29, 52.32, 50.65, 42.01, 36.41, 28.94, 25.60, 25.23, 24.89, 22.76, 21.93, 3.40.

4.2.4.6 Synthesis of leucine functionalized arildiyne derivative (18)

A solution of 0.9 g (2.73 mmol) of tetrabutylammonium fluoride trihydrate in 5 mL of THF was added dropwise to 8 mL of THF containing 835 mg (1.06 mmol) of **(17).** The obtained dark mixture was stirred overnight. The reaction was quenched by adding 50 mL of water and extracted three times with dichloromethane. The organic phase was dried over Na$_2$SO$_4$ and the solvent was evaporated under vacuum. The crude product was purified by flash chromatography (CH$_2$Cl$_2$/AcOEt 5:1 as eluent) affording 602 mg of **(18)** (0.94 mmol, 89% yield) as yellowish solid. ^{1}H NMR (CDCl$_3$, 298 K), δ (ppm): 6.92 (s, 2H), 5.78 (d, 2H), 4.63 (td, 2H), 3.96 (t, 4H), 3.71 (s, 6H) 3.33 (s, 2H), 2.23 (t, 4H), 1.81 (quint, 4H), 1.70 (quint, 4H), 1.61 (m, 5H), 1.52 (m, 5H), 0.91

(t, 12H). ^{13}C NMR (CDCl$_3$, 298 K) δ (ppm): 173.71, 172.66, 153.70, 118.18, 114.15, 82.36, 81.45, 69.89, 52.35, 50.63, 42.01, 36.41, 28.95, 25.60, 25.23, 24.89, 22.81, 22.12.

4.2.4.7   *Synthesis of LeuHex-PPE (19)*

In a round bottom flask were placed under nitrogen atmosphere 220 mg (0.34 mmol) of **(18)**, 290 mg (0.34 mmol) of **(16)**, 17.5 mg (15 μmol, 4.5%) of Pd(PPh$_3$)$_4$ and 3 mg (15 μmol, 4.5%) of CuI. Thus 3 mL of Et$_3$N and 7 mL and CH$_2$Cl$_2$ were added and the obtained dark solution was refluxed under stirring for 48 h. Then the system was allowed to reach room temperature, diluted with CH$_2$Cl$_2$ and extracted three times with water. The organic phase was dried over Na$_2$SO$_4$ and concentrated to about 15 mL. Then about 50 mL of Et$_2$O were added and the formed precipitate was separated by centrifugation. Thus the solid was dissolved again in 15 mL of chloroform and precipitated with 50 mL of Et$_2$O. The precipitate was collected by centrifugation washed with Et$_2$O and dried under vacuum. We obtained 315 mg (76% yield) of **(19)** as yellow orange powder. Mol. Wt.: M$_n$ = 8950 Da PDI = 1.72 determined by GPC with uniform polystyrene standards in CHCl$_3$. ^{1}H NMR (CDCl$_3$, 298 K), δ (ppm): 7.00 (bs, 2H), 6.45 (bm, 2H), 4.59 (bm, 2H), 4.03 (bm, 4H), 3.69 (bs, 6H), 2.25 (bm, 4H), 1.85 (bm, 4H), 1.72 (bm, 4H), 1.6-1.4 (bm, 10H), 0.91 (bm, 12H). ^{13}C NMR (CDCl$_3$, 298 K) δ (ppm): 173.91, 172.80, 153.66, 115.91, 113.63, 91.27, 69.75, 52.35, 50.68, 41.75, 36.37, 29.21, 25.83, 25.22, 24.87, 22.56, 21.92.

4.2.5   **Preparation of Aminoacid Functionalized PPE Copolymers.**

Aminoacid functionalized PPE copolymers were prepared according to Scheme 22

4.2.5.1   *Synthesis of valine functionalized diiodoarene derivative (20)*

In strict anhydrous conditions valine methyl ester hydrochloride (470 mg, 2.8 mmol), 3 mL of Et$_3$N and 25 ml of dry CH$_2$Cl$_2$ were placed in a round bottom flask and cooled with an ice/water bath. Then compound **(15)** (800 mg, 1.27 mmol) in 15 mL of

CH$_2$Cl$_2$ was added. After 2 h, the reaction mixture was allowed to warm to room temperature and further stirred for 24 h.

R = iBu (16)
 iPr (20)
 Bn (21)
 tBu (22)
 H (23)

R = iBu (24)
 iPr (25)
 Bn (26)
 tBu (27)
 H (28)
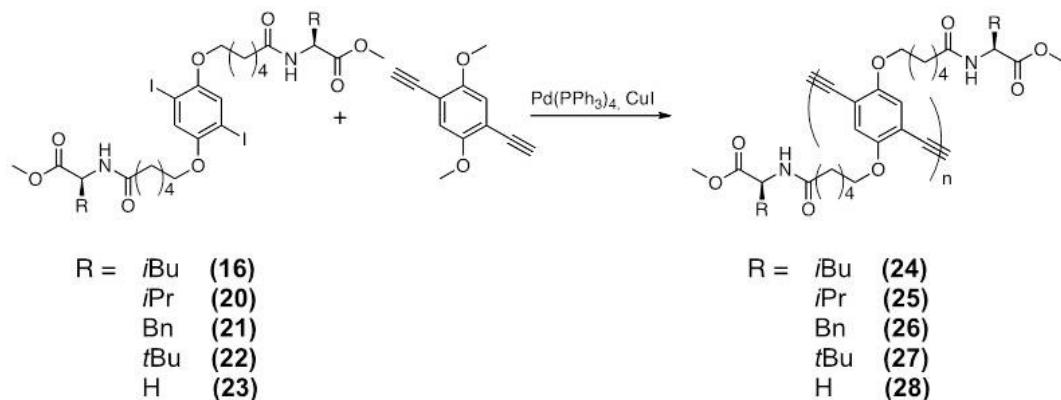
SCHEME 22: PREPARATION OF AMINOACID FUNCTIONALIED PPE COPOLYMERS

The solvent was removed under vacuum and the crude product was purified by flash chromatography (silica gel, CH$_2$Cl$_2$/AcOEt 4:1) to give 880 mg (1.07 mmol, 85% yield) of **(20)** as a white solid. ^{1}H NMR (CDCl$_3$, 298 K), δ (ppm): 7.14 (s, 2H), 5.90 (d, 2H), 4.57 (m, 2H), 3.91 (t, 4H), 3.72 (s, 6H), 2.27 (t, 4H), 2.13 (sest, 2H), 1.80 (quint, 4H), 1.70 (quint, 4H), 1.53 (quint, 4H), 0.90 (dd, 12H). ^{13}C NMR (CDCl$_3$, 298 K) δ (ppm): 172.91, 172.35, 150.95, 123.12, 88.75, 69.35, 57.13, 52.15, 36.50, 31.12, 29.06, 25.69, 25.35, 18.98, 18.03.

4.2.5.2 Synthesis of phenylalanine functionalized diiodoarene derivative (21)

Compound **(21)** was prepared exactly as described for **(20)** using phenylalanine methyl ester hydrochloride (604 mg, 2.8 mmol) instead of the valine precursor. We obtained 962 mg (1.05 mmol, 83% yield) of **(21)** as a white solid. ^{1}H NMR (CDCl$_3$, 298 K), δ (ppm): 7.28 (t, 4H), 7.20 (t, 2H), 7.14 (s, 2H), 7.07 (d, 4H), 5.84 (d, 2H), 4.89 (m, 2H), 3.89 (t, 4H), 3.70 (s, 6H), 3.11 (ddd, 4H), 2.22 (t, 4H), 1.78 (quint, 4H), 1.68 (quint, 4H), 1.49 (quint, 4H). ^{13}C NMR (CDCl$_3$, 298 K) δ (ppm):173.01, 172.15, 151.55, 135.92,

129.23, 128.57, 126.95, 122.96, 88.78, 69.22, 56.65, 52.26, 37.75, 36.29, 28.95, 25.55, 25.10.

4.2.5.3 Synthesis of tert-leucine functionalized diiodoarene derivative (22)

Compound **(22)** was prepared exactly as described for **(20)** using *tert*leucine methyl ester hydrochloride (508 mg, 2.8 mmol) instead of the valine precursor. We obtained 860 mg (1.01 mmol, 80% yield) of **(22)** as a white solid. ^{1}H NMR (CDCl$_3$, 298 K), δ (ppm): 7.28 (t, 4H), 7.20 (t, 2H), 7.14 (s, 2H), 7.07 (d, 4H), 5.84 (d, 2H), 4.89 (m, 2H), 3.89 (t, 4H), 3.70 (s, 6H), 3.11 (ddd, 4H), 2.22 (t, 4H), 1.78 (quint, 4H), 1.68 (quint, 4H), 1.49 (quint, 4H). ^{13}C NMR (CDCl$_3$, 298 K) δ (ppm): 173.51, 172.32, 152.57, 122.95, 86.29, 70.10, 59.77, 51.70, 36.64, 34.75, 28.83, 26.55, 25.83, 25.29.

4.2.5.4 Synthesis of glycine functionalized diiodoarene derivative (23)

In strict anhydrous conditions glycine methyl ester hydrochloride (351 mg, 2.8 mmol), 3 mL of Et$_3$N and 25 ml of dry CH$_2$Cl$_2$ were placed in a round bottom flask and cooled with an ice/water bath. Then compound **(15)** (800 mg, 1.27 mmol) in 15 mL of CH$_2$Cl$_2$ was added. Almost immediately the formation of a white precipitate was observed. After 2 h, the reaction mixture was allowed to warm to room temperature and further stirred for 24 h. The solvent was removed under vacuum and the obtained solid was washed several times water affording 827 mg (1.13 mmol, 89% yield) of **(23)** as a white powder. ^{1}H NMR (DMSO, 298 K), δ (ppm): 7.14 (s, 2H), 5.94 (bs, 2H), 4.04 (d, 4H), 3.91 (t, 4H), 3.75 (s, 6H), 2.28 (t, 4H), 1.81 (quint, 4H), 1.73 (quint, 4H), 1.55 (quint, 4H).

4.2.5.5 Synthesis of leucine functionalized copolymer (24)

In a round bottom flask were placed under nitrogen atmosphere 64 mg (0.34 mmol) of 1,4-diethynyl-2,5-dimethoxybenzene, 290 mg (0.34 mmol) of **(16)**, 17.5 mg (15 μmol, 4.5%) of Pd(PPh$_3$)$_4$ and 3 mg (15 μmol, 4.5%) of CuI. Thus 3 mL of Et$_3$N and 7 mL and CH$_2$Cl$_2$ were added and the obtained dark mixture was refluxed under stirring for 48 h. Then the system was allowed to reach room temperature, diluted with CH$_2$Cl$_2$ and extracted three times with water. The organic phase was dried over

Na_2SO_4 and concentrated to about 15 mL. Then about 50 mL of Et_2O were added and the formed precipitate was separated by centrifugation. Thus the solid was redissolved in 15 mL of chloroform and precipitated with 50 mL of Et_2O. The precipitate was collected by centrifugation washed with Et_2O and dried under vacuum. We obtained 208 mg (78% yield) of **(24)** as yellow orange powder. Mol. Wt.: M_n = 10120 Da PDI = 1.81 determined by GPC with uniform polystyrene standards in $CHCl_3$. ^{1}H NMR ($CDCl_3$, 298 K), δ (ppm): 7.03 (bm, 4H), 5.89 (bm, 2H), 4.59 (bm, 2H), 4.04 (bm, 4H), 3.90 (bs, 6H), 3.70 (bs, 6H), 2.21 (bm, 4H), 1.87 (bm, 4H), 1.73 (bm, 4H), 1.6-1.4 (bm, 10H), 0.91 (bm, 12H). ^{13}C NMR ($CDCl_3$, 298 K) δ (ppm): 173.91, 172.87, 154.02, 153.61, 116.94, 115.91, 114.46, 113.63, 91.26, 69.72, 56.46, 52.32, 50.66, 41.75, 36.37, 29.12, 25.80, 25.22, 24.87, 22.76, 21.29.

4.2.5.6   Synthesis of valine functionalized copolymer (25)

Copolymer **(25)** was prepared exactly as described for **(24)** using derivative **(20)** (278 mg, 0.34 mmol) instead of **(16)**. We obtained 200 mg (77% yield) of **(25)** as yellow-orange fibers. Mol. Wt.: M_n = 9150 Da PDI = 1.62 determined by GPC with uniform polystyrene standards in $CHCl_3$. ^{1}H NMR ($CDCl_3$, 298 K), δ (ppm): 7.03 (bm, 4H), 5.90 (bm, 2H), 4.53 (bm, 2H), 4.05 (bm, 4H), 3.90 (bs, 6H), 3.71 (bs, 6H), 2.25 (bm, 4H), 2.12 (bm, 2H), 1.89 (bm, 4H), 1.75 (bm, 4H), 1.56 (bm, 4H), 0.88 (bm, 12H). ^{13}C NMR ($CDCl_3$, 298 K) δ (ppm): 172.81, 172.67, 153.90, 153.53, 116.99, 115.75, 114.10, 113.68, 91.67, 69.30, 56.90, 56.59, 52.08, 36.42, 31.25, 29.06, 25.67, 25.36, 18.98, 17.82.

4.2.5.7   Synthesis of phenylalanine functionalized copolymer (26)

Copolymer **(26)** was prepared exactly as described for **(24)** using derivative **(21)** (310 mg, 0.34 mmol) instead of **(16)**. We obtained 205 mg (70% yield) of **(26)** as yellow-orange fibers. Mol. Wt.: M_n = 9180 Da PDI = 1.86 determined by GPC with uniform polystyrene standards in $CHCl_3$. ^{1}H NMR ($CDCl_3$, 298 K), δ (ppm):7.25 (bm, 8H), 7.08 (bm, 6H), 5.89 (bm, 2H), 4.85 (bm, 2H), 4.04 (bm, 4H), 3.85 (bs, 6H), 3.68 (bs, 6H), 3.07 (bddd, 4H), 2.18 (bm, 4H), 1.84 (bm, 4H), 1.66 (bm, 4H), 1.50 (bm, 4H).

^{13}C NMR (CDCl$_3$, 298 K) δ (ppm):172.36, 172.14, 153.93, 153.60, 135.89, 129.23, 128.57, 127.14, 117.02, 115.81, 114.17, 113.76, 91.58, 69.26, 56.61, 52.93, 52.26, 37.85, 36.29, 29.00, 25.55, 25.17.

4.2.5.8 Synthesis of tertleucine functionalized copolymer (27)

Copolymer (27) was prepared exactly as described for (24) using derivative (22) (290 mg, 0.34 mmol) instead of (16). We obtained 210 mg (78% yield) of (27) as yellow-orange fibers. ^{1}H NMR (CDCl$_3$, 298 K), δ (ppm): 7.01 (bm, 4H), 5.96 (bm, 2H), 4.47 (bm, 2H), 4.04 (bm, 4H), 3.89 (bs, 6H), 3.70 (bs, 6H), 2.24 (bm, 4H), 1.89 (bm, 4H), 1.72 (bm, 4H), 1.58 (bm, 4H), 0.94 (bs, 18H). ^{13}C NMR (CDCl$_3$, 298 K) δ (ppm):172.54, 172.28, 154.04, 153.53, 117.03, 115.76, 113.59, 91.77, 69.31, 59.86, 56.67, 51.83, 36.54, 34.63, 29.06, 26.53, 25.63, 25.33.

4.2.5.9 Synthesis of glycine functionalized copolymer (28)

Copolymer (28) was prepared exactly as described for (24) using derivative (23) (250 mg, 0.34 mmol) instead of (16). We obtained 74 mg (32% yield) of (28) as yellow powder. ^{1}H NMR (DMSO, 298 K), δ (ppm): 7.02 (bm, 4H), 6.08 (bm, 2H), 4.06 (bm, 4H), 3.97 (bm, 4H), 3.89 (bs, 6H), 3.70 (bs, 6H), 2.23 (bm, 4H), 1.87 (bm, 4H), 1.74 (bm, 4H), 1.58 (bm, 4H).

4.2.6 Preparation of N-Methylleucine functionalized PPE Copolymer
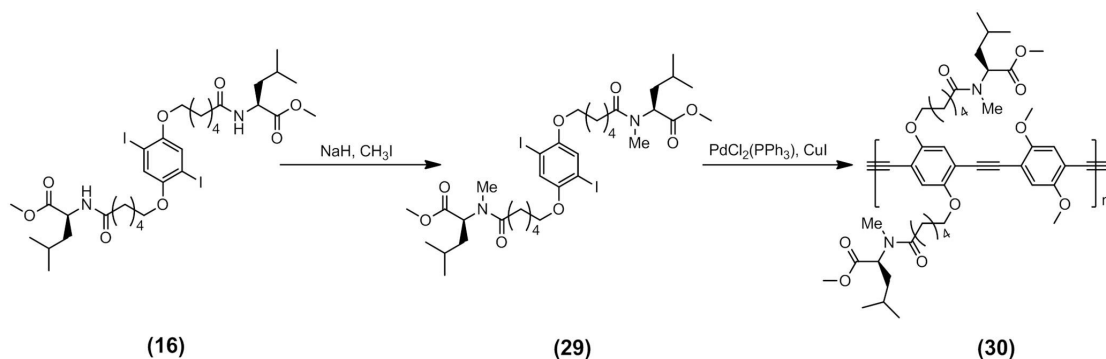
SCHEME 23: PREPARATION OF MeLeuHexMeO-PPE

4.2.6.1   Synthesis of N-Methylleucine functionalized derivative (29)

A solution of **(16)** (350 mg, 0.41 mmol) in DMF (25 mL) was cooled to 0 °C. To this solution was sequentially added whilst stirring NaH (65 mg, 2.7 mmol) and MeI (193 µl, 3.1 mmol). The reaction mixture was stirred at 0 °C for 45 min and then quenched slowly with saturated NH_4Cl aqueous solution. The resulting mixture was extracted with Et_2O and the combined organic phase was washed with brine, dried over Na_2SO_4, and evaporated yielding **(29)** (347 mg, 0.4 mmol, 97% yield) as a yellowish oil. ^{1}H NMR ($CDCl_3$, 298 K), δ (ppm): 7.14 (s, 2H), 5.35 (dd, 2H), 3.92 (t, 4H), 3.67 (s, 6H), 2.90 (s, 6H), 2.35 (m, 4H), 1.82 (m, 4H), 1.7-1.6 (m, 10H), 1.55 (m, 4H), 0.99 (dd, 12H).

4.2.6.2   Synthesis of N-Methylleucine functionalized copolymer (30)

In a round bottom flask were placed under nitrogen atmosphere 64 mg (0.34 mmol) of 1,4-diethynyl-2,5-dimethoxybenzene, 300 mg (0.34 mmol) of **(29)**, 17.5 mg (15 µmol, 4.5%) of $Pd(PPh_3)_4$ and 3 mg (15 µmol, 4.5%) of CuI. Thus 3 mL of Et_3N and 7 mL and CH_2Cl_2 were added and the obtained dark mixture was refluxed under stirring for 48 h. Then the system was allowed to reach room temperature, diluted with CH_2Cl_2 and extracted three times with water. The organic phase was dried over Na_2SO_4 and concentrated to about 10 mL. Then about 50 mL of methanol were added and the formed precipitate was separated by centrifugation. Thus the solid was redissolved in 10 mL of chloroform and precipitated with 50 mL of petroleum ether. The precipitate was collected by centrifugation washed with methanol and petroleum ether and dried under vacuum. We obtained 200 mg (75% yield) of **(30)** as yellow orange powder. Mol. Wt.: M_n = 19100 Da PDI = 1.51 determined by GPC with uniform polystyrene standards in $CHCl_3$. ^{1}H NMR ($CDCl_3$, 298 K), δ (ppm): 7.02 (bs, 4H), 5.33 (bm, 2H), 4,05 (bm 4H), 3.90 (bs, 6H), 3.66 (bs, 6H), 2.90 (bs, 6H), 2.35 (bm, 4H), 1.91 (bm, 4H), 1.7-1.4 (m, 14H), 0.99 (bm, 12H).

5 References

[1] H. Shirakawa, E. J. Louis, A. G. MacDiarmid, C. K. Chiang, A. J. Heeger*, Chem. Commun.,* **1977**, 578

[2] a) U. Scherf, E. J. W. List, *Adv. Mater*., **2002**, *14*, 477. b) S. Setayesh, D. Marsitzky, K Mullen, *Macromolecules*, **2000**, *33*, 2016. c) U. Scherf, *J. Mater. Chem.*, **1999**, *9,* 1853. d) J. Kido, H. Shionoya, K. Nagai, *Appl. Phys. Lett.*, **1995**, *67*, 2281. e) C. Zhang, A. J. Heeger, *J. Appl. Phys.,***1998**, *84*, 1579.

[3] R. E. Peierls, **1955**, *Quantum Theory of Solids* (Clarendon, Oxford).

[4] a)A. J. Heeger, S. Kivelson, J. R. Schrieffer, W.-P. Su, *Rev. Mod. Phys.*, **1988**, *60*, 781; b) Z. G. Soos, S. Ramasesha, D. S. Galvao, *Phys. Rev. Lett.*, **1993**, *71*, 1609; c) Z. G. Soos, S. Ramasesha, D. S. Galvao, R. G. Kepler, S. Etemad, *Syn. Met.*, **1993**, *54*, 35.

[5] a) N. S. Sariciftci (ed.), *Primary Photoexcitations in Conjugated Polymers: Molecular Exciton versus Semiconductor Band Model*, **1997**, World Scientific, Singapore; b) K.Y. Law, *Chem. Rev*. **1993,** *93,* 449 c) P. M. Borsenberger, D. S. Weiss, *Organic Photoreceptors for Xerography*, **1998**, Marcel Dekker, New York.

[6] A. Mozumder, *J. Chem. Phys*. **1974**, *60*, 4300.

[7] M. Redecker, D.D. C. Bradley, M. Inbasekaran, E. P. Woo, *Appl. Phys. Lett.*, **1998**, *73*, 1565.

[8] J. Shinar, V. Savvateev : *Introduction to Organic Light-Emitting Devices* in *"Organic Light Emitting Devices, a Survey"* **2004,** Springer-Verlag New York, *Chapter 1*, page 44.

[9] D. T. McQuade, A. E. Pullen, T. M. Swager, *Chem. Rev.*, **2000**, *100*, 2537.

[10] a) B. J. Schwartz. *Ann. Rev. Phys. Chem.*, **2003**, *54*, 141; b) R. Chang, J. H. Hsu, W. S. Fann, K. K. Liang, C. H. Chang, M. Hayashi, J. Yu, S. H. Lin, E. C. Chang, K. R. Chuang, S. A. Chen, *Chem. Phys. Lett.*, **2000**, *317*, 142; c) J. Yu, D. Hu, P. F. Barbara, *Science*, **2000**, *289*, 1327.

[11] a) K. S. Schweizer. *J. Chem. Phys.*, **1986**, *85*, 1156; b) M. Schreiber, S. Abe *Synth. Met.*, **1993**, *55*, 50; c) O. Lhost, J. L. Brédas, *J. Chem. Phys.*, **1992**, *96*, 5279; d) Z. G. Soos, S. Ramasesha, D. S. Galvao, S. Etemad, *Phys. Rev. B*, **1993**, *47*, 1742.

[12] S. Heun, R. F. Mahrt, A. Greiner, U. Lemmer, H. Bässler, D. A. Halliday, D. D. C. Bradley, P. L. Burn, A. B. Holmes, *J. Phys.: Condens. Matter.*, **1993**, *5* ,247.

[13] a) S. N. Yaliraki, R. J. Silbey, *J. Chem. Phys.*, **1996**, *104*, 1245; b) B. E. Kohler, I. D. W. Samuel. *J. Chem. Phys.*, **1995**, *103*, 6248; c) B. E. Kohler, J. C. Woehl, *J. Chem. Phys.*, **1995**, *103*, 6253.

[14] a) G. Rossi, R. R. Chance, R. Silbey, *J. Chem. Phys.*, **1989**, *90*, 7594; b) J. D. White, J. H. Hsu, S. C. Yang, W. S. Fann, G. Y. Pern S. A. Chen, *J. Chem. Phys.*, **2001**, *114*, 3848; c) C. F. Wang, J. D. White, T. L. Lim, J. H. Hsu, S. C. Yang, W. S. Fann, K. Y. Peng, S. A. Chen. *Phys. Rev. B*, **2003**, *67*, 35202.

[15] F. Schindler and J. M. Lupton. *ChemPhysChem*, **2005**, *6*, 926.

[16] a) R. Kersting, U. Lemmer, R. F. Mahrt, K. Leo, H. Kurz, H. Bässler, E. O. Göbel, *Phys. Rev. Lett.*, **1993**, *70*, 3820; b) S. Mukamel, S. Tretiak, T. Wagersreiter, V.

Chernyak. *Science*, **1997**, *277*, 781; c) H. Bässler, B. Schweitzer, *Acc. Chem. Res*, **1999**, *32*, 173.

[17] L. Rothberg. Photophysics of conjugated polymers in " G. Hadziioannou and G.G. Malliaras, *Semiconducting Polymers: Chemistry, Physics and Engineering*, Wiley-VCH, **2006**, *volume 1*, page 768.".

[18]a) D. Oelkrug, A. Tompert, J. Gierschner, H.J. Egelhaaf, M. Hanack, M. Hohloch, E. Steinhuber. *J. Phys. Chem. B*, **1998**, *102*,1902; b) X. Yang, T. E. Dykstra, G. D. Scholes, *Phys. Rev. B*, **2005**, *71*, 045203.

[19] S. Tretiak, A. Saxena, R. L. Martin, A. R. Bishop. *Phys. Rev. Lett.*, **2002**, *89*, 097402.

[20] F.C. Grozema, L.D.A. Siebbeles, G.H. Gelinck, and J.M. Warman. *Top. Curr. Chem.*, **2005**.

[21] a) F. Garnier, R. Hajlaoui, A. Yassar, P. Srivastava, *Science*, **1994**, 265 1684; b) J. A. Rogers, Z. Bao, M. Meier, A. Dodabalapur, O. J. A. Schueller, G. M. Whitesides, *Synth. Met.*, **2000**, *115*, 5; c) J. A. Rogers, Z. Bao, K. Baldwin, A. Dodabalapur, B. Crone, V. R. Baju, V. Kuck, H. E. Katz, K. Amundson, J. Ewing, P. Drzaic, *Proc. Natl. Acad. Sci. U.S.A.*, **2001**, *98*, 4835 d) H. Sirringhaus, T. Kawase, R. H. Friend, T. Shimoda, M. Inbasekaran, W. Wu, E. P. Wu, *Science*, **2000**, *290*, 2123; e) S. P. Speakman, G. G. Rozenburg, K. J. Clay, W. I. Milne, A. Ille, I. A. Gardner, E. Bressler, J. H. G. Steinke, *Org. Electron.*, **2001**, *2*, 65.

[22] a) F. J. M. Hoeben, P. Jonkheijm, E. W. Meijer, A. P. H. J. Schenning, *Chem. Rev.*, **2005**, *105*, 1491; b) J. Kim, *Pure Appl. Chem.*, **2002**, *74*, 2031.

[23] J. M. Lehn, *Science* **2002**, *295*, 2400.

[24] J. W. Steed, J. L. Atwood, *Supramolecular Chemistry*; **2000** Wiley &Sons: Chichester.

[25] C. A. Hunter, J. K. M. Sanders, *J. Am. Chem. Soc.,* **1990**, *112*, 5525.

[26] a) B. Askew, P. Ballester, C. Buhr, K. S. Jeong, S. Jones, K. Parris, K. Williams, J. Rebek Jr, *J. Am. Chem. Soc.*, **1989**, *111* , 1082; (b) S. C. Zimmerman, C. M. VanZyl, G. S. Hamilton, *J. Am. Chem. Soc*, **1989**, *111*, 1373.

[27] K. Morokuwa, *Acc. Chem. Res.*, **1977**, *10*,294.

[28] L. J. Prins, D. N. Reinhoudt, P. Timmerman, *Angew. Chem. Int. Ed.* **2001**, *40,* 2382.

[29] W. den Hoeve, H. Wynberg, E. E. Havinga, E. W. Meijer, *J. Am. Chem. Soc.*, **1991**, *113*, 5887.

[30] S. D. D. V. Rughooputh, S. Hotta, A. Heeger, J. F. Wudl, *J.Polym. Sci., Part B: Polym. Phys.,* **1987**, *25*, 1071.

[31] a) S. A. Chen, J. M. Ni, *Macromolecules,* **1992**, *25*, 6081; b) G. Daoust, M. Leclerc, *Macromolecules,* **1991**, *24*, 455; c) G. W. Heffner, D. S. Pearson, *Macromolecules,* **1991**, *24*, 6295; d) C. Roux, M. Leclerc, *Macromolecules,* **1992**, *25*, 2141.

[32] a) R. D. McCullough, S. Tristram-Nagle, S. P. Williams, R. D. Lowe, M. Jayaraman, *J. Am. Chem. Soc.,* **1993**, *115*, 4910; b) T. Yamamoto, D. Komarudin, M. Arai, B. L. Lee, H. Suganuma, N. Asakawa, Y. Inoue, K. Kubota, S. Sasaki, T. Fukuda, H. Matsuda, *J. Am. Chem. Soc.,* **1998**, *120*, 2047; c) K. Fäıd, M. Fréchette, M. Ranger, L. Mazerolle, I. Lévesque, M. Leclerc, T. A. Chen, R. D. Rieke, *Chem. Mater.,* **1995**, *7*, 1390; d) I. Lévesque, M. Leclerc, *Chem. Mater.*, **1996**, *8*, 2843.

[33] a) B. J. Schwartz, *Annu. Rev. of Phys. Chem.* **2003**, *54*, 141; b) U. H. F. Bunz, *Chem. Rev.* **2000**, *100*, 1605.

[34] a) J. Cornil, D. Beljonne, J. P. Calbert, J. L. Bredas., Adv. Mater. **2001**, 13, 1053; b) J. L. Bredas, J. Cornil, D. Beljonne, D. dos Santos, Z. G. Shuai. Acc. Chem. Res.,**1999**, 32, 267; c) J. Cornil, D. A. dos Santos, X. Crispin, R. Silbey, J. L. Bredas. J. Am. Chem. Soc.,**1998**, 120, 1289; d) J. Cornil, A. J. Heeger, J. L. Bredas. Chem. Phys. Lett., **1997**, 272, 463; e) R. Jakubiak, C. J. Collison, W. C. Wan, L. J. Rothberg, B. R. Hsieh, *J. Phys. Chem. A*, **1999**, *103*, 2394; f) S. Tretiak, A. Saxena, R. L. Martin, A. R. Bishop. *J. Phys. Chem. B* , **2000**, *104*, 7029.

[35] a) J. Kim , T. M. Swager, Nature, **2001**, 411, 1030; b) J. Kim, I. A. Levitsky, D. T. McQuade, T. M. Swager, J. Am. Chem. Soc., **2002**, 124, 7710; c) R. Deans, J. Kim, M. R. Machacek, T. M. Swager. J. Am. Chem. Soc., **2000**, 122, 8565; d) J. Kim, D. T. McQuade, S. K. McHugh, T. M. Swager. Angew. Chem., Int. Ed., **2000**, *39*, 3868; e) D. T. McQuade, J. Kim, T. M. Swager., *J. Am. Chem. Soc.*, **2000**, *122*, 5885; f) S. A. Jenekhe. Adv. Mater., **1995**, *7*, 309; g) S. A. Jenekhe, J. A. Osaheni. *Science*, **1994**, *265*, 765; h) J. A. Osaheni, S. A. Jenekhe, *Macromolecules* **1994**, 27, 739; i) J. W. Blatchford, T. L. Gustafson, A. J. Epstein, D. A. VandenBout, J. Kerimo, D. A. Higgins, P. F. Barbara, D. K. Fu, T. M. Swager, A. G. MacDiarmid, *Phys. Rev. B,* **1996**, *54*, R3683; j) J. W. Blatchford, S. W. Jessen, L. B. Lin, T. L. Gustafson, D. K. Fu, H. L. Wang, T. M. Swager, A. G. MacDiarmid, A. J. Epstein, *Phys. Rev. B* , **1996**,*54*, 9180; k) E. Conwell. Trends Polym. Sci., **1997**, *5*, 218.

[36] a) D. R. Greve, N. Reitzel, T. Hassenkam, J. Bogelund, K. Kjaer, P. B. Howes, N. B. Larsen, M. Jayaraman, R. D. McCullough, T. Bjornholm. *Synth. Met.*, **1999**, *102*, 1502; b) J. Kim, S. K. McHugh, T. M. Swager. *Macromolecules* **1999**, *32*, 1500; c) G.Pescitelli, F. Babudri, D. Colangiuli, L. Di Bari, G. M. Farinola, O. H. Omar, F. Naso,

Macromolecules, **2006**, *39*, 5206; d) G. Pescitelli, O. H. Omar, A. Operamolla, G. M. Farinola, L. Di Bari, *Macromolecules*, **2012**, *45*, 9626.

[37] a) M. Levitus, K. Schmieder, H. Ricks, K. D. Shimizu, U. H. F. Bunz, M. A. Garcia-Garibay., *J. Am. Chem. Soc*., **2001**, 123, 4259; b) T. Miteva, L. Palmer, L. Kloppenburg, D. Neher, U. H. F. Bunz. *Macromolecules*, **2000**, *33*, 652; c) U. H. F. Bunz. *Acc. Chem. Res*., **2001**, *34*, 998.

[38] M. Levitus, G. Zepeda, H. Dang, C. Godinez, T. A. V. Khuong, K. Schmieder, M. A. Garcia-Garibay. *J. Org. Chem*., **2001**, *66*, 3188.

[39] a) J. S. Yang, T. M. Swager, *J. Am. Chem. Soc.*, **1998**, *120*, 5321; b) J. S. Yang, T. M. Swager*., J. Am. Chem. Soc*., **1998**, *120*, 11864.

[40] M. Halim, J. N. G. Pillow, D. W. Samuel, P. L. Burn., *Adv. Mater*., **1999**, *11*, 371.

[41] H. G. Gilch, W. L. Wheelwright*, J. Polym. Sci.:A*, **1966**, *4*, 1337.

[42] B. R. Hsieh, Y. Yu, A. C. Van Laeken, H. Lee, *Macromolecules*, **1997**, *30*, 8094.

[43] C. J. Neef, J. P. Ferraris, *Macromolecules*, **2000**, *33*, 2311.

[44] a) L. Hontis, V. Vrindts, L. Lutsen, D. Vanderzande, J. Gelan, *Polymer*, **2001**, *42*, 5793; b) L. Hontis, L. Lutsen, D. Vanderzande, J. Gelan, *Synth. Met*. **2001**, *119*, 135.

[45] H. P. Weitzel, A. Bohnen, K. Müllen, *Makromol. Chem*., **1990**, *191*, 2815.

[46] H. Becker, H. Spreitzer, W. Kreuder, E. Kluge, H. Schenk, I. Parker, Y. Cao, *Adv. Mater.*, **2000**, *12*, 42.

[47] a) H. Becker, H. Spreitzer, W. Kreuder, E. Kluge, H. Vestweber, H. Schenk, K. Treacher, *Synth. Met*., **2001**, *122*, 105; b) H. Becker, H. Spreitzer, W. Kreuder, E. Kluge,

H. Schenk, I. Parker, Y. Cao, *Adv. Mater*., **2000**, *12*, 42; c) K. L. Brandon, P. G. Bentley, D. D. C. Bradley, D. A. Dunmer, *Synth. Met*., **1997**, *91*, 305.

[48] S. Pfeiffer, H. H. Hörhold, *Macromol. Chem. Phys*. **1999**, *200*, 1870.

[49] M. J. Marsella, D.-K. Fu, T. M. Swager, *Adv. Mater*. **1995**, *7*, 145.

[50] a) F. Babudri, S. R. Cicco, G. M. Farinola, F. Naso, A. Bolognesi. W. Porzio, *Macromol. Rapid. Commun.*, **1996**, *17*, 905; b) L. Chiavarone, M. Di Terlizzi, G. Scamarcio, G. M. Farinola, F. Bubudri, F. Naso, *Appl. Phys. Lett.,***1999**, *75*, 2053; c) F. Naso, F. Babudri, G. M. Farinola, *Pure Appl. Chem.*, **1999**, *71*, 1485; d) F. Babudri, S. R. Cicco, L. Chiavarone, G. M. Farinola, L. G. Lopez, F. Naso, G. Scamarcio, *J. Mater. Chem.*, **2000**, *10*, 1573; e) F. Babudri, G. M. Farinola, L. C. Lopez, M. G. Martinelli, F. Naso, *J. Org. Chem.*, **2001**, *66*, 3878.

[51] F. Koch, W. Heitz, *Macromol. Chem. Phys.*, **1997**, *198*, 1531.

[52] a) Y. H. Kim, J. H. Ahn, D. C. Shin, S. K. Kwon, *Polymer* , **2004**, *45*, 2525; b) L. C. Lopez, P. Strohriegl, T. Stübinger*, Macromol. Chem. Phys.*, **2002**, *203*, 1926.

[53] a) E. Thorn-Csönyi, P. Kraxner, *Macromol. Chem. Phys.*, **1997**, *198*, 3827; b) R. Reetz, O. Norwark, O. Herzog, S. Brocke, E. Thorn-Csönyi, *Synth. Met*. **2001**, *119*, 539.

[54] a) S. Tasch, W. Graupner, G. Leising, L. Pu, M. P. Wagaman, R. H. Grubbs, *Adv. Mater.* **1995**, *7*, 903; b) L. Pu, M. Wagaman, R. H. Grubbs, *Macromolecules* **1996**, *29*, 1138.

[55] a) F. Babudri, D. Colangiuli, P. A. Di Lorenzo, G. M. Farinola, O. Omar Hassan, F. Naso, *Chem. Commun.*, **2003**, 130; b) A. Mori, T. Kondo, Y. Kato, Y. Nishihara, *Chem. Lett.*, **2001**, 286.

[56] U. H. F. Bunz, *Chem*. *Rev*. **2000**, *100*, 1605–1644.

[57] *Circular Dichroism: Principles and Applications*, ed. N. Berova, K. Nakanishi, R.W. Woody, Wiley-VCH, New York, 2nd ed., **2000**.

[58] F. Ciardelli, E. Benedetti , O. Pieroni, *Makromol. Chem.*, **1967**, *103*, 1.

[59] L. Pu, *Chem. Rev.*, **1998**, *98*, 2405.

[60] Z. B. Zhang, M. Motonaga, M. Fujiki, C. E. McKenna, *Macromolecules*, **2003**, *36*, 6956.

[61] H. Goto, Y. Okamoto, E. Yashima, *Chem. Eur. J.*, **2002**, *8*, 4027.

[62] W. Vanormelingen, A. Smeets, E. Franz, I. Asselberghs, K. Clays, T. Verbiest, G. Koeckelberghs, *Macromolecules*, **2009**, *42*, 4282.

[63] a) B. M. W. Langeveld-Voss, D. Beljonne, Z. Shuai, R. A. J. Janssen, S. C. J. Meskers, E. W. Meijer, J. L. Brédas, *Adv. Mater.*, **1998**, *10*, 1343. b) B. M. W. Langeveld-Voss, R. A. J. Janssen, E. W. Meijer, *J. Mol. Structure*, **2000**, *521*, 285.

[64] a) J. C. Nelson, J. G. Saven, J. S. Moore, P. G. Wolynes, *Science*, **1997**, *277*, 1793; b) S. Lahiri, J. L. Thompson, J. S. Moore, *J. Am. Chem. Soc.*, **2000**, *122*, 11315.

[65] X. Y. Zhao, K. S. Schanze, *Langmuir*, **2006**, *22*, 4856.

[66] K. Suda, K. Akagi, *Macromolecules*, **2011**, *44*, 9473.

[67] a) M. M. Bouman, E. E. Havinga, R. A. J. Janssen E. W. Meijer, *Mol. Cryst. Liq. Cryst.*, **1994**, *256*, 439; b) M. M. Bouman, E. W. Meijer, *Adv. Mater.*, **1995**, *7*, 385.

[68] M. Lemaire, D. Delabouglise, R. Garreau, A. Guy, J. Roncali, *J. Chem. Soc., Chem. Commun.*, **1988**, 658.

[69] R. D. McCullough, R. D. Lowe, M. Jayaraman, D. L. Anderson, *J. Org. Chem.*, **1993**, *58*, 904.

[70] G. Bidan, S. Guillerez, V. Sorokin, *Adv. Mater.*, **1996**, *8*, 157.

[71] B. M. W. Langeveld-Voss, R. J. M. Waterval, R. A. J. Janssen, E. W. Meijer, *Macromolecules*, **1999**, *32*, 227.

[72] G. Koeckelberghs, M. Vangheluwe, C. Samyn, A. Persoons, T. Verbiest, *Macromolecules*, **2005**, *38*, 5554.

[73] C. R. G. Grenier, S. J. George, T. J. Joncheray, E. W. Meijer, J. R. Reynolds, *J. Am. Chem. Soc.*, **2009**, *129*, 10694.

[74] E. Peeters, M. P. T. Christiaans, R. A. J. Janssen, H. F. M. Schoo, H. P. J. M. Dekkers, E. W. Meijer, *J. Am. Chem. Soc.*, **1997**, *119*, 9909.

[75] E. Peeters, R. A. J. Janssen, E. W. Meijer *Synth. Met.*, **1999**, *102*, 1105

[76] R. Fiesel, U. Scherf, *Macromol. Rapid Commun*., **1998**, *19*,427.

[77] S. Zahn, T. M. Swager, *Angew. Chem. Int. Ed.*, **2002**, *41*, 4226.

[78] a) S. Changsarn, R. Traiphol, T. Pattanatornchai, T. Srikhirin, P. Supaphol, *J. Polym. Sc. B: Polymer Physics*, **2009**, *47*, 696; b) *O.* Dammer *et al., Materials Chemistry and Physics* **2009**, *115*, 352 c) Y. Li, Y. Sun, Y. Li, F. Ma, *Computational Mater. Sci.* **2007**, *39*,575; d) S. Quana, F. Tenga, Z. Xua, L. Qiana, T. Zhanga, D. Liua, Y. Houa, Y. Wanga, X. Xua, *Journal of Luminescence* **2007,** *124*, 81; e) S. J. Martin, D. D. C. Bradley, P. A. Lane, H. Mellor, P. L. Burn, *Phys Rev. B*, **1999***, 59,* 15133. f) N.N. Barashkov 1, D.J. Guerrero, H.J. Olivos, J.P. Ferraris, *Synth. Met.*, **1995**, *75*, 153.

[79] A. J. Heeger, D. Braun, *PCT Intl. Patent Appl.* WO 92/16,023, **1992**; *Chem. Abstr.* **1992**, 118, 157401j

[80] a) B. C. Anić, M. Majerić-Elenkov, Z. Hameršak, V. Šuric, *Food, Technol & biotechnol*, **1999**, *37*, 65; b) B. C. Anić, Z. Hameršak, *Chirality*, **2009**, *21*, 894.

[81] A. M. Spring, C. Y. Yu, M. Horic, M. L. Turner, *Chem. Commun. ,***2009**, 2676

[82] J. S. Yang, T. M. Swager, *J. Am. Chem. Soc.* **1998**, *120*, 11864.

[83] T. Mangel, A. Eberhardt, U. Scherf, U. H. F Bunz,.K. Mullen, *Macromol. Rapid Commun.* **1995***, 16,* 571.

[84] a) C. Weder, C. Sarwa, A. Montali, G.Bastiaansen, P. Smith, *Science* **1998**, *279*, 835; b) A. Montali, G. Bastiaansen, P. Smith, C. Weder, *Nature* **1998**, *392*, 261

[85] a) L. A Bumm, J. J.Arnold, M. T. Cygan, T. D.Dunbar, T. P. Burgin, L. Jones, D. L. Allara, J. M. Tour, P. S. Weiss, *Science* **1996**, *271*, 1705.

[86] R. Giesa, J. M. S.-Rev. Macromol. Chem. Phys. **1996**, 36, 631

[87] R. Giesa, R. C. Schulz, Macromol. Chem. Phys. **1993**, 191, 857

[88] a) M. Moroni, J. LeMoigne, S. Luzzati, *Macromolecules* **1994**, *27*, 562; b) R. Fiesel, U. Scherf, *Macromol. Rapid Commun.* **1998**, *19*, 427; c) D. Steiger, P. Smith, C. Weder, *Macromol. Rapid Commun.* **1997**, *18*, 643.

[89] a) T. M. Swager, C. J. Gil, M. S. Wrighton, *J. Phys. Chem.* **1995**, *99*, 4886; b) C. Weder, M. S. Wrighton, *Macromolecules* **1996**, *29*, 5157; c) C. Weder, M. S. Wrighton, R. Spreiter, C. Bosshard, P. Gunter, *J. Phys. Chem.* **1996**, *100*, 18931.

[90] S. Dellsperger, F. Dötz, P. Smith, C. Weder, Macromol. Chem. Phys., **2000**, 201, 192-198

[91] a) B. Erdogan, J. N. Wilson, U. H. F. Bunz, *Macromolecules* **2002**, *35*, 7862; b) F. Babudri, D. Colangiuli, P. A. Di Lorenzo, G. M.Farinola, O. Omar Hassan, F. Naso, *Chem. Commun.* **2003**, 130; c) J. J.Lavigne, D. L. Broughton, J. N. Wilson, B. Erdogan, U. H. F.Bunz, *Macromolecules* **2003**, *36*, 7409. d) M. D. Sisney, J. Zheng, T. M. Swager, P. H. Seeberger, *J. Am. Chem. Soc.* **2004**, *126*, 13343.

[92] C. J. Yang, M. Pinto, K. Schanze, W. Tan, *Angew. Chem., Int. Ed.* **2005**, *44*, 2572.

[93] a) S. A. Kushon, K. Bradford, V. Marin, C. Suhrada, B. A. Armitage, D. McBranch, D. Whitten, *Langmuir* **2003**, *19*, 6456. b) J. N. Wilson, Wang, Y. Q. J. J. Lavigne, U. H. F. Bunz, *Chem. Commun.* **2003**, 1626.

[94] E. R. Jarvo, S. J. Miller, *Tetrahedron* **2002**, *58*, 2481.

[95] O. R. Weigang, *J. Chem. Phys.*, **1965**, *43*, 71.

[96] a) C. D.Dimitrakopolous, P. R. L. Malenfant, *Adv. Mater.*, **2002**, *14*, 99; b) D. Braun, *Mater. Today* **2002**, *5*, 32, c) C. J Brabec, V. Dyakonov, J. Parisi, N. S. Sariciftci, *Organic Photovoltaics Concepts and Realization*; Springer-Verlag: London, **2003**.

[97] W.C. Still. M. Kahn, A. Mitra, *J. Org. Chem*, **1978**, *43*, 23.

[98] a) A. I. Vogel, Textbook of Practical Organic Chemistry, fifth edition, Longman Scientific and Technical, Harlow, UK, 1989. b) D. D. Perrin, W. L. F. Armarego, Purification of Laboratory Chemical, third edition, Pergamon Press, 1988.